MODELLING THE PROXIMAL SOURCE OF INTERCEPTED EXOTIC INSECTS

A thesis submitted in partial fulfilment of the
requirements for the degree of
Doctor of Philosophy
at
Lincoln University
by
Sylvain Guichard

Lincoln University
2009

Abstract of a thesis submitted in partial fulfilment of the requirements for the Degree of Ph.D.

Modelling the proximal source of intercepted exotic insects

by

S. Guichard

Biological invasions are major threats to any nation's economy and biodiversity. To detect new biological incursions of some species biosecurity agencies deploy pheromone sentinel traps for targeted species at high risk sites such as airports, seaports and transitional facilities. A good example is the gypsy moth surveillance program in New Zealand. Following the detection of an incursion by an unwanted organism, ground-based searches to locate the source can be very expensive, but are essential to identify the introduction pathway and to increase the chances of success eradicating the unwanted organism. In such circumstances, the possibility of better targeting the search for the source of the incursion using a modelling approach is worthy of investigation

A stochastic mechanistic model to hindcast moth flight from a recapture location to the release location was developed based on insect behaviour in response to wind and pheromones. The model was composed of two main processes, 1) downwind dispersal, assumed to result from an appetitive behaviour, indicated by an analysis of a previous mark-release-recapture experiment on painted apple moth (*Teia anartoides*, Walker) and, 2) anemotaxic dispersal inspired by pheromone anemotaxis theory but up-scaled from a fine-scaled behaviour model to a 2 m scale.

A genetic algorithm was used to fit some model parameters. A specialised fitness function was developed to allow the genetic algorithm to identify parameters that resulted in models that reflected both the spread and density patterns in the trapping data. The resulting function allowed the stochastic model results to be compared with the inherently stochastic trapping data.

The resulting individual based model simulates the spatio-temporal dispersal pattern of painted apple moth recorded during a previous mark-release-recapture experiment. While the proposed model is shown to have limitations with respect to accuracy and precision it is also demonstrated to greatly improve biosecurity incursion response capability, by more efficient targeting of search effort for the proximal source of an incursion.

Keywords: anemotaxis, appetitive, biosecurity, casting, downwind, goodness of fit, individual based model, invasive alien species, Lymantriidae, *Lymantria dispar*, moth, pheromone, *Teia anartoides*

To my Whanau,

To my Mentors,

TABLE OF CONTENTS

LIST OF FIGURES AND TABLES

CHAPTER I

Introduction

CHAPTER I

Introduction

I.1. Context

According to the International Union for the Conservation of Nature and Natural Resources (2000), biological invasions follow human population growth and its associated activities as the major cause of biodiversity loss throughout the world (Pimentel, 2002a). To limit pest importation, the New Zealand government along with many other countries have signed the Convention on Biological Diversity in which article 8h requires parties to "prevent the introduction of, [and to] control or eradicate those alien species which threaten ecosystems, habitats or species" (Convention on Biological Diversity, 2004). In addition to this treaty, New Zealand has provided additional protection with national legislation such as the Biosecurity Act 1993 (Parliament of New Zealand, 1993) and the Hazardous Substances and New Organisms (HSNO) Act 1996 (Ministry for the Environment, 1996) to guard against invasive species introductions.

I.1.1 Historical context and actual situation

New Zealand was separated from the ancient supercontinent Gondwana (southern part of the Pangaea) 80 million years ago and was protected from insect invasions by the large distances of ocean that surrounds the country (Cook *et al.*, 2002). Around 1000 years ago, the first human colonisation by Polynesian migrations, occurred and with those migrants came the first introductions of alien species (Cook *et al.*, 2002). From 1800 to the first half of the 20th century, European arrivals and agricultural development that involved deliberate and accidental importations of plants, animals and associated pests further contributed to alien introduction and establishment of alien species (Cook *et al.*, 2002).

While biological invasions have been occurring over several centuries, the rate of invasion has increased markedly during recent decades. Since the Second World War, intercontinental transfers by air and sea have increased the volume of goods and number of travellers, while travel times have decreased (Cook *et al.*, 2002).

Table I.1. *Traffic to New Zealand (Whyte, 2005); P: Percentage of increase over the last years.*

	Traffic in 2004-2005	P
Air passengers	4 Million	30%
Air cargo consigment	-	40%
Sea containers	0.5 Million	57%
Used vehicles and machinery	0.18 Million	35%

Air and sea traffic in New Zealand have increased markedly in the last five years (Table I.1) and new entry pathways have also appeared with diversification of flights at smaller airports and with the development of new international airlines (Whyte, 2005). Major changes in traffic rates to New Zealand over the last few years are the main reasons for the huge rise of alien species incursions. An incursion is defined as "an isolated population of a pest recently detected in an area, not known to be established, but expected to survive for the immediate future" (IPPC, 2008).

Sea containers have become one of the major pathways of alien species incursion and invasion. In Australia, a study of 3001 empty sea cargo containers (which represent 2 days of Australian traffic) showed the presence of a total of 1339 live insects in 6% of the containers and dead timber pests in 3.5% of the containers (Stanaway *et al.*, 2001). In 1999-2000, 25% of the 360,000 sea containers entering New Zealand annually were inspected by biosecurity staff and 20% of the inspected containers were found to be contaminated with plant and animal materials (Cook *et al.*, 2002).

In 1990, 3 new incursions of potential pest species (from among weeds, viruses, invertebrates, fungi and bacteria but excluding forestry pests) were detected while in 2003 there were over 30 (Kriticos *et al.*, 2005). These authors extrapolated this trend to suggest that around 52 new incursions could be detected in 2016. In New Zealand, between 1958 and 1989, the number of interceptions of potential insect pests of *Pinus radiata*, was on average 58.2 insects per year (a total of 1,806 insect pests of *P. radiata* were intercepted over 31 years) and records observed in living plantations were, on average, 2.2 insects species per year between 1950-1987 (a total of 82 intercepted insect species over 37 years for 30 biological regions) (Carter, 1989). The tendency over recent decades is a marked increase in interceptions and incursions and over the next few decades, invasive alien species introductions and impact are expected to increase due to predicted climate changes (Cannon, 1998).

Between 2000 and 2002, 152 interceptions of lymantriid species were reported at New Zealand ports in used vehicles: 124 were identified as Asian gypsy moth (81%), 2 were identified as white spotted tussock moth and 1 as nun moth (Armstrong *et al.*, 2003). All these species are included in the list of high risk pests to New Zealand (Ministry of Agriculture and Forestry, 2006a) where seven tussock moth species have been classified based on their pest status and polyphagous nature (Armstrong *et al.*, 2003).

Williamson and Fitter (1996) developed the so-called tens rule whereby they suggest that approximately 0.1% of the exotic species that arrive in a new country become an invasive pest species (Figure I.1). Getting estimates of the number of exotic species imported into a new country is difficult. In a study of 3001 containers, Stanaway *et al.* (2001) detected 69 different insect species in 1996; but 44 of them were found only in one container. The authors probably didn't cover the whole range of exotic species imported and it would be unrealistic to extrapolate this figure to an annual proportion knowing the authors estimated the annual traffic around 770 000 shipping containers.

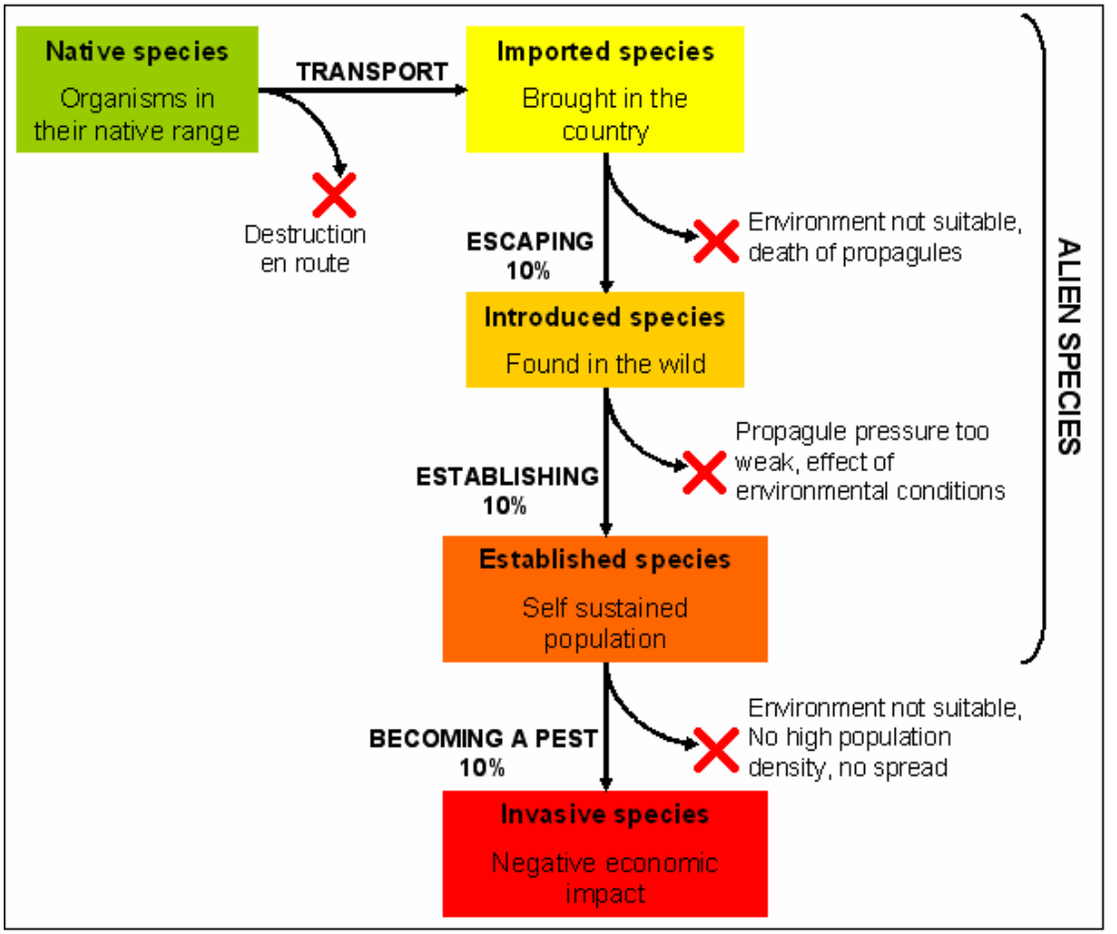

Figure I.1. *How an immigrant species becomes an alien and an invasive pest species according to the tens rule (from Williamson & Fitter, 1996; Mack* et al.*, 2000).*

We can however estimate the number of established species. Over the period 1990-2003, following General Surveillance activity, MAF Biosecurity reported the detection of an average of 3.9 ± 1.5 new to New Zealand invertebrates per year established in the country (excluding organisms associated with forestry) (Wilson *et al.*, 2004). According to the tens rule (Williamson & Fitter, 1996) that would represent between 250 and 550 exotic species imported into New Zealand per year, and would represent 1 invasive species inducing negative economic impact every 2 to 4 years.

I.1.2 Ecological and economic impacts of bioinvasions

Biological invasions represent an important ecological cost for any country. A well known example in New Zealand is the Australian brush-tailed possum, *Trichosurus vulpecula*, that affects native forests and birds. More than 230 species of weeds, 34 predatory or herbivorous mammals and many alien insects, birds and fish have also become pests since New Zealand was colonised by humans (Craig *et al.*, 2000). Specific insect examples include the introduced wasp species, *Vespula vulgaris*, that has been shown to be in food competition with kaka, *Nestor meridionalis*, and is implicated in the decline of this New Zealand endemic forest parrot species (Beggs & Wilson, 1991). The extinction of *Zizina oxleyi* (the New Zealand endemic blue butterfly) in different areas of the country could also be the result of the competition with the Australian introduced *Zizina labratus* (Hoare, 2001). Another example, a tortricid parasite, *Trigonospila brevifacies*, also introduced but for biological control, has extended its effect to non- target species such as native species of non tortricid Lepidoptera (Green, 1984).

Invasive species have a huge impact on agricultural and forestry production. In 1999, *Herpetogramma licarsisalis* (tropical grass webworm) became invasive in New Zealand (Hoare, 2001). Large populations of *H. licarsisalis* were responsible for conspicuous damage to some areas of dairy pasture in Northland during the autumn of 1999 (Hardwick *et al.*, 2000).

The cost due to invasive species can be divided into two parts 1) direct economic losses (*i.e.* reduction of outputs) and 2) indirect costs (*i.e.* expenditure on research and control to limit pest impacts). The estimated costs (direct and indirect) of alien invertebrate plant pests is estimated to be NZ$880 million per year with around NZ$540 million attributed to direct costs (Barlow & Goldson, 2002). Considering all insect pests (with high or low economic impact), the average Biosecurity New Zealand response cost is about NZ$540 000 for each incursion. Kriticos *et al.* (2005) suggesting that from 2005 to 2017, the cumulative estimated cost of incursions could reach NZ$921 million. Unfortunately, the ecological cost of biological invasions is difficult to quantify but is considered to present a very high economic cost.

I.1.3 New Zealand biosecurity context and incursion management

In biosecurity risk management the prevention of both entry and establishment is, and always will be the most important and cost effective method to avoid alien species invasion (Myers *et al.*, 2000; Baker *et al.*, 2005). In New Zealand, continuing establishment of unwanted exotic species has placed increasing demands on pre-border and border biosecurity systems (Barker *et al.*, 2003). To respond to these trends, more rapid and effective methods are needed. These methods are outlined by Baker *et al.* (2005). This study proposes to develop a new rapid response method that increases the response capacities and efficiency during the earliest steps of an incursion and is outlined below.

There are two components of the biosecurity system in New Zealand:
1) The exclusion of insects at the pre-entry and entry phases by inspection and treatment of cargo at the port of origin and maintenance of biosecure entry points.
2) Surveillance of exotic species within New Zealand and maintaining a response capacity for their control or eradication (Cook *et al.*, 2002).

As soon as an incursion is detected, The New Zealand Ministry of Agriculture and Forestry (MAF) agency Biosecurity New Zealand applies the incursion response procedure with delimitation surveys, containment measures and eradication (Figure I.2).

- ✓ Positively identify the suspect exotic organism
- ✓ Initial determination of the range likely impacts
- ✓ Clarify whether it is already an unwanted organism and, if not, determine unwanted status where that is appropriate
- ✓ Determine the initial level or response, including whether to establish a response team
- ✓ Investigate the means by which the organism was introduced, make any necessary border control or risk-management adjustements and take enforcement action
- ✓ Consult and inform key organisations and individuals
- ✓ Consider the need for, and obtain, expert, industry and community advice
- ✓ Carry out a delimiting and environmental survey
- ✓ Ensure appropriate legal instruments are in place
- ✓ Commence any immediate eradication, containment or other management actions

Figure I.2. *Initial response phase process (O'Neil, 2001).*

Clearly, rapid responses to an incursion are strategically important, with huge impacts on efficacy and costs of the response. One of the factors influencing the success of an eradication program is the early detection and the rapid initiation of an eradication program against an exotic species (Myers *et al.*, 1998). It allows elimination on a relatively small scale and with a greater probability of success owing to the less widespread distribution of the insects (Myers *et al.*, 2000). Throughout the invasion process (Figure I.3), the spread of insects during the delay or lag phase is initially low, followed by a rapid exponential increase until a specific threshold is reached (Mack *et al.*, 2000; Memmott *et al.*, 2005). Most extinctions of immigrant populations occur in this lag phase (Mack *et al.*, 2000).

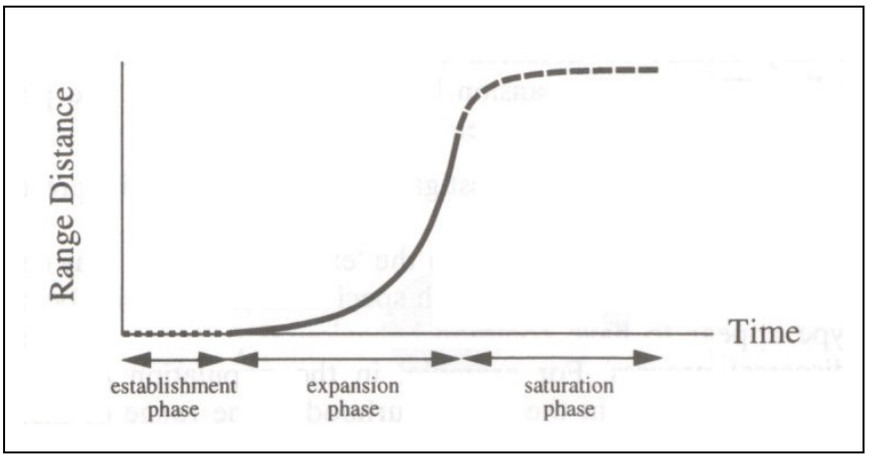

Figure I.3. *Relationship between range size and time during an invasion process. Classically, three phases can be observed: the establishment phase (also called the lag phase), the expansion phase and the saturation phase (Shigesada & Kawasaki, 1997).*

Clearly, the critical phases of the invasion process are the escape and establishment phases (Figure I.1). To prevent establishment and to eradicate and control all the insects in an incursion, biosecurity officers need to rapidly identify the founder population. Identification of the source of incursion is also vital to manage the pathway to prevent further similar incursions.

Since November 2005, Biosecurity New Zealand has used a new High Risk Site Surveillance scheme (HRSS, Figure I.4) to detect new incursions and monitor existing ones (Murphy, 2005).

The risk of incursion has been widened from concentrating on a few ports, to monitoring around 7 500 transitional facilities around the country where containers are unloaded (Murphy, 2005). Transitional facilities are MAF-approved sites, often well away from the ports (Murphy, 2005). High Risk Site Surveillance (Figure I.4) includes surveillance of traditional high risk sites such as ports, military bases and even sites of suspected post-border incursions, but also the identified transitional facilities and any vegetation rich areas such as parks and reserves, as well as invasion pathways associated with high risk sites (Murphy, 2005).

Faced with this increase in locations that require monitoring, and the more complex situation where there are now in reality more sites from where an invader can escape into the new environment, rapid identification of the founder population and its associated foci should be a key tool in incursion management.

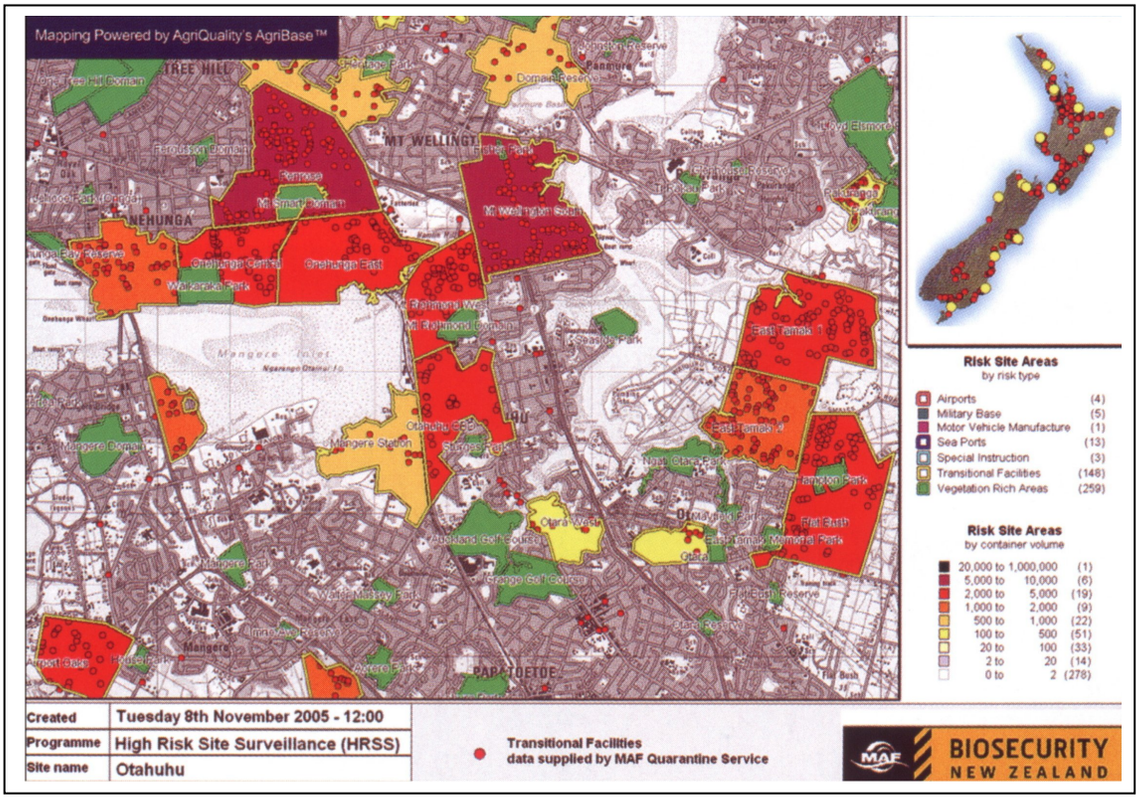

Figure I.4. *Map of high risk sites in a part of Auckland (Murphy, 2005).*

I.2 Case study species

Within the context of New Zealand biosecurity, the overall aim of the present study is to focus on the escape phase of a potential invader by modelling the proximal source of intercepted Lepidoptera species. Painted apple moth (*Teia anartoides*, Walker) was chosen as a case study based on its invasive traits such as a high rate of reproduction, high dispersal capacity, polyphagous regime and behaviour that is associated with human activities (Williams & Meffe, 1998; Jeschke & Strayer, 2008). This species is included in the unwanted species database for New Zealand (Ministry of Agriculture and Forestry, 2006a) has already been introduced to New Zealand and has been the subject of an eradication programme.

I.2.1 Biology of Painted apple moth

Teia anartoides (painted apple moth), (Lepidoptera, Lymantriidae) is native to Australia. *Teia anartoides* males fly during the day, and females are flightless (Common, 1990). Larvae are highly polyphagous and have been recorded on plants of importance to forestry, horticulture and urban amenity plantings, but the preferred host plants are acacias (Common, 1990). *Teia anartoides* moths lay egg masses on host plants, but also on different media such as walls, containers or cars (Hoare, 2001).

I.2.2 Painted apple moth incursion history in New Zealand

Teia anartoides was found in New Zealand in Glendene (West Auckland suburb) in May 1999. The first ground based attempts at eradication were undertaken and were supplemented by aerial sprayings of *Bacillus thuringiensis* (Richardson *et al.*, 2005) and mass release of sterile insects (Suckling *et al.*, 2007).

If it had not been under an eradication programme, *T. anartoides* could have cost New Zealand around NZ$3 million per year resulting from damage to forestry (Barlow & Goldson, 2002). Another estimate of the economic impact of *T. anartoides* establishment in New Zealand ranged from NZD 58 to 356 million over 20 years due to its wide host range (Self, 2003).

In 2006, a trapping programme was still continuing but the *Teia anartoides* population had been hugely reduced as reflected by the low numbers caught in baited traps. In January 2002, 1 784 moths were caught; in January 2003, 48 moths; January 2004, 1 moth (Gear, 2004) and from May to December 2005, 5 moths were caught (Kean, personal communication). *Teia anartoides* was declared eradicated in 2006 (Ministry of Agriculture and Forestry, 2006b). The eradication including health monitoring and communication and the operation was budgeted at an estimated NZD 100 million (Turner *et al.*, 2004), which was later revised closer to NZD 62.4 million actually spent (Ministry of Agriculture and Forestry, 2006b).

I.3 Technical issues in modelling insect dispersal

To model the proximal focus of intercepted Lepidoptera species it is necessary to model their dispersal. The large number of simulations of the dispersal from the interception location, the landing location to the takeoff location allows pinpointing the source location, the proximal locus. To illuminate the issues and requirements for modelling insect dispersal, the following section introduces the dispersal mechanisms of insects. These include, 1) factors affecting dispersal behaviour and the flight capacity of insects, and 2) flight tracks and searching strategies (paying particular attention to pheromone plumes and induced flight behaviour).

I.3.1 Factors affecting dispersal behaviour and flight capacity

Insects are poikilotherms and therefore flight capacities are dependant on external factors as well as internal conditions. Before young adults can achieve effective flight, the cuticle needs to be hard enough, and also they must be sufficiently mature (Johnson, 1969; Ostrand *et al.*, 2001). The teneral stage is a developmental stage when the insect is able to fly but cannot migrate; this stage could last from a few hours to some weeks, depending on the species (Johnson, 1969).

When the details of flight are considered, even something simple like take off requires factors like temperature, light intensity and wind to be well-suited to species requirements (Johnson, 1969).

When the temperature is below a specific threshold, muscles cannot generate enough energy for wings to beat with a sufficient amplitude and frequency for take off (Johnson, 1969). Atmospheric humidity interacts with temperature where dry air increases the threshold temperature and moist air reduces it (Johnson, 1969). High wind, rain and reduced sunlight tend to reduce take off (Green, 1962; Johnson, 1969). Strong winds reduce the body temperature and could induce antennal or sensillae movements so that in many insects flight is inhibited (Johnson, 1969). Green (1962) showed that periodic rain inhibited the flight of *Rhyaciona buoliana* inducing a sporadic flight pattern that varied inversely with the intensity of the rainfall. Johnson (1969) refers to instances where temporary cloudiness often prevents take off in dragonflies, butterflies and locusts.

The flight velocity of an insect is an important parameter in dispersal modelling and can be expressed in terms of air speed or ground speed. Generally, the smallest insects fly slower and they are more affected by the wind (Johnson, 1969). Insects can modulate their flight speed by integrating the changing image on the retina. This integration allows an evaluation of the insect's air speed so that it can keep control of its track and switch from flying behaviour to landing behaviour in extreme conditions. For example, Kennedy (1939) showed that in a wind tunnel, mosquitoes (*Aedes aegysti*) appear to keep the "retinal velocity", or the speed of image movement on the retina, around a value of 13-17 $cm.s^{-1}$. In still air they fly at a ground speed of 13-17 $cm.s^{-1}$. With wind speed of 33 $cm.s^{-1}$, their air speed increases to 50 $cm.s^{-1}$. In still air with the background moving from front to back faster than 13-17 $cm.s^{-1}$, the mosquitoes turned and moved across the pattern and if wind speed was too high it induced a change of flight direction or landing. Responses of flying insects to the ground pattern are the subject of Kennedy's optomotor theory of flight.

Using the capacity to fly at different heights, bees seem to keep a constant value of the rate between the ground speed and the flight height (Riley & Osborne, 2001). Riley & Osborne (2001) applied this hypothesis to estimate the height of flight from the equation: height = ground speed / 3.5 where 3.5 is the "preferred" constant value of image changes over the bee retinae.

The optomotor theory of flight, Kennedy (1951) explained the difference in the flying behaviour of insects over land and over water. During flight, the change of image sensitivity above the ground and above the sea induces a particular behavioural response. An example of change of image sensitivity is the junction between air and sea; it should increase insect flight in one direction away from the sea and reduce flights over it (Johnson, 1969). As well Heran & Lindauer (1963) cited in Riley & Osborne, (2001) state that honeybee species lose the ability to compensate wind drift when they are flying over water due to the loss of image changes. The speed of image movement on the retina could influence the movement rules in a dispersal model. The change of image sensitivity could determine the flight behaviour over water and give a supplementary tool to model flight direction change and landing.

I.3.2 Energy requirements for flight

The distance a flying insect can fly can be calculated from the amount of stored energy available in the body and the energy cost of travel. The two main sources of energy used by insects are carbohydrates and stored fat (lipids). Hymenoptera seem to use carbohydrates as fuel and Lepidoptera seem to use stored fat (Johnson, 1969). Johnson (1969) determined that stored fat in Lepidoptera represents 8% to 15% of fresh weight and that can support a flight time of 7 h to 20 h. Relative lipid mass in *Urania fulgens* (Lepidoptera: Uraniidae) ranges from 4% to 15% of the total body mass which should allow an estimated flight of 37 km to 110 km (Dudley & DeVries, 1990). To fly up to an airspeed of 4.5 $m.s^{-1}$, bumblebee workers expend a relatively constant amount of mass specific power (Dudley & Ellington, 1990; Riley & Osborne, 2001) whereas *Urania fulgens* requires increasing mechanical power at higher airspeeds over the range 1.5-4.5 $m.s^{-1}$ (Dudley & DeVries, 1990).

The energy cost (E, $J.kg^{-1}.m^{-1}$), of a journey for insects is a function of the mass specific power P(a) for a given air speed (a, $m.s^{-1}$), wind speed (v_w, $m.s^{-1}$) and angle between the insect track and downwind wind direction (θ) and between the insect body and track (θ_1): $E = P(a) / [a.\cos(\theta_1) + v_w.\cos(\theta)]$ (Riley & Osborne, 2001).

According to Gordon (1977) cited in Dudley & DeVries (1990), the total energy content can be calculated by conversion of lipid reserve to energy using an energetic conversion factor of 37.7 $J.mg^{-1}$ fat.

In many species of Lepidoptera, carbohydrates and lipid are utilized in combination, whereas lipid, especially triacylglycerol, the neutral lipid, from the insect fat body is the main fuel during sustained flight (Beenakkers *et al.*, 1984; Blacklock & Ryan, 1994). It has been shown that lipid content is correlated with weight and size in coccinellids (Mills, 1981) and in bark beetles (Anderbrant, 1988). Whole body lipids were extracted from dried beetles using petroleum ether (Anderbrant, 1988). In the pool of lipids we can distinguish triglycerides, as an energy source stored in the fat body and non-triglyceride lipids as structural lipids such as components of the cuticle (Downer & Matthews, 1976).

Fatty acids have been studied in gypsy moth adults, and were found to be mainly composed by n-Heptadecanoic acid (C16:0), n-Octadecanoic acid (C18:0), linoleic (C18:2), linolenic (C18:3) fatty acids and were assumed to be the principal energy resource (Clark *et al.*, 1990). With regard to triglyceride use during flight, Sakamoto *et al.*, (2004) showed that *Spodoptera litura* (Lepidoptera: Noctuidae), used unsaturated fatty acids first, followed by saturated fatty acids. To quantify triglycerides, lipids are first extracted from dried specimens using a methanol-chloroform protocol and triglycerides can then be separated by thin layer chromatography and quantify by laser densitometry (Zera *et al.*, 1994).

Flight duration can be studied in a flight mill or wind tunnel with a moving floor. In the later, the floor pattern is moved downwind to increase the apparent ground speed for the insect, which reacts by reducing its airspeed, preventing the insect reaching the pheromone source rapidly (Fadamiro *et al.*, 1998). In a flight mill, insects are tethered to the flight mill that is composed of a horizontal arm which rotates around a vertical arm (Jactel & Gaillard, 1991). Macaulay (1974) showed that in *Plusia gamma* (Lepidoptera, Noctuidae), its weight at emergence is positively correlated to the flight duration in both free flight and tethered flight.

I.3.3 Pheromone plumes and induced flight behaviour

A robust model for the capture of an alien species in a surveillance trap requires an understanding of how the pheromone plume from a pheromone trap behaves and how the insect responds to its stimulus. The shape of the pheromone plume created around the trap depends on a number of factors, especially air movement. At different scales, the pheromone plume has different characteristics.

At the scale of the human experience, the pheromone plume appears similar to a trail of smoke from a chimney (Figure I.5). David *et al.* (1982) showed in two studies comprising wind from NW-S at 1.6 $m.s^{-1}$ and wind from SW-N-NE at variable speeds ranging in 0.1 to 2.7 $m.s^{-1}$, that when continuous smoke is emitted in variable conditions of winds, smoke plumes snake (Figure I.5).

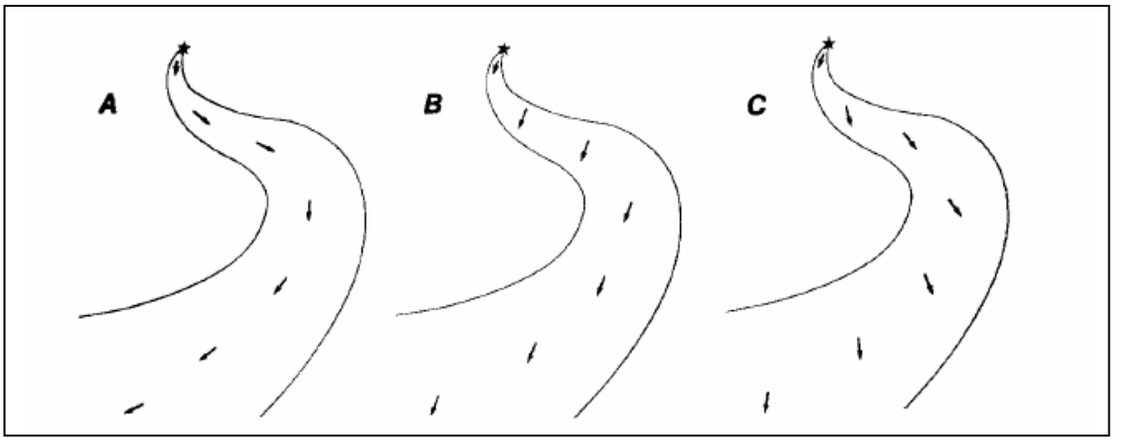

Figure I.5. *Large scale shape of a pheromone plume (star: smoke source, lines: plume outlines, arrows: wind direction). A and B, wrong first preconceptions; C, observed (David et al., 1982).*

This large scale pattern covers an area of encounter for an insect which we will call the "stimulation range". This is the area inside which biological effects, in particular attraction, occurs or is induced in flying insects (Wall & Perry, 1987). In the model developed in this work, this area will determine the boundary between "outside plume behaviour" and "inside plume behaviour".

The threshold of pheromone detection varies between insect species and will influence the area of the pheromone plume which corresponds to the range of stimulation. Assuming no aerial turbulence, species with a low threshold of detection, *i.e.* they can detect low levels of pheromone, are able to respond to the plume at some distance, in the order of hundreds of metres, from the source. In this situation, it makes little difference whether the pheromone is released continuously or in pulses (Dusenbery, 1989b). However, if the insect has a high threshold of detection, stimulation or detection only occurs near the source, that is within the order of tens of metres, and pulsed release induces a higher range of detection than constant release (Dusenbery, 1989b).

Wall and Perry (1987) define the range of stimulation as "the maximum distance at which an attractive source can be shown to elicit a response". This range varies with the species considered (Table I.2).

Table I.2. *Summary of observed ranges of stimulation (Wall & Perry, 1987).*

	Range of simulation (m)	**Reference**
Cydia nigricana	500	(Wall & Perry, 1987)
Other Tortricidae	140	(Baker & Roelofs, 1981)
Sessidae	200	(Kishaba *et al.*, 1970)
Noctuidae	97	(Kishaba *et al.*, 1970)
Lymantriidae	80	(Elkinton *et al.*, 1984)

At a medium scale, such as the scale of an insect, pheromone plumes appear as filaments of pheromone separated by gaps of clean air. Figures I.6 and I.7 show schematic representations of such filaments. In Figure I.7, the modelled pheromone puff trajectories are a simplification of the expected trajectory illustrated by Figure I.5C.

Even if the signals are emitted continuously, the resulting plume in the field characterised by a wind speed of 4-5 $m.s^{-1}$, is a structure composed of a succession of odour tracks, typically 0.4-0.5 m long, separated by gaps of clean air typically 2-2.5 m long (Murlis & Jones, 1981).

Murlis & Jones (1981) showed that the duration and frequency of odour peaks does not greatly vary within the plume from 2 to 15 m from the source, but the ratio of pheromone to clean air fluctuates with the distance from the pheromone source.

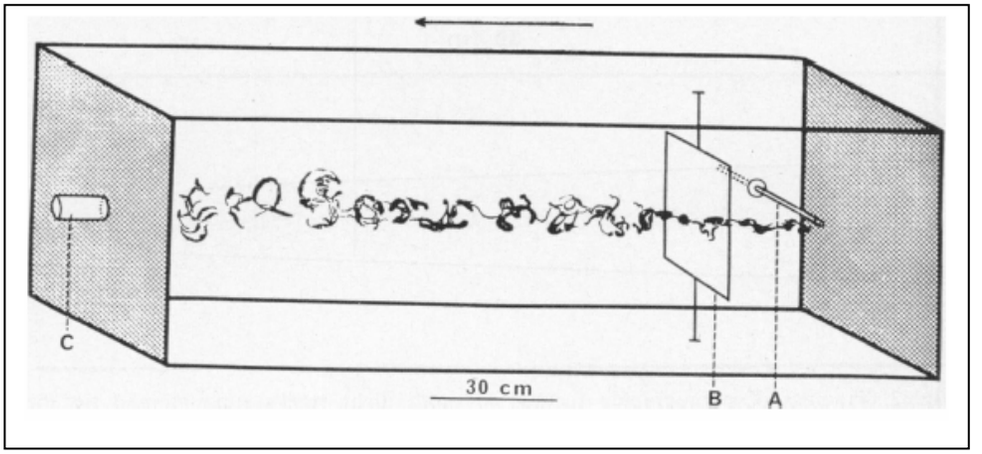

Figure I.6. *Representation of an odour plume in a flight tunnel based on a photograph of a visible smoke plume. A, pheromone source; B, wire hoop; C, release cage for insects. Arrow, direction of the air flow (Farkas & Shorey, 1972).*

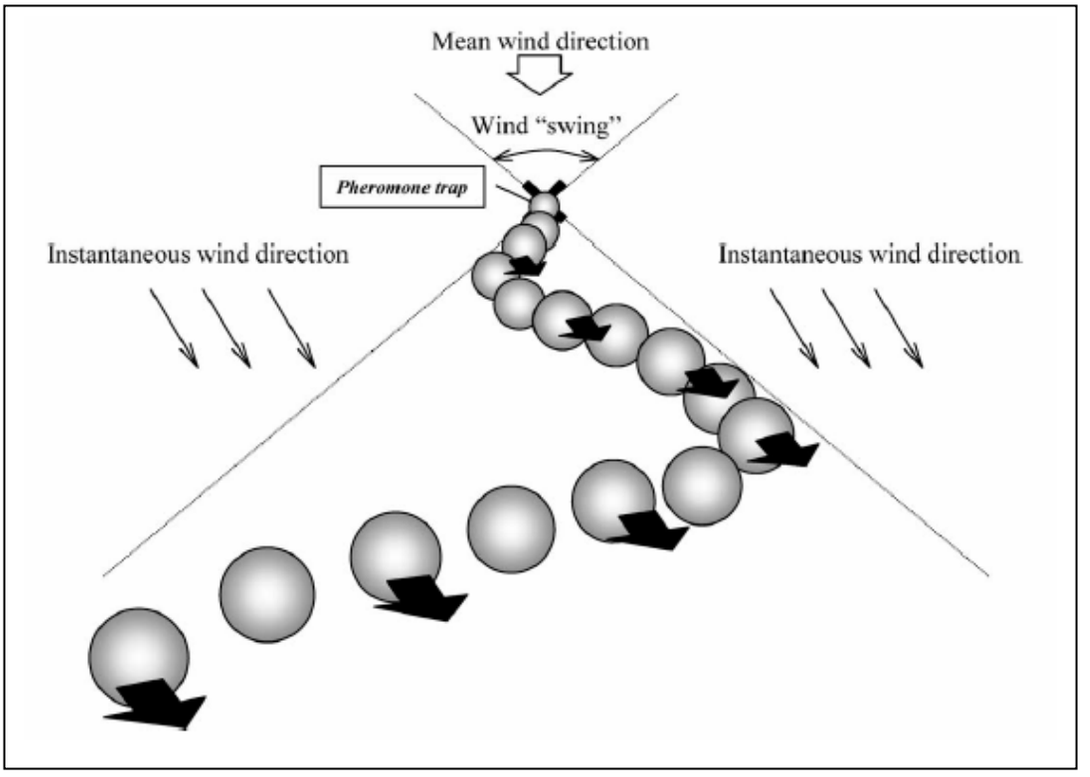

Figure I.7. *Modelled representation of the pheromone puff trajectories (Yamanaka et al., 2003).*

An odour track is not uniform but is a series of variable odour peaks. Indeed, in an open field characterised by a wind speed of 2-4 $m.s^{-1}$ and a relatively stable wind direction, the ion plume is shown to be intermittent, with 80% of clean air at 2.5 m from the source, and around 90% at 20 m (Murlis *et al.*, 2000). Thus, at the medium scale, variation in pheromone plume shape is primarily characterised by increasing space between filaments of pheromone as the distance increases from a continuous source.

The pheromone plume shape at the medium scale could vary with insect calling (pheromone emission) behaviour, wind direction and speed. Conner *et al.* (1985) report that during calling in a temperature of about 25°C and zero wind speed, different Arctiid moths extrude their sex pheromone gland rhythmically, from about 68 $extrusions.min^{-1}$ to 170 $extrusions.min^{-1}$ depending on the species. The highest rates are seen in species calling at dusk, when the wind speed is generally high, while the lowest rates are seen in species calling at dawn, when the wind speed is generally low (Conner *et al.*, 1985). The resulting plume structure should be a typical succession of pheromone tracks separated by clean air gaps. For different wind speeds, adjustment of pheromone release rate could maintain the distance between each pheromone track in a range compatible with male behaviour (Dusenbery, 1989b).

An increase in wind speed does not generally produce longer plumes, but instead more turbulent ones (Dusenbery, 1989a). In laboratory studies, pheromone plumes may be generated artificially by pulses with variable duration and frequency. High frequency pulses make turbulent plumes, while low frequency pulses make continuous plumes (Mafra-Neto & Cardé, 1994). Mafra-Neto & Carde (1994) in a study of *Cadra cautella* in wind speed of 0.45 $m.s^{-1}$ over a study range of 1 m, that the angle between the insect course and wind direction is 40.4° ± 14.04° when the pheromone plume is created at 5 $pulses.s^{-1}$, but is 73.9° ± 7.19° at 0.6 $pulses.s^{-1}$. In a wind speed of 0.6 $m.s^{-1}$, insect tracks are tortuous with a bimodal distribution around -90° and +90° of the angle between the insect course and wind direction when filament frequency is about $4.s^{-1}$ (Vickers & Baker, 1994). A unimodal distribution around 0° and straight upwind tracks are observed when filament frequency is about $10.s^{-1}$ (Vickers & Baker, 1994).

According to Vickers & Baker (1994) who studied *Heliothis virescens* over a study range of ~3.5 m in a wind speed of 0.6 $m.s^{-1}$, when frequencies are 1 and 2 $pulses.s^{-1}$, insects aren't stimulated to fly upwind in the pheromone plume. As shown in these studies, insect behaviour varies with the turbulence of the plume such that the more frequently pheromone is released, and the more turbulent the plume, the more direct the insect flight to the source of pheromone.

Changes in the wind direction, *i.e.* the wind swing, can also induce variations in the orientation of pheromone filaments. At about 25m from a pheromone source, with a wind blowing between 0.1 $m.s^{-1}$ and 2.7 $m.s^{-1}$, 77% of smoke tracks have an angular deviation of 0-5° from the source and 94% of smoke tracks have a deviation of 0-10° from the source (David *et al.*, 1982). In this experiment a wind swing up to an amplitude of 225 degrees was used (Figure I.8). Unfortunately information about the variance of the wind direction is not available from this publication.

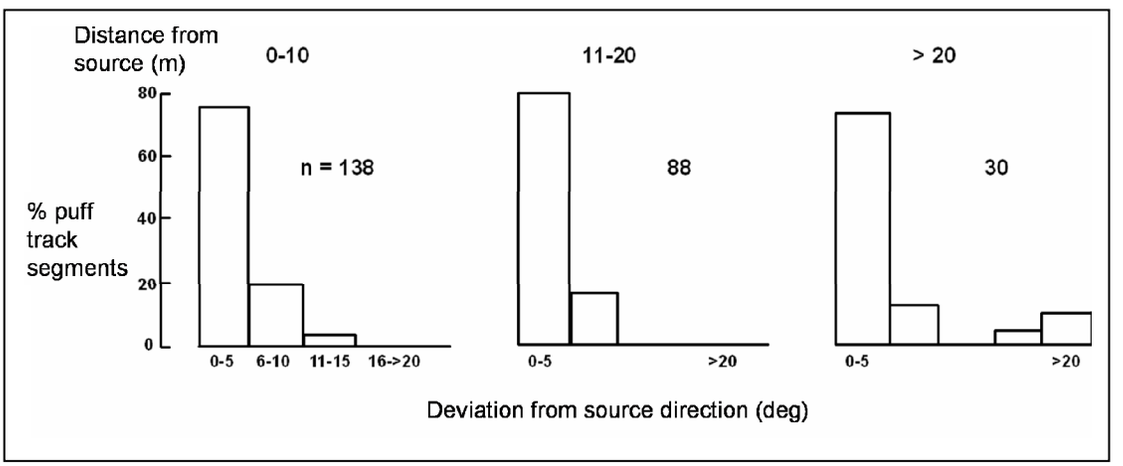

Figure I.8. *Frequency distribution of angles between pheromone filaments and a line from the source to the midpoint of the filament (adapted from David et al., 1982).*

In another field experiment, Elkinton *et al.* (1987) demonstrated that 30 s and 60 s after release, the smoke puff direction was significantly and highly correlated with instantaneous wind direction at source rather than with initial puff direction. Differences between wind direction taken at the release point and smoke puff direction at 5 m and 20 m at the same time were on average 20° to 35° respectively (Elkinton *et al.*, 1987).

Some studies have investigated the structure of the pheromone plume at a finer scale, in other words at the molecular level of the pheromone filament. Inside the pheromone plume, the quantity and the concentration of odour in each odour track is variable, unsurprisingly the odour is most concentrated near the source (Murlis & Jones, 1981). Even at the finer scale, each filament is characterised by variable amounts of pheromone which induce different antennal responses. With an electroantennogram (EAG) technique, intensity and duration of antennal responses to pheromone stimuli are measured. The responses give an estimate of the signal structure inside different filaments. Baker & Haynes (1989) in their study of *Grapholita molesta*, over a range of 30 m with a pheromone concentration of 1000 µg and wind speed of 1.27-1.55 $m.s^{-1}$ showed electroantennogram peak amplitudes increase as the insect approaches the source of pheromone while the electroantennogram peak frequencies are relatively constant with the distance. When they increased wind speed from 0.1 to 1 $m.s^{-1}$ and also when they increased air speed from 0.3 to 0.8 $m.s^{-1}$, wind speed and air speed did not significantly influence electroantennogram peak amplitudes whereas it tended to increase the electroantennogram peak frequencies. Baker & Haynes (1989) suggest that for *Grapholita molesta* male, behavioural response in upwind flight is more correlated to electroantennogram peak amplitudes than electroantennogram peak frequencies. However, other studies such as that by Murlis *et al.* (2000) on gypsy moth found that no relation could be shown between electroantennogram response and ion signals and concluded that Gypsy moth does not respond to the fine scale structure of the plume. On the other hand, high concentration odour could be the stimulus that switches flying behaviour to landing behaviour, the latter relying mainly on visual cues (Murlis & Jones, 1981), the specifics of which depend on the species.

The foregoing information were used to design a model of the behaviour of pheromone plumes in different meteorological conditions and the behavioural responses of the target insects.

I.3.4 The flight track and flight strategies

Insects use three main methods to disperse, 1) passive dispersal where they are blown by the wind, 2) active flight where they may fly across the wind direction, or 3) active flight mainly upwind.

Many insects can actively utilise some meteorological systems, such as inversion layers depressions and different layers of air to disperse. There is a boundary layer of air near the earth surface where some friction from such things as vegetation, buildings and topography slows wind (Johnson, 1969). Similarly, the boundary layer for an insect is the layer of air near the earth surface "in which air movement is less than flight speed or within which the insect's sensory mechanisms and behaviour permit active orientation to the ground" (Johnson, 1969). Clearly, the insect boundary layer is always less than the meteorological boundary layer of air.

Gradient winds blow above the boundary layer of air and are stronger than the winds in the boundary layer. Some insects fly above the boundary layer to be transported by the stronger winds over large distances (Johnson, 1963). Above the boundary layer, insects can control orientation which will affect their track but they cannot control their track (Johnson, 1969). Johnson (1969) comments that insects seem to migrate downwind in the upper atmosphere layers where they are blown by strong winds whereas they migrate upwind, crosswind or downwind, depending on wind speed in the boundary layer.

Insects can also use the inversion layer or general meteorological systems like depressions for dispersal and migration. Moth migration in general begins in the late evening when insects climb from the cold layer of air near the ground into the warmer inversion layer flying first at a height of 7-8 m, then at 50-75 m around midnight when the inversion layer has increased in height (Johnson, 1969). Johnson (1969) reported that some Lepidoptera species can fly from a few meters to many kilometres, for example up to 400 km for *Pectinophora gossypiella*. Some species fly at different altitudes that could range from 60 to 600 m and at a maximum ground speed of 6-7 $m.s^{-1}$ in the case of *Loxostege sticticalis*.

According to Johnson (1969) migration can also begin with the arrival of a depression such that take off occurs in the warm sector of the depression and landing occurs in the tail. In a depression in the South hemisphere, the wind blows clockwise and the track is more or less circular. Insect speed induced by wing beating is clearly negligible in comparison to the wind speed within a depression that can range from 11 to 27 $m.s^{-1}$ or to the overall depression speed such that insects can migrate over large distances using a general meteorological system. For example, Johnson (1969) suggests insects can migrate 1400-3200 km over 3-5 days at high altitudes at about 300-1500 m. Migrations of Lepidoptera from Australia to New Zealand often follow a period of strong westerly or north-westerly winds, which may be associated with a depression (Fox, 1978). Fox (1978) and Hoare (2001) record many different species of butterflies and moths that have flown across the Tasman Sea.

A well studied flying behaviour is the one induced by the pheromone plume. Insects flying in a pheromone plume show two different flight behaviours, 1) rapid straight flight in pheromone filament and, 2) zigzagging around filaments (Figure I.9).

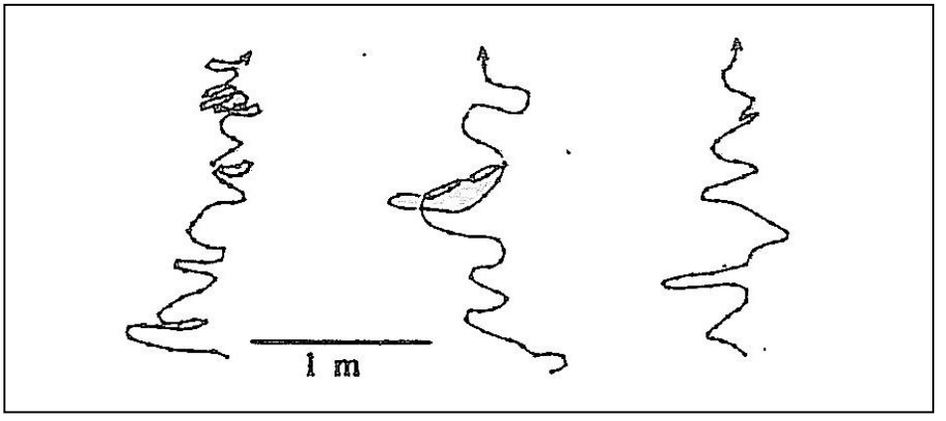

Figure I.9. *Upwind flight path of Lymantria dispar males at a distance of 2.5 m from a source of female sex pheromone. The wind is blowing from top to bottom (Willis et al., 1991).*

David *et al.* (1983) studied gypsy moth behaviour and showed that in a 400 m² zone, inside the pheromone plume, 56% of insect tracks have an angular variation of 0-15° from the wind and 21% of insect tracks have a variation of 76-105°. Inside the pheromone plume, the particular filament structure formed by the succession of filaments separated by gaps of clean air, plays an important role in the specific insect behaviour of alternating zigzagging (also called casting) as well as upwind flight.

Kennedy *et al.* (1980) showed in a study of *Adoxophyes orana* in an air flow of 0.24 $m.s^{-1}$ and a study range up to 1.9 m, a lack of response on re-entering a homogeneous pheromone cloud. Kennedy *et al.* (1980) showed that when the insects spend less than 2 s out of the pheromone cloud, they don't fly upwind. When more than 2 s are spent in clean air, the authors showed that about 35% of flying behaviour is an upwind flight re-entering the pheromone cloud. Vickers & Baker (1994) in a study of *Heliothis virescens* in a study range up to 3.5 m, and wind speed of 0.6 $m.s^{-1}$ showed when a male of this species leaves a pheromone filament, it takes 0.27 s ± 0.1 s before it begins to zigzag and when it encounters a new pheromone filament there is a latency time of 0.30 s ± 0.16 s before an upwind course that lasts 0.38 s ± 0.12 s.

Murlis *et al.* (1992) point out that while behaviour inside the pheromone plume is well described in the literature, only a few examples are available that describe flying behaviour of insects before contact with the pheromone plume. This knowledge gap is compensated for by theoretical studies but required some additional experiments in the present research. Retinal velocity can explain part of the flying behaviour in strong wind conditions but we need to model insect behaviour outside of a pheromone plume. Some authors use random behaviour to simulate the flying behaviour outside the pheromone plume (Yamanaka *et al.*, 2003). David *et al.* (1983) report crosswind behaviour but do not give precise quantification. They simply state that, in a 400 m^2 zone, outside the pheromone plume, gypsy moth tracks are mainly oriented at 76-105° from the wind.

Theoretically, the behaviour outside the pheromone plume is guided by searching for an odour plume. The optimal strategy to find an odour plume would be to maximise the searched volume (S) per time unit (t). The searched volume corresponds to the apparent active space (σ) that is the cross sectional area of the plume perpendicular to insect movement multiplied by the ground speed (v_g): $S/t = \sigma.v_g$ (Dusenbery, 1989a). Apparent active space is a function of the direction (θ) chosen by the insect, measured from the downwind direction that depends on the shape of the plume (Dusenbery, 1989a). A prolate ellipsoid (semi-axes a, b and c with $a > (b = c)$) has an apparent active space of $\sigma(\theta) = \pi.c(a^2.\sin^2(\theta) + b^2.\cos^2(\theta))^{1/2}$ as illustrated in Figure I.10 (Dusenbery, 1989a).

Ground speed is dependent on wind speed (v_w), air speed (v_a) and the angle between insect direction and wind direction (θ): $v_g = (v_w^2 + v_a^2 + 2v_w v_a.\cos(\theta))^{1/2}$ (Dusenbery, 1989a). For example, based on an ellipsoid plume of 1 m^3 where a/b = 10, with wind speed of 1 $m.s^{-1}$ and air speed of 1 $m.s^{-1}$, the optimal flying angle to find the plume is 89° (Figure I.10). In other words the effective course is oriented 44° from downwind (Dusenbery, 1989a).

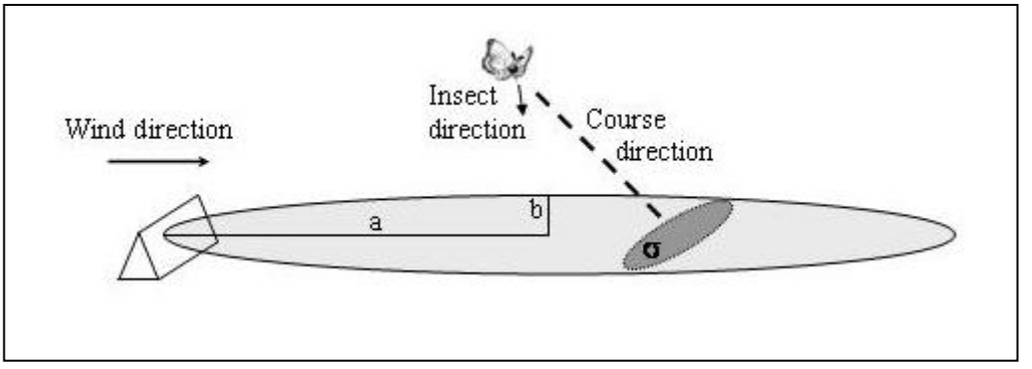

Figure I.10. *Schematic representation of the Dusenbery (1989a) model. The optimal strategy to find an odour plume depends on wind direction, insect direction and on the resulting apparent active space (σ). a, major semi-axis is perpendicular to semi-axis b; semi-axes a and b are perpendicular to semi-axis c (not represented).*

Other authors have used the same approach but consider also the variation of the wind direction. The strategy to find an odour plume under conditions of variation in wind direction, involves integrating the inspected area, or the area in which an animal has odour information when it moves. This so-called anemotactic strategy is optimal when the inspected area is maximised (Sabelis & Schippers, 1984; Hardie *et al.*, 2001). The values of the inspected area (I) are given by the equations in Table I.3.

Table I.3. *Values of inspected area (I) calculated for different levels in variation of wind direction and different direction of searching movement (Sabelis & Schippers, 1984). α: half of the variation of wind direction; β: travelled direction (e.g. upwind movement 90°≤ β_1≤180°) and β = 180- β_1; I: inspected area; r: maximal distance of detection; p: distance travelled.*

α	**β**		**I, r, p**
$0° \leq \alpha \leq 90°$	$\beta \leq \alpha$	$\beta \leq 90° - \alpha$	$I = r.p.[\sin(\alpha + \beta) + \sin(\alpha - \beta)]$
$0° \leq \alpha \leq 90°$	$\beta \leq \alpha$	$\beta \geq 90° - \alpha$	$I = r.p.[1 + \sin(\alpha - \beta)]$
$0° \leq \alpha \leq 90°$	$\beta \geq \alpha$	$\beta \leq 90° - \alpha$	$I = r.p.\sin(\alpha + \beta)$
$0° \leq \alpha \leq 90°$	$\beta \geq \alpha$	$\beta \geq 90° - \alpha$	$I = r.p$
$90° \leq \alpha \leq 180°$	$\beta \leq \alpha - 90°$		$I = 2r.p$
$90° \leq \alpha \leq 180°$	$\beta \geq 90° - \alpha$		$I = r.p.[1 + \sin(\alpha - \beta)]$

To maximise the inspected area, the movement should be across the wind when the wind direction varies up to 30° from the mean direction and upwind or downwind when the wind direction varies more than 30° from the mean direction (Sabelis & Schippers, 1984). Based on the same assumptions as used by (Sabelis & Schippers, 1984), Dusenbery (1990) demonstrates for wind variation higher than 30° from the mean wind direction, that the upwind movement is more strategic than downwind movement for searches of total path length. This applies not only in search to reach the plume but to reach the odour source.

However the theories presented here assume that an insect can estimate the mean wind direction (Murlis *et al.*, 1992). The model used by Sabelis and Schippers (1984) also assumes that movement is slow compared to plume swinging and that the cost of movement is equivalent in any direction. Unfortunately, as Dusenbery (1990) points out these assumptions do not generally apply to flying animals. Some authors openly disagree with any hypothesis of searching behaviour. For example, Hardie *et al.* (2001) suggest that insects don't actively search or "find" resources; they encounter them and respond to those resources as stimuli. When insects are not disrupted by stimuli they continue to fly until they randomly encounter an odour plume. Hardie *et al.* (2001) showed that for some insects flight paths are quite simple. For example, *Drosophila* fly across the wind in stable wind and parallel to the mean wind direction in variable wind, whereas tsetse flies generally fly downwind in the field.

I.4 Research objectives

The information detailed in the foregoing sections will be utilized to build a stochastic mechanistic model of the dispersal of a flying insect. This model is intended to provide probabilistic predictions of the source of an invasive insect intercepted in a pheromone sentinel trap with a view to targeting the search for the proximal source of an incursion more efficiently.

In the following chapters the key elements of this study are presented:

Pheromone anemotaxis theory has been developed by several studies since first proposed by Kennedy (1939) to explain insect behaviour in response to pheromone elicitation. This theory is based mainly on wind tunnel experiments and describes fine scale variations in insect behaviour. In Chapter II, the pheromone anemotaxis theory was up-scaled from fine scaled published observations to a coarser operational scale.

Anemotaxis describes insect behaviour in the pheromone plume. Prior to any contact with the pheromone, *Appetitive* behaviour (Elkinton & Cardé, 1983) has been reported as random (Elkinton & Cardé, 1983), downwind (Riley *et al.*, 1998; Reynolds *et al.*, 2007) or crosswind (Reynolds *et al.*, 2007) behaviour. In Chapter III, data from a previous mark-release-recapture experiment were re-analyzed to determine elements of dispersion in relation to the wind.

Having identified dispersal components of a moth flying towards a trap, initial modelling trials revealed the need for a specific fitness function to fit model results to insect recapture patterns. Pattens are typically represented by a right skewed frequency distribution of recaptures in relation to distance between the trap and release location. Cohen's kappa statistic (Cohen, 1960) captures the qualitative pattern, and the sum of square difference the quantitative pattern, however the later is highly influenced by traps with the highest recapture rates. In Chapter IV, a fitness function was developed to incorporate density and spatial patterns into a single goodness of fit estimate incorporating also the stochasticity involved in trap recapture.

In Chapter V, the results obtained in the previous three chapters were combined and an individual-based semi-mechanistic model to hindcast the area of origin of an insect detected in a pheromone trap was developed and validated using a previous mark-release-recapture experiment. The limitations of the model were assessed, and the performance of the model in relation to biosecurity practices was compared with a simple point diffusion search.

CHAPTER II

Upscaling moth movement patterns

CHAPTER II

Modelling pheromone anemotaxis for biosecurity surveillance. Upscaling moth movement patterns reveals a downwind component

II.1 Abstract

Insect pheromone traps are becoming an increasingly important tool especially in biosecurity and pest surveillance, alerting managers to the presence of unwanted organisms. To expand the role of these traps beyond their present sentinel role, it is necessary to develop reliable operational models of moth dispersal. Following the detection of an insect incursion using a pheromone trap, such models could simulate the dispersal of the moth from its emergence site to the point of detection, enabling biosecurity managers to estimate the most likely proximal source of the incursion. An individual-based moth movement model was developed to simulate observed patterns of moth movement in response to the presence or absence of a pheromone. Using parameters derived from a genetic algorithm, it was possible to fit a model based on the three behavioural components (upwind, upwind with zigzags and casting) described in insect anemotaxis theory to a subset of observed movement patterns (0-135 ° to the wind), but not to the whole spectrum of movement patterns. When insects were also allowed to move downwind, it was possible to explain observed flight patterns over the full range of observations. It appears that current insect anemotaxis theory is missing a downwind flight component. Whilst the frequency of downwind movements is small; their apparent speed could lead to significant downwind displacement, having a disproportionately strong influence on a moth movement model, and hence projections of the likely source or target locations.

Keywords: casting, crosswind, flight behaviour, Lepidoptera, moth, pheromone, upwind, zigzagging

II.2 Introduction

The rate of biological invasions is increasing due to increasing worldwide trade and international travel (after Perrings *et al.*, 2005; McCullough *et al.*, 2006). Biological invasions are also expected to increase in frequency in response to global warming and elevated CO_2 (Logan *et al.*, 2007; Ward & Masters, 2007; Currano *et al.*, 2008). Pest incursions incur significant costs related to detection and monitoring activities, eradication efforts and pest management or control (Pimentel, 2002b; Hosking *et al.*, 2003; Kriticos *et al.*, 2005; Colautti *et al.*, 2006).

Pheromones are chemicals that are emitted by insects as sex attractants. These chemicals can be isolated and synthesised to create highly specific trap lures (El-Sayed & Trimble, 2002). Pheromone traps are used in biosecurity particularly for range delimitation (Kriticos *et al.*, 2007), monitoring (Sharov *et al.*, 1997; Augustin *et al.*, 2004; Cannon *et al.*, 2004), phenology assessment (Suckling *et al.*, 2005b) and management (Sharov *et al.*, 1995; 1998; Kean & Suckling, 2005) of insect invaders. In some jurisdictions, grids of pheromone traps are used permanently at high risk sites to monitor for insect incursions (Stephenson *et al.*, 2003).

The spatial scale of biosecurity surveillance and the response to an incursion ranges from hundreds of meters to hundreds of kilometres (Maynard *et al.*, 2004; Logan *et al.*, 2007; Tobin *et al.*, 2007). When an unwanted insect invader is detected in a pheromone or other trap, it is standard practice to attempt to delimit the range of the incursion, and to discover its source. These range delimitation surveys are typically expensive, involving intensive ground-based surveys of potential habitat within the estimated maximum likely dispersal range of the insects that triggered the incursion response (Carter, 1989). Techniques that could predict the most likely source of the incursion could significantly reduce response costs and possibly more importantly the time taken to delimit the invading population and commence eradication or control efforts. Such tools would need to be based on knowledge of the likely dispersal paths taken by the insect prior to being caught in the trap.

Current understanding of the behaviour of insects in response to pheromone plumes, is based on work by Kennedy (1939). Flight behaviour in response to a pheromone plume known as pheromone anemotaxis theory is now widely accepted as the mechanism used by many flying insects to locate an odour source and to track a mate (Kennedy, 1983; Colvin *et al.*, 1989; Murlis *et al.*, 1992; Fadamiro *et al.*, 1998; Cardé & Willis, 2008). A pheromone plume produced by a calling female is not a cloud of uniform pheromone concentration, but a collection of pheromone filaments separated by gaps of air. Pheromone filaments maintain high concentrations of pheromone for considerable distance downwind (Murlis & Jones, 1981; Mafra-Neto & Cardé, 1994; Murlis *et al.*, 2000). The pheromone anemotaxis theory has three components: 1) direct upwind flight when a pheromone filament is detected, 2) upwind flight with short crosswind movements (zigzags) into the pheromone plume, and 3) casting flight with large crosswind flights outside of the pheromone plume (Kennedy & Marsh, 1974; David *et al.*, 1982; 1983; Kennedy, 1983; Murlis *et al.*, 1992; Baker & Haynes, 1996; Vickers & Baker, 1997; Zanen & Cardé, 1999). These behaviours are believed to represent optimal adaptations to the intermittency of a pheromone signal in an environment where the wind is shifting (Balkovsky & Shraiman, 2002). Many laboratory studies have been conducted to validate the theory, both in wind tunnels (Marsh *et al.*, 1978; Cardé & Hagaman, 1979; Marsh *et al.*, 1981; Kennedy, 1983; Preiss & Kramer, 1986; Willis & Cardé, 1990; Charlton *et al.*, 1993; Kuenen & Cardé, 1994; Cardé & Knols, 2000) and in the field (David *et al.*, 1982; 1983; Elkinton *et al.*, 1987; Willis *et al.*, 1991; 1994).

To improve the efficiency and effectiveness of biosecurity surveillance and pest management we sought to create and parameterise a spatially-explicit individual-based dispersal model for the attraction of individual insects to monitoring traps. However, to parameterise such a model requires more detail than is typically published from wind tunnel and field studies. For example, David *et al.* (1983) presented frequency histograms for tracking the direction of gypsy moth movements in response to pheromone plumes, but did not report the velocity associated with such behaviour. In this study, we use a discrete-time mechanistic dispersal model for insect anemotaxis to recreate the empirical results measured by David *et al.* (1983) in the field.

Our increased understanding of insect anemotaxis may then be used to develop a pheromone tracking model that operates over a large spatial scale and that can be used to make decisions for biosecurity monitoring and surveillance.

II.3 Materials and methods

Our model of insect anemotaxis simulates the movement of an individual moth in two-dimensional space, determined by air speed and flight direction relative to the wind (Figure II.1). The flight direction was expressed as a Gaussian function over the range 0 °-180 ° to the upwind direction. The flight direction relative to the wind ranged between -180° and +180° following the sign of the heading angle (Figure II.1).

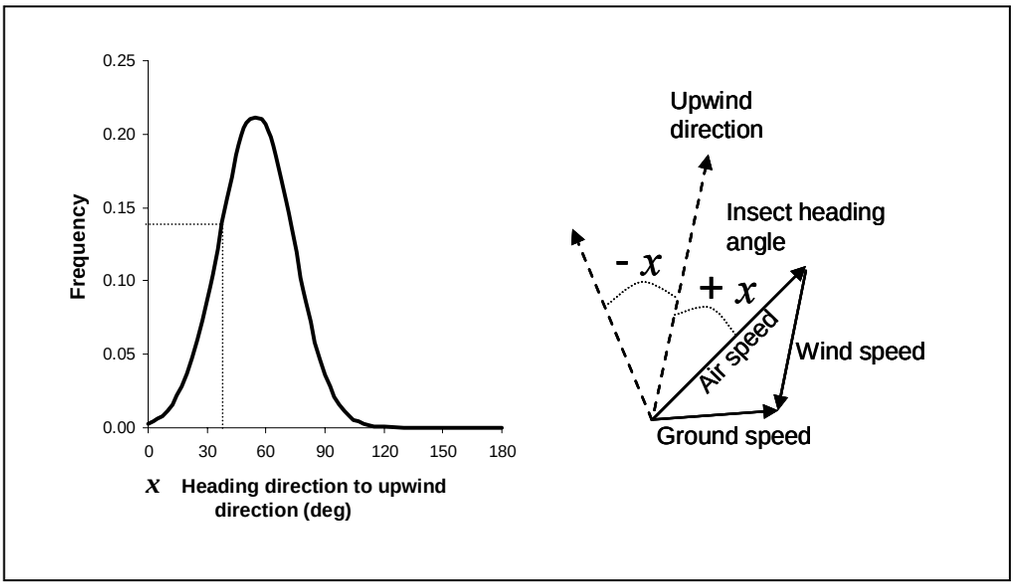

Figure II.1. *Representation of the parameters that control the movement of insects in the simulation. Insect heading angle in relation to the upwind direction follows a Gaussian function; in this example, for x = 38 ° the frequency is 0.14. The sign of the heading angle can be negative or positive: angle - x or + x to the upwind direction. The triangle of velocities (Marsh* et al.*, 1978) denotes the terminology of the speed vectors: air speed, wind speed and ground speed.*

Equation (1) illustrates the flight direction models with x being the heading angle to the upwind direction (in degrees), y the probability of selecting angle x; μ is the position of the centre of the curve's peak, *i.e.* mean angle (in degrees), and σ represents the width of the peak, *i.e.* standard deviation.

$$y = \frac{\exp\left[\frac{-(x-\mu)^2}{2\sigma^2}\right]}{\sigma\sqrt{2\pi}} \qquad (1)$$

Appropriate parameter sets were determined for the three different anemotaxis behaviours: 1) direct upwind travel for upwind behaviour, 2) upwind travel with short crosswind movements for zigzagging behaviour, and 3) large crosswind movements for casting behaviour. The proportion of each behaviour model (upwind, upwind with zigzags and casting behaviour) was set as a parameter to be fitted (see below). The upwind with zigzags comprised the combination of upwind and zigzagging behaviours. Based on the definitions of upwind, zigzagging and casting behaviours, the heading angle to the wind for the upwind behaviour model would be expected to be small whereas for the zigzagging and casting behaviour models the angles were expected to be greater. Table II.1 summarizes the ranges for each parameter for the three behaviour models.

Behaviour model	**Flight direction to wind (deg)**
Upwind flight	μ [0-30]
	σ [5-30]
Zigzagging flight	μ [45-60]
	σ [5-30]
Casting flight	μ [45-90]
	σ [5-50]

Table II.1. *Parameter range of the three behaviour models (upwind, zigzagging and casting flights) used to simulate insect paths in the bounding box. Angles are expressed in degrees.*

A fitted parameter defined the sign of the heading angle (Figure II.1) by the frequency at which the sign is reversed for each behaviour model. This frequency ranged from zero to one, *ie.* no change to a change for every displacement. The air speed for gypsy moths tracking a pheromone source in the field was expected to be in the range 1.5-2.5 ms^{-1} based on studies by Willis *et al.* (1991; 1994). The air speed was uniform for the three behaviour models; its value was fitted in the range [1.5, 2.5].

In the simulations, we used a time step of 0.1 s, as did Charlton *et al.* (1993) for analysing fine scale insect tracks using video recording. The wind (direction and velocity) was considered as a mean wind and assumed to be constant at 1 ms^{-1} for the duration of the simulations. For each time step the displacement of the insect was calculated by applying 1) a randomly chosen heading direction given the behaviour function, 2) the air speed and 3) the wind drift (Figures II.1 and II.2). Firstly, velocities and angles were transformed into vectors following equations in Table II.2.

	$\cos\theta < 0$	$\cos\theta > 0$
$\sin\theta < 0$	$\begin{vmatrix} -\cos(\theta - 270) * v \\ \sin(\theta - 270) * v \end{vmatrix}$	$\begin{vmatrix} \cos(90 - \theta) * v \\ \sin(90 - \theta) * v \end{vmatrix}$
$\sin\theta > 0$	$\begin{vmatrix} -\cos(270 - \theta) * v \\ -\sin(270 - \theta) * v \end{vmatrix}$	$\begin{vmatrix} \cos(\theta - 90) * v \\ -\sin(\theta - 90) * v \end{vmatrix}$

Table II.2. *Equations to convert a vector expressed in polar coordinates (angle, θ and velocity, v) into a vector expressed in rectangular coordinates (x-coordinates and y-coordinates). Angles are given in degrees in the range [0-360°].*

The calculation represented in equation (2) is the vectorial sum of air speed and wind speed vectors; the resulting vector for the displacement is represented as the ground speed vector in Figure II.1.

$$\begin{vmatrix} g_x \\ g_y \end{vmatrix} = \begin{vmatrix} a_x + w_x \\ a_y + w_y \end{vmatrix} \tag{2}$$

with ground speed vector $\begin{vmatrix} g_x \\ g_y \end{vmatrix}$, air speed vector $\begin{vmatrix} a_x \\ a_y \end{vmatrix}$ and wind speed vector $\begin{vmatrix} w_x \\ w_y \end{vmatrix}$.

Ground speed is calculated using equation (3):

$$ground\ speed = \sqrt{g_x^2 + g_y^2} \tag{3}$$

Simulated flight paths were analysed in terms of "track segments", which David *et al.* (1983 p805) defined as 'a portion of flight track … that achieves a net horizontal displacement of two or more metres without deviations in excess of 0.5 m'. To represent the flight track segment, model simulations were terminated whenever the simulated insect left a bounding box of 2 m long and 1 m wide drawn around the flight path. The orientation of the bounding box with respect to the wind direction was then calculated, and simulated flight paths were categorized as 0 °-15 °, 15 °-45 °, 45 °-75 °, 75 °-105 °, 105 °-135 °, or 135 °-180 ° to reproduce the categories used by David *et al.* (1983). Simulations were only included in the frequency distribution of track segments if the simulated flight path fitted within the bounding box, thereby representing a successful track segment. The results from 500 track segments were compared to the corresponding frequencies reported by David *et al.* (1983) from their field study (400 track segments) and the number of track simulations discarded was calculated (Figure II.2).

We used an objective method to fit the parameters of the behaviour models to match the two frequency distributions; the frequencies were paired by category of flight angle and the objective function scores the difference. The best fitting parameters for each flight angle category were those that reproduced the same frequency distribution of successful tracks after re-sampling using the "track segment" definition.

For the first flight angle category (0 °-15 °), David *et al.* (1983) also distinguished nearly straight track segments from track segments showing narrow zigzags with frequencies of 43 and 57% respectively. In addition, we used this information in the objective function to discriminate upwind and upwind with zigzags behaviours.
A genetic algorithm (Beasley *et al.*, 1993) was used to fit the parameters. Inspired by natural selection processes in the evolution of biological organisms, genetic algorithms are fast and efficient methods for fitting parameters (Beasley *et al.*, 1993). They are capable of rapidly narrowing the search for optimal parameters from a series of parameters with wide ranges of starting values, and they don't suffer from getting hung up on local minima in the objective function. Genetic algorithms utilise a "population" of vectors, each containing values for each of the parameters to be fitted.

The genetic algorithm was used to fit the parameters for the two frequency distributions of track segments and it was initialised with the parameter range of the three behaviour models (Table II.1) using an initial population of 500 sets of parameters. The "fitness" of each vector was determined by comparing the model projections with observations from David *et al.* (1983) applying the objective function described previously. The fitness score was used to rank the vectors, and the best were hybridized and used in the next iteration of the algorithm (Figure II.2). By repeating this procedure many times it is possible to select sets of parameter values that produce models with the highest possible fitness. The run was considered to have converged when the most beneficial "genes" had diffused through the population, *i.e.* when the standard deviation of the fitness scores for one generation of different sets of parameters was less than 1 % of the mean fitness score (Figure II.2).

For the best-fitting set of parameters, the average frequency of successful tracks over 100 replicates for each angle category was compared to the frequency distribution of "segment tracks" reported in David *et al.* (1983) using Pearson's chi-square (χ^2) (S-plus 6.1). The scaled-up velocity, the time to transit the bounding box divided by the net displacement, was calculated by using departure and arrival locations and the transit time for the best fitting models.

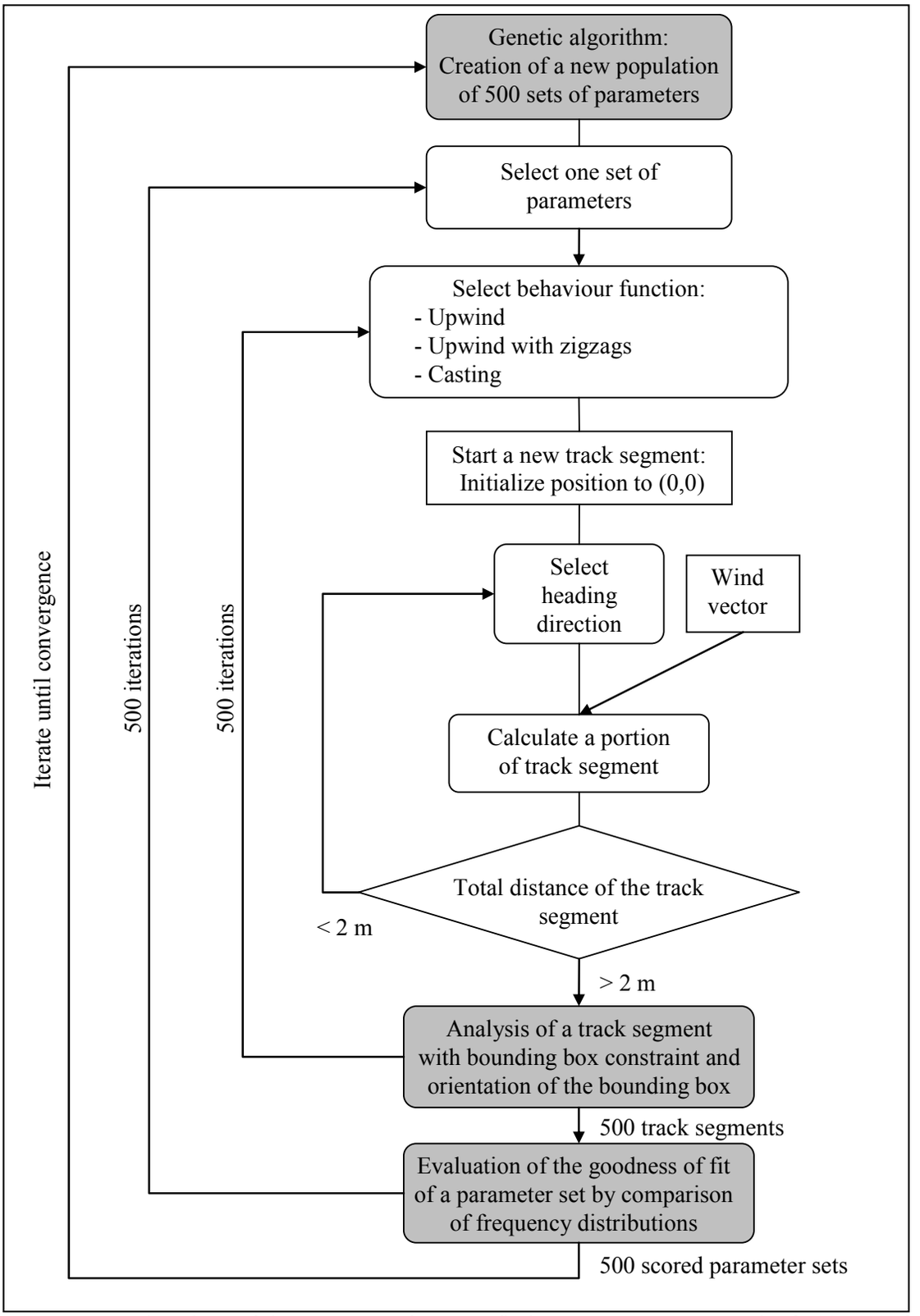

Figure II.2. *Flowchart of the process to fit insect flight parameters. For each of 500 sets of parameters, 500 track segments were generated before evaluating the goodness of fit of each parameter set in comparison with the results of David* et al. *(1983). The genetic algorithm generates new parameter sets from a population of 500 scored sets of parameters.*

II.4 Results

The best fitting model, obtained after the evaluation of 13 488 different sets of parameter combinations, did not reproduce the track segments observed by David *et al.* (1983) for track segments oriented 135 °-180 ° to the wind. Even if some successful track segments were modelled for this range of angles, the parameters of the models were not selected during evolution of the genetic algorithm because the quality of fit for other angle categories was poor.

A second model was fitted excluding the 135 °-180 ° category. The best fitting model was obtained after 60 generations (11 578 different sets of parameters). For the best models obtained here, the successful tracks were not significantly different to the frequency distribution reported by David *et al.* (1983) as illustrated in Figure II.3 (χ^2 = 0.891, df = 4, P = 0.926).

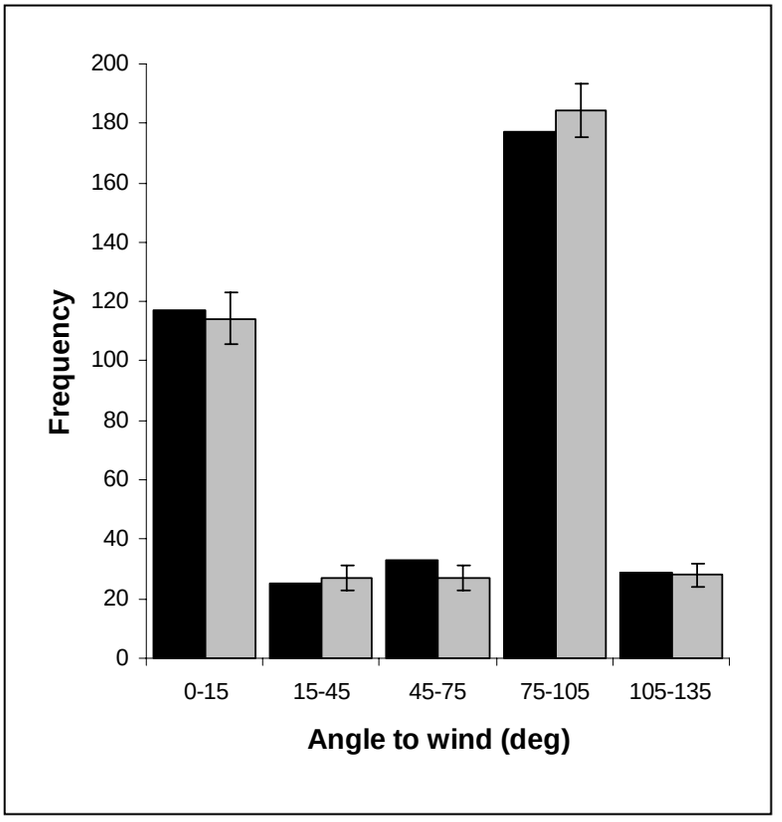

Figure II.3. *Frequency distribution (□) of track segments from David* et al. *(1983) and the frequency distribution (■) of successful tracks from the best fitting model with 5 categories of flight angle (see text for details). Error bars represent the variation in frequency obtained over 100 replicates of the best fitting models.*

A small proportion (0.024%, 12 from 50 000 track segments) of simulated flight paths using the best fitting model failed to traverse the conceptual bounding box from end to end, and so did not qualify as track segments as defined by David *et al.* (1983), and were discarded.

The best performing flight behaviour models are represented in Figure II.4, with the model equations and parameters given in Table II.3.

Table II.3. *Best fitting parameters of the three behaviour models (upwind, zigzagging and casting flights) used to simulate insect paths in the bounding box. The flight direction was expressed in relation to the wind direction by equation (1).*

Behaviour model	**Flight direction to wind (deg)**	**Proportion of each model**
Upwind flight	$\mu = 8.59$ $\sigma = 10.92$	0.14
Zigzagging flight	$\mu = 54.85$ $\sigma = 18.61$	0.23
Casting flight	$\mu = 46.85$ $\sigma = 48.86$	0.63

The upwind, zigzagging and casting flight behaviour models were characterized by flights oriented respectively at mainly 8.6 °, 54.9 ° and 46.8 ° to the wind (Figure II.4). For the best fitted set of parameter, the sign of the heading angle was uniform in the bounding box (frequency of change = 0) to reproduce casting behaviour whereas for upwind and upwind with zigzags behaviours the frequency was 23% and 46%, respectively. The associated velocity for the best fitting parameters was 2.49 ms^{-1}.

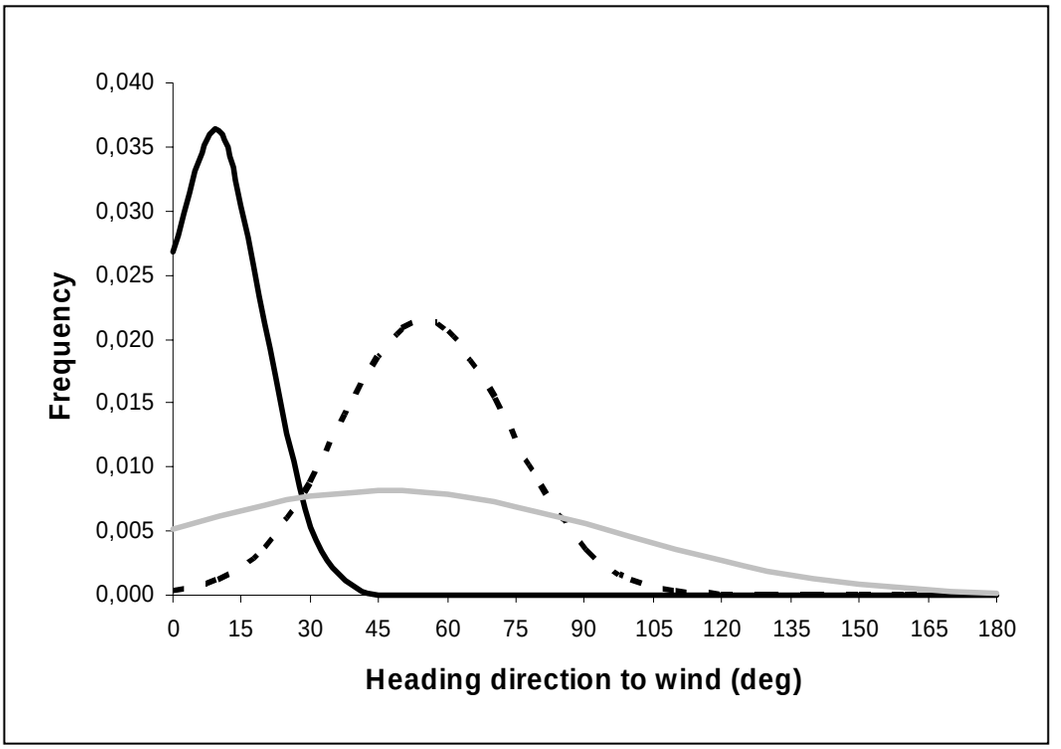

Figure II.4. *Probability density function of insect heading direction for the best fitting model. The three behaviour models: upwind (——), zigzagging (- - -) and casting (——) are described by the heading angle to the wind direction.*

The simulated paths for the best fitting model (Figure II.5) produced flight patterns that closely resemble observed moth flights (Cardé & Hagaman, 1979; David *et al.*, 1983; Willis & Cardé, 1990; Charlton *et al.*, 1993; Kuenen & Cardé, 1994; Willis *et al.*, 1994; Cardé & Knols, 2000).

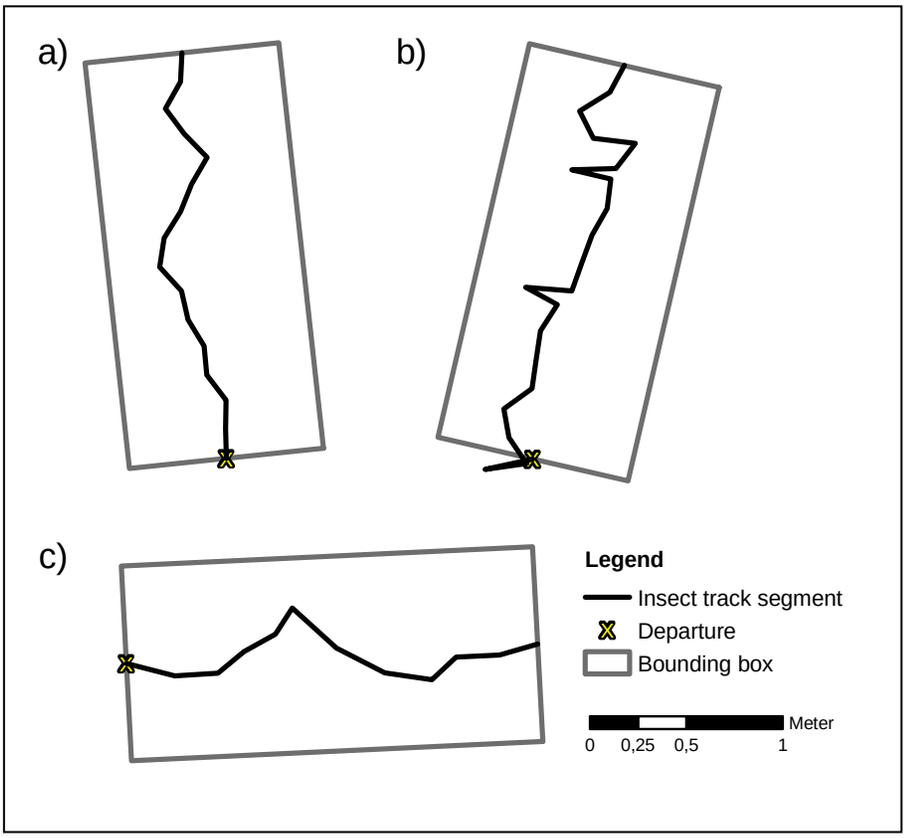

Figure II.5. *Examples of modelled flight tracks using the bounding box for different behaviour models a) upwind model, the "track segment" is oriented 6 ° to the wind; b) upwind with zigzags model, the "track segment" is oriented 13 ° to the wind c) casting model, the "track segment" is oriented 87 ° to the wind. The wind is blowing from top to bottom of the figure.*

The scaled up velocities associated with different insect track directions to the wind are given in Figure II.6. The scaled up velocities range between 1.2 ms^{-1} for a low deviation range from the wind direction and up to 2.05 ms^{-1} for flights with higher deviations from the wind direction (45 °-135 °).

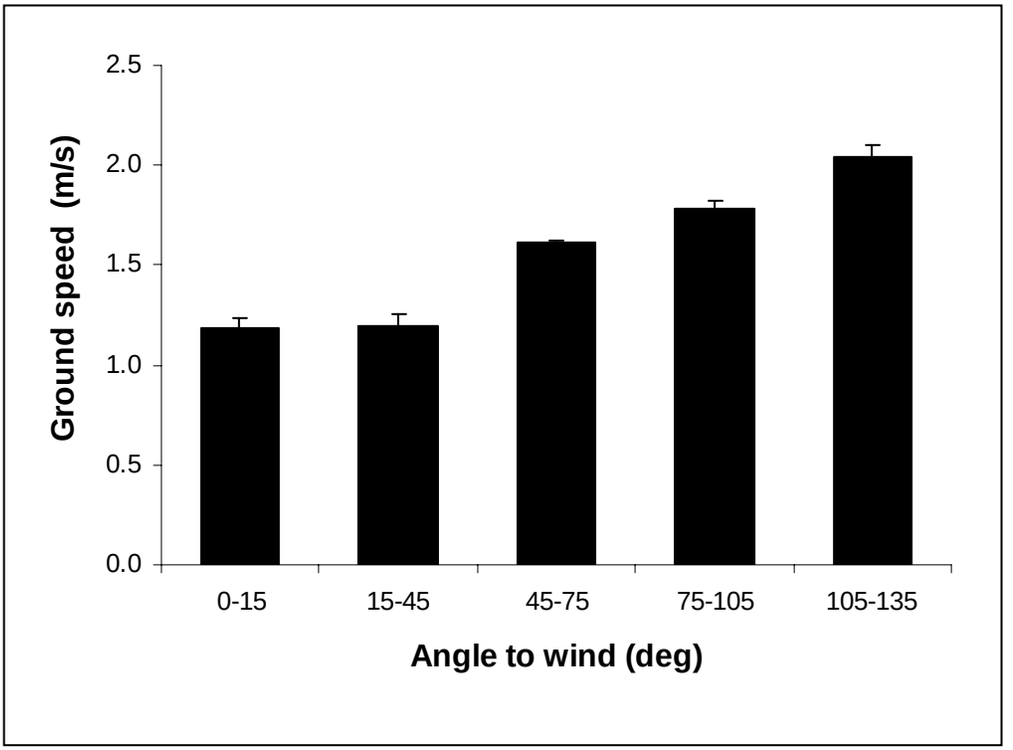

Figure II.6. *Ground speed estimated at the bounding box scale. Each speed is calculated for a straight line of successful track segments to cross the bounding box for the best fitting models. Error bars represent the variation in speed obtained with 100 replicates of the best models.*

II.5 Discussion

Using three simple behaviour models (upwind, upwind with zigzags and casting), we were able to reproduce the flight patterns of gypsy moths observed in the field by David *et al.* (1983) only when the flight angle was constrained to 0 °-135 ° to the wind. Under this constraint, the pheromone anemotaxis theory that guided the choices of these three behaviour models reproduced the flight pattern observed by David *et al.* (1983) extremely well. The bimodal frequency distribution of angles in Figure II.3 reflects the propensity for moths to fly upwind or transverse across the wind during pheromone tracking.

However, these three behaviour models (upwind, upwind with zigzags and casting) were not sufficient to reproduce the observed flight behaviours when angles of 135 °-180 ° to the wind were included. Pheromone anemotaxis theory as reported in the literature is missing a downwind component.

The fact that the three behaviour models could not account for observed flight behaviours for the 135 °-180 ° category could be explained by the fact that wind velocity was assumed to be constant in our model, whereas gusts of wind occur in the field, that could induce the downwind displacement evident in the field results of David *et al.* (1983). However, previous studies suggest that moths do not get blown downwind as wind speed increases, but rather, compensate for wind speed by increasing their air speed (Kuenen & Baker, 1982; Mafra-Neto & Cardé, 1998). Another explanation for the observed result is to consider that pheromone anemotaxis theory describes a net upwind behaviour that insects use to track a pheromone scent. The downwind net displacement as described by moth track segments oriented 135 °-180 ° to the wind could be the result of another behaviour. Indeed, a net downwind behaviour has been sporadically reported in other studies (Willis & Arbas, 1991; Baker & Haynes, 1996; Riley *et al.*, 1998) and attributed to a seeking behaviour either to find a pheromone plume (Riley *et al.*, 1998) or to recover the loss of the pheromone plume (Willis & Arbas, 1991; Baker & Haynes, 1996).

Even if downwind behaviour occurs only on few occasions, it clearly should be incorporated in future modelling when more realistic models are required (Worner, 1991). For example, in biosecurity settings, it is necessary to include such behaviours in order to infer the proximal source of a trapped pest, and subsequently the remainder of its cohort. In particular conditions, however, we would expect a higher proportion of downwind flight. First, if downwind behaviour is a mechanism to recover a lost pheromone plume, specific conditions such as high wind shift or turbulence (for example in forest habitat) would increase the meandering of the pheromone plume and the probability of the moth losing the scent (Murlis *et al.*, 2000). Second, if the downwind behaviour is an appetitive behaviour occurring prior to the initial detection of a pheromone filament, insect tracking models may have to be separated into sub models, one for behaviour prior to the first encounter of the pheromone and another for, when pheromone anemotaxis has been elicited.

For operational insect dispersal models for biosecurity monitoring and pest management, simulating the downwind behaviour is crucial to identify the potential source of trap catches, and subsequently the delimitation of the invading population.

If the model excludes the possibility of downwind behaviour, and this is a feature of the behaviour of the insect being modelled, the model may be incapable of correctly indicating the correct source location of the trapped insect, making it useless for biosecurity, and probably most other applications.

The differences between the scaled-up velocities for the different deviations to the wind are explained by the nature of the behaviour. For upwind flight, with deviation range from 0 ° to 45 ° to the wind, the low net ground speed (Figure II.6) is directly attributed to the impact of wind drift during upwind flights plus a short crosswind movement due to zigzag upwind flight (Figure II.5b). The increase of the net ground speed for deviations above 45 ° to the wind (Figure II.6) can be attributed to a reduction of wind drift. The scaled-up velocity (Figure II.6) and the frequency distribution reported by David *et al.* (1983) comprise the basis for pheromone track modelling based on insect behaviour at a 2 m scale, explicitly discarding fine-scale movements. By the use of the "track segment" definition, David *et al.* (1983) explicitly discarded detailed insect behaviour, in other words, side deviations smaller than 0.5 m to the track.

This study provides the foundation for the development of a detailed pheromone tracking model at the scale of several meters, similar to the smallest scales for biosecurity and pest management applications. This study suggests that current theory needs to be modified to include a downwind component in pheromone tracking behaviour of insects. Further studies are needed to better understand the frequency of this downwind behaviour among individuals and species, and whether it is a behaviour that can occur anytime during dispersal, or whether it is only displayed at certain times, for example, prior to the insect experiencing pheromone stimulation.

II.6 Acknowledgements

We would like to thank A. Leriche and M. Borgas for helpful comments on the paper. This work was funded by the New Zealand Foundation for Research, Science & Technology through contract C02X0501 and the Better Border Biosecurity (B3) programme (www.b3nz.org)

CHAPTER III

Experimental evidence of downwind dispersal

CHAPTER III

Evidence of active or passive downwind dispersal in mark-release-recapture of moths

III.1 Abstract

Modelling moth dispersal in relation to wind direction and strength could greatly enhance the role of pheromone traps in biosecurity and pest management applications. Anemotaxis theory that describes moth behaviour in the presence of a pheromone plume is used as a framework for such models. Currently, however, that theory includes only three components: upwind, zigzagging, and sideways casting behaviour. We test anemotaxis theory by analysing the data from a series of mark-release-recapture experiments where the wind direction was known and the insects were trapped using an irregular grid of pheromone traps. The trapping results provide evidence of a downwind component to the flight patterns of the released insects. This active or passive downwind dispersal is likely to be an appetitive behaviour, occurring prior to the elicitation of pheromone-oriented flight patterns (pheromone anemotaxis). Given the potential for significant displacement during downwind dispersal, this component will have impact on final trap captures and should be considered when constructing moth dispersal models.

Keywords: anemotaxis, appetitive behaviour, biosecurity, Lepidoptera, Lymantriidae, pheromone, *Teia anartoides*

III.2 Introduction

Pheromone baited traps are used widely for biosecurity surveillance to detect new incursions of unwanted organisms, and to delimit their ranges (Augustin *et al.*, 2004; Suckling *et al.*, 2005a,b; Bogich *et al.*, 2008; Liebhold & Tobin, 2008). They have been used for several decades in pest management for monitoring to alert land managers to the presence of a pest in time and space, providing insight into phenology as well as geographic distribution (Suckling *et al.*, 2005b). Pheromone traps have also been used to delimit populations for pest risk modelling (Kriticos *et al.*, 2007). When deployment of a surveillance grid of traps is warranted to monitor for biological invasions, the detection of an unwanted organism typically triggers a delimitation survey to identify the proximal source of the incursion, the extent of the incursion population, the feasibility of eradication, and possibly the pathway by which the organism entered the jurisdiction (Canadian Food Inspection Agency, 2007). As such surveys are resource intensive, new technologies are needed to target them better. If the flight path or even direction of an insect from the proximal source of the invasive population to the pheromone trap could be inferred with some reliability, then on-ground delimitation surveys can be prioritised to those areas most likely to include the source location from which the trapped individual originated, and the most likely location of the remainder of its cohort.

Modelling the flight paths of individual insects from point of origin to trapping point requires knowledge of their anemotaxis (any purposeful behaviour that is oriented in relation to the wind direction). Odour-mediated anemotaxis is the mechanism that insects employ to locate an odour source such as a female emitting a pheromone (Kennedy & Marsh, 1974; David *et al.*, 1983; Kennedy, 1983; Vickers, 2000; Cardé & Willis, 2008). Within a pheromone plume, insects experience the fine structure of pheromone intermittency with pheromone filaments separated by gaps of clean air (Murlis & Jones, 1981; Baker & Haynes, 1989; Mafra-Neto & Cardé, 1994; Riffell *et al.*, 2008). The response of the insect as it alternately senses the pheromone or clean air at millisecond frequencies is the so-called "pheromone anemotaxis behaviour", which results in a net upwind displacement that ultimately guides flying insects to an odour source.

When a filament of pheromone is detected, the insect flies upwind, but as the pheromone filament is lost, the insect begins to fly in a zigzag pattern to locate another pheromone filament from the same plume (Kennedy *et al.*, 1980; Vickers & Baker, 1996; Zanen & Cardé, 1999). When the insect exits from the pheromone plume, large crosswind movements are observed (Baker & Haynes, 1987; Kuenen & Cardé, 1994; Mafra-Neto & Cardé, 1998). Presumably this behaviour is triggered or promoted by a long time period without encountering a pheromone filament. This behaviour was originally demonstrated with moths but it has also been observed for various other insect taxa such as some beetles (Fadamiro *et al.*, 1998; Kuenen & Rowe, 2006; Williams *et al.*, 2007).

Pheromone anemotaxis theory focuses on insect behaviour within the pheromone plume, and is mainly based on wind tunnel studies. Behaviour at a broader scale than within the odour plume is not so well understood. Several authors have suggested that the optimal strategy to locate a pheromone source depends, unsurprisingly, on the wind conditions. Dusenbery (1989a) suggests that in a steady wind, the most effective flight course is oriented around 45º from downwind, whereas with a wind shifting up to 30º from the mean direction, the most effective strategy is crosswind flight (Sabelis & Schippers, 1984). For winds that shift over a wider range, Sabelis & Schippers (1984) suggested a search strategy parallel to the wind but Dusenbery (1990) used a more complete analysis to conclude that the optimal strategy is upwind flight rather than downwind. Reynolds *et al.* (2007) confirmed these studies in an analysis accounting for a more realistic plume shape: downwind flights were preferable than crosswind when the width of the plume was greater than its length, when for example the plume was meandering due to a shifting wind. Reynolds *et al.* (2007) demonstrated that a biased Lévy flight searching strategy, optimal with a scaling exponent between 1 and 2, was consistent with their observations.

In contrast to the number of studies of insect behaviour within a pheromone plume (Murlis *et al.*, 1992; Cardé & Willis, 2008), few experimental studies have investigated "appetitive" insect behaviour, defined by Elkinton & Cardé (1983) as the behaviour before any contact with the pheromone. Those few studies include field experiments by Elkinton & Cardé (1983), who reported a random behaviour for the appetitive flight of gypsy moth, and Riley *et al.* (1998), who reported occasional

appetitive downwind flights in *Agrotis segetum* (Denis & Schiffermüller) moths. Monitoring flight patterns with harmonic radar, Reynolds *et al.* (2007) demonstrated a trend of crosswind or downwind movements at the departure location before anemotaxis behaviour commenced following an initial encounter with the pheromone.

We believe that describing insect behaviour before any contact with a pheromone, as well as the behaviour within the pheromone plume are key elements required to identify the source location of insects caught in pheromone traps. In the present study, we re-analysed data from a study by Suckling *et al.* (2005a) on mark-release-recapture of sterile painted apple moths, *Teia anartoides* (Walker) (Lepidoptera: Lymantriidae), together with generalised wind field. Moth flight was related to wind speed and direction to determine elements of dispersal in relation to the wind.

Teia anartoides is an Australian native lymantriid (Common, 1990) that became established in Auckland, New Zealand, in the 1990s (Hoare, 2001). Larvae are polyphagous and can affect the growth of plants of importance to horticulture and forestry such as pine trees but can also feed on New Zealand indigenous trees. The estimated cost of *T. anartoides* establishment in New Zealand ranged from NZD 58 to 356 million over 20 years due to its wide host range (Self, 2003). An eradication program against *T. anartoides* was undertaken from 1999 to 2006, and it was declared successfully eradicated in 2006 on the basis of a trapping model using sterile males (Kean & Suckling, 2005; Suckling *et al.*, 2007). The eradication including health monitoring, communication and the operation was budgeted at an estimated NZD 100 million (Turner *et al.*, 2004), which was later revised to closer to NZD 62.4 million actually spent (Ministry of Agriculture and Forestry, 2006b). In this study, the analysis of moth dispersion in relation to the wind provided elements of discussion on moth strategy to find a mate and therefore on the understanding and interpretation of pheromone trap catches.

III.3 Materials and Methods

III.3.1 Release recapture data

Experiments were conducted in Auckland between February and May 2003 with an average of 1 452 traps to cover the study area (Suckling *et al.*, 2005a). Delta traps baited with virgin female moths were deployed because the main component of the synthetic pheromone is instable (El-Sayed *et al.*, 2005). Adult moths were marked with fluorescent powders coloured differently for each of three release locations [Hobsonville (36º47'35"S, 174º39'12"E), Waikumete Cemetery (36º54'04"S, 174º38'42"E) and Ranui (36º51'59"S, 174º35'52"E), see figure III.1] (Suckling *et al.*, 2005a). The habitat of release and recapture sites varied from urban and suburban type around Auckland to forest, mainly on the Western side of the area.

The data considered in the present study were limited to the period from 19 February 2003 to 31 March 2003 when more than 1% of insects were recaptured but also when insects were released weekly. Low recapture rates in subsequent release periods were likely due to suboptimal conditions immediately following release including temperatures below the threshold for flight (Suckling *et al.*, 2005a). Some releases in subsequent periods were also done twice a week. Painted apple moths survived in the field for approximately 4 days (Suckling *et al.*, 2005a) and so recaptures cannot be clearly distinguished between two releases separated by less than 5 days. During the 6-week duration of the mark-release-recapture experiment, a total of 16 355 moths were released at all locations and 1 481 or 9% of the total were recaptured in female-baited traps (Table III.1). The average number of insects released was 962 males (range: 330 - 1 444) per release location and week (Table III.1).

Table III.1. *Number of painted apple moths released and recaptured at the different locations in Auckland, New Zealand,and release date considered in the present study (from Suckling* et al.*,2005a).*

Location	**Hobsonville**		**Waikumete Cemetery**		**Ranui**	
Period	***Release***	***Recapture***	***Release***	***Recapture***	***Release***	***Recapture***
19-25 February	413	63	434	32	0	0
28 Feb.- 4 March	1128	103	1436	324	330	39
6-10 March	814	81	795	131	892	175
13-20 March	1444	34	1292	101	1440	111
21-25 March	1191	25	1129	59	1036	13
28-31 March	866	19	850	154	865	17

Insects were released around 10:00 hours which corresponded to the beginning of the period of flight activity. Prior to each release, traps were reset with new sticky bases and baited with a fresh virgin female, and each trap was checked at least once per week. Therefore, a recapture recorded on a particular day had occurred between that day and the more recent of the release days or the last day the trap was checked. Parameters affecting female moth performance have been examined elsewhere (Suckling *et al.*, 2006).

III.3.2 Weather data collection and meteorological modelling

Six meteorological stations (Figure III.1) recorded wind direction and speed at 1- or 10-min intervals using a Vector A101M Pulse® output anemometer (Vector Instruments, Rhyl, United Kingdom). One-minute wind direction and speed were averaged over 10 min after transformation of wind polar coordinates into rectangular coordinates (Batschelet, 1981). These meteorological stations also provided relative humidity and temperature measurements for every minute and these data were also averaged over 10 min.

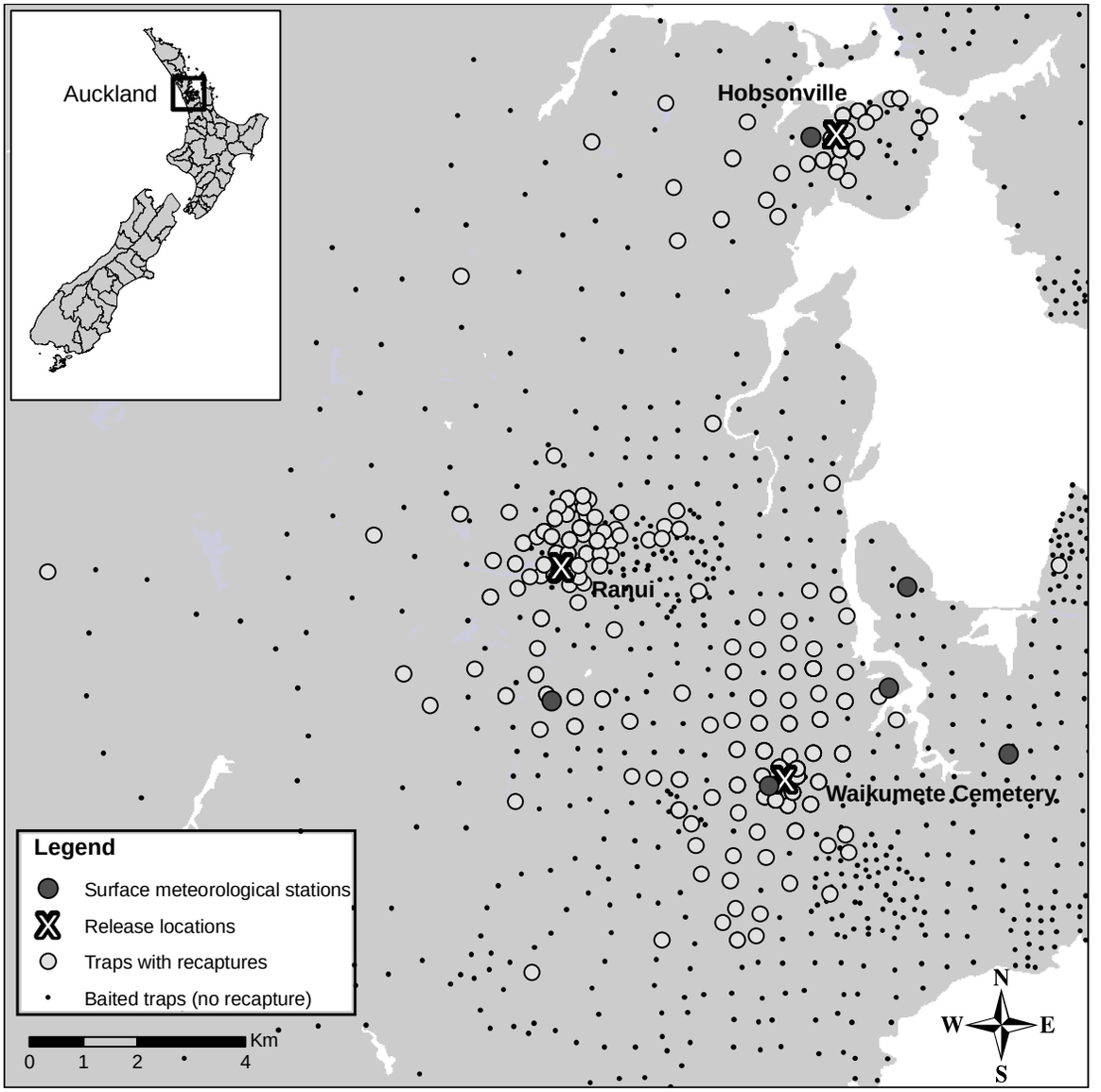

Figure III.1. *Distribution of recaptures around the three release locations in Auckland, New Zealand.*

Atmospheric pressure, cloud cover, and cloud height were extracted from the New Zealand National Climate Database for three nearby meteorological stations (36º59'28"S, 174º52'12"E; 37º00'18"S, 174º47'21"E; and 36º47'34"S, 174º37'26"E). The hourly values for these variables were linearly interpolated to 10-min values. Twice daily, vertical profiles of pressure, elevation, temperature, wind direction, and wind speed for each sounding level were extracted from the New Zealand Climate Database for the nearest upper air meteorological station (36º47'34"S, 174º37'26"E). The wind direction and wind speed data for the duration of each release-recapture period were interpolated onto a 200 × 200 m series of 10-min grids covering the study area using CALMET modelling software (Scire *et al.*, 1998; Wang *et al.*, 2008).

III.3.3 Estimation of mean wind direction

For each release location the mean wind direction was calculated from wind rectangular coordinates at 10-min intervals from 10:00 to 15:00 hours for the day of release, corresponding to the main flight period of painted apple moth (Table III.2).

Table III.2. *Average wind direction and velocity (from 10-min intervals) for the main flying period of painted apple moth (10:00-15:00 hours) at the three release locations in Auckland, New Zealand.*

Location	**Hobsonville**		**Waikumete Cemetery**		**Ranui**	
	Direction	***Velocity***	***Direction***	***Velocity***	***Direction***	***Velocity***
Date	***(°N)***	***(m/s)***	***(°N)***	***(m/s)***	***(°N)***	***(m/s)***
19 February	135	1.24	127	1.79	-	-
28 February	235	3.47	235	5.06	265	4.28
6 March	359	2.44	348	2.67	345	2.22
13 March	28	5.16	64	6.73	38	5.29
21 March	252	2.64	277	3.88	268	3.51
28 March	247	4.28	309	6.89	266	5.62

A transformation was required to convert wind polar coordinates (given by the angle and velocity of the wind) into rectangular coordinates (given by the coordinates of the wind vector) (Batschelet, 1981).

III.3.4 Wind direction and recapture pattern

The influence of wind characteristics during the day of release on the subsequent recapture patterns of the released moths was investigated by comparing recapture distances, after segregating the data by wind direction. A line orthogonal to the mean wind direction across the release location was used to split the data between upwind and downwind recaptures. Each trap distance was expressed as the shortest distance to the trap from this line. This transformation allowed measurement of downwind or upwind displacement ignoring any crosswind displacement. The same method was applied to split the data left and right relative to the wind, thereby removing the downwind and upwind components to highlight net crosswind displacement.

After this reclassification into either net left-right or upwind-downwind flight, the frequency distributions of recapture net displacement were compared using a Pearson's χ^2 test (S-plus 6.1; TIBCO Software Inc., Palo Alto, USA) to test for any dominant dispersal direction.

To measure directedness in the recapture patterns, in other words, the main direction of the distribution of recaptures, we also investigated the relative position of the centre of mass of the recaptures. The direction of each recapture was calculated relative to the mean wind on the day of release and the data were expressed as (1) distance from the release location, and (2) deviation from the downwind direction. The latter was calculated as the difference between recapture and wind directions. The distribution of resulting points represented the recapture pattern with respect to the mean wind on the day of release, and allowed replicates from different release dates and locations to be compared. We then calculated the location of the centre of mass of this distribution of points, considering all recaptures as independent events. For n sample points defined by their coordinates (x, y), the centre of mass ($\bar{x}, \bar{y}$) was estimated by the average vector (1) for the sample.

$$\bar{x} = \frac{1}{n}\sum_i^n x_i \text{ and } \bar{y} = \frac{1}{n}\sum_i^n y_i \quad (1)$$

To test whether the recaptures were oriented about a mean direction, we determined the confidence ellipse for the centre of mass and applied Hotelling's test of significance (Appendix III.A) (Batschelet, 1981). Based on a distribution of sample points, the confidence ellipse covers the region where the centre of mass for the population is located (Batschelet, 1981). In the present study, we defined the level of significance (α) for the confidence ellipse at 0.01. If the confidence ellipse contained the origin, there was no significant evidence for the drift in the population and the hypothesis that moths showed an overall directed movement was rejected.

III.4 Results

Over all directions, marked moths were recaptured over a range from the release location of 33-9 528 m with an average of 1 404 m. Seventeen replicates comprising six releases at three locations (except for one date where releases were done at two locations) with a total of 16 355 insects released and 1 481 insects recaptured were included in the comparison between wind pattern for the day of release and the recaptures summarized on a weekly basis.

The net distances for the recaptures ranged from 7-9 523 m downwind (median = 790 m, n = 894) (Figure III.2) and 3-3 720 m upwind (median = 266 m, n = 587). The net distances for the classified recaptures ranged from 6-4 023 m crosswind to the left (median = 404 m, n = 681) and 1-5 697 m crosswind to the right (median = 494 m, n = 800).

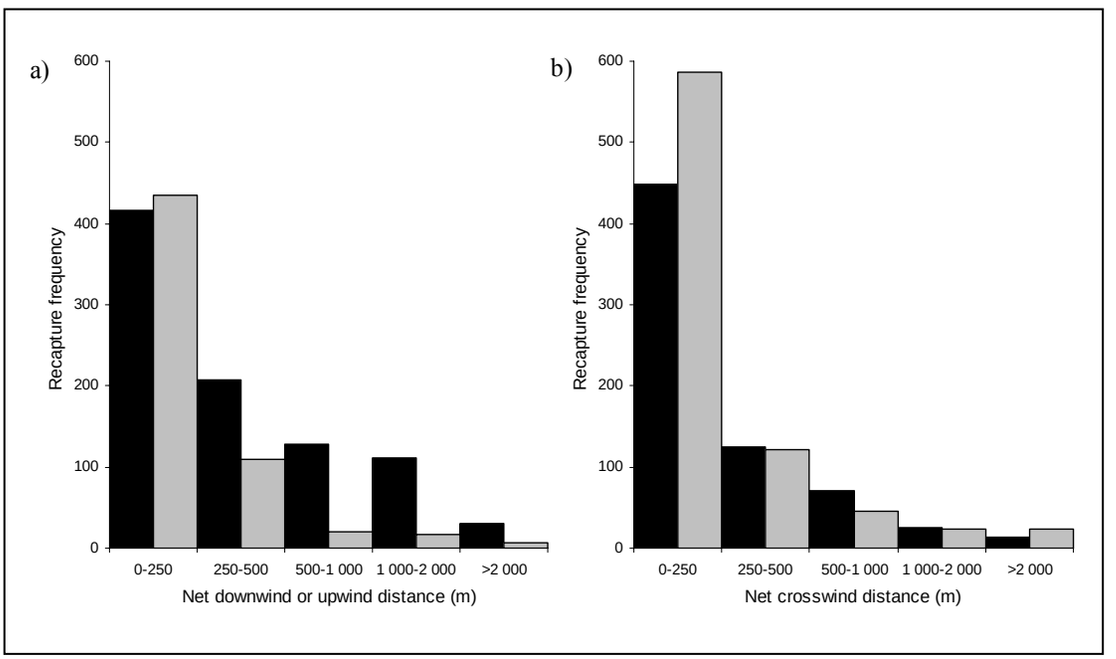

Figure III.2. *Segregation of recaptures by direction. Frequency distribution of the recaptures classified by the shortest distance between the recapture location and a line orthogonal to the mean wind at the release location for the day of release (a) downwind (■) and upwind (□), frequencies are significantly different using χ^2 test; (b) to the right (■) or left (□) relative to the mean wind direction, frequencies are not significantly different for net distances greater than 250 m (see text for details).*

The frequency distributions are significantly different for upwind *vs.* downwind (Figure III.2a; $\chi^2 = 137.789$, d.f. = 4, $P<0.00001$) and also for left *vs.* right (Figure III.2b; $\chi^2 = 16.939$, d.f. = 4, $P = 0.002$). The significant difference for left *vs.* right results from the contribution of the first class 0-250 m to the overall χ^2, because for net distances >250 m, the frequencies are not significantly different ($\chi^2 = 6.841$, d.f. = 3, $P = 0.077$). Conversely, the up- and downwind components differ only for net displacement >250 m (Figure III.2a) where more recaptures in traps located downwind to the release location were observed.

After normalization of recapture patterns by wind direction, where each recapture is expressed by its angular deviation to the wind, the distributions of recaptures are represented in Figure 3 for each release location. In each case, the furthest distances are observed on the positive ordinate axis which corresponds to the downwind direction. For the three release locations and the pooled data (Figures III.3 and III.4), Hotelling's test was significant ($T^2 > T^2table_{(2,n-2,\alpha)}$ for $\alpha = 0.01$ with n = 325, 801, 355, and 1 481 for Hobsonville, Waikumete cemetery, Ranui, and all the release locations, respectively), indicating that the sample centre of mass deviated significantly from the origin and pointing towards a displacement in the prevailing wind direction. The centre of mass of all 1 481 recaptures was located around 250 m downwind from the release sites (Figure III.4d).

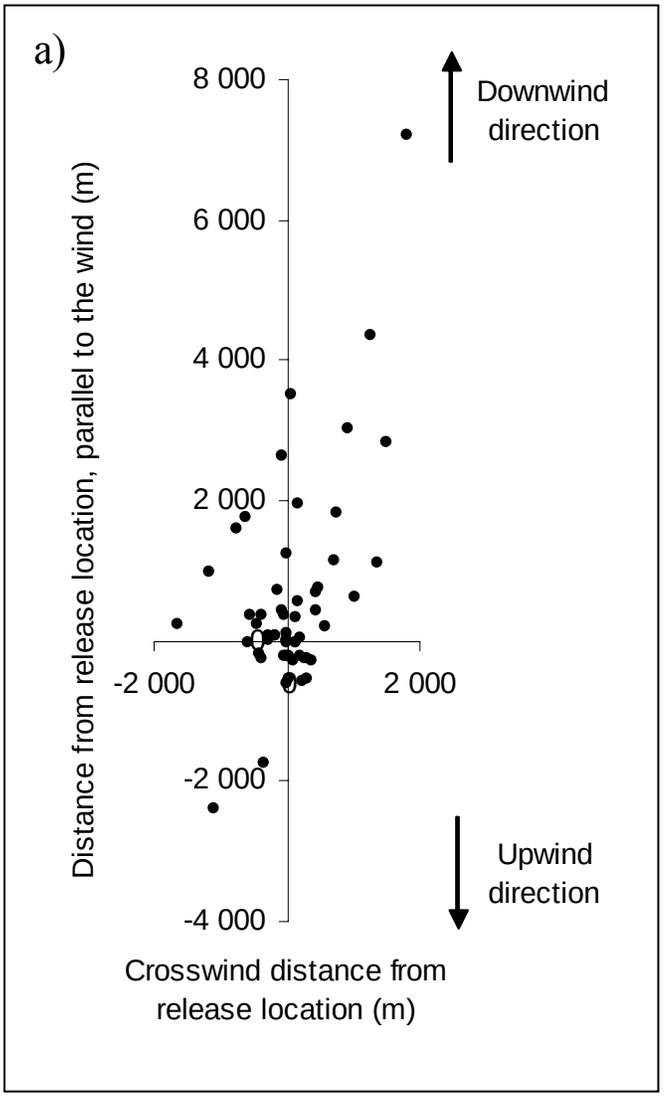

Figure III.3. *Recapture pattern (•) after normalization of the recapture direction by the mean wind for the three release locations: a) Hobsonville; (next pages): b) Waikumete Cemetery, c) Ranui and d) for the whole dataset. The downwind direction is represented by the positive ordinate axis.*

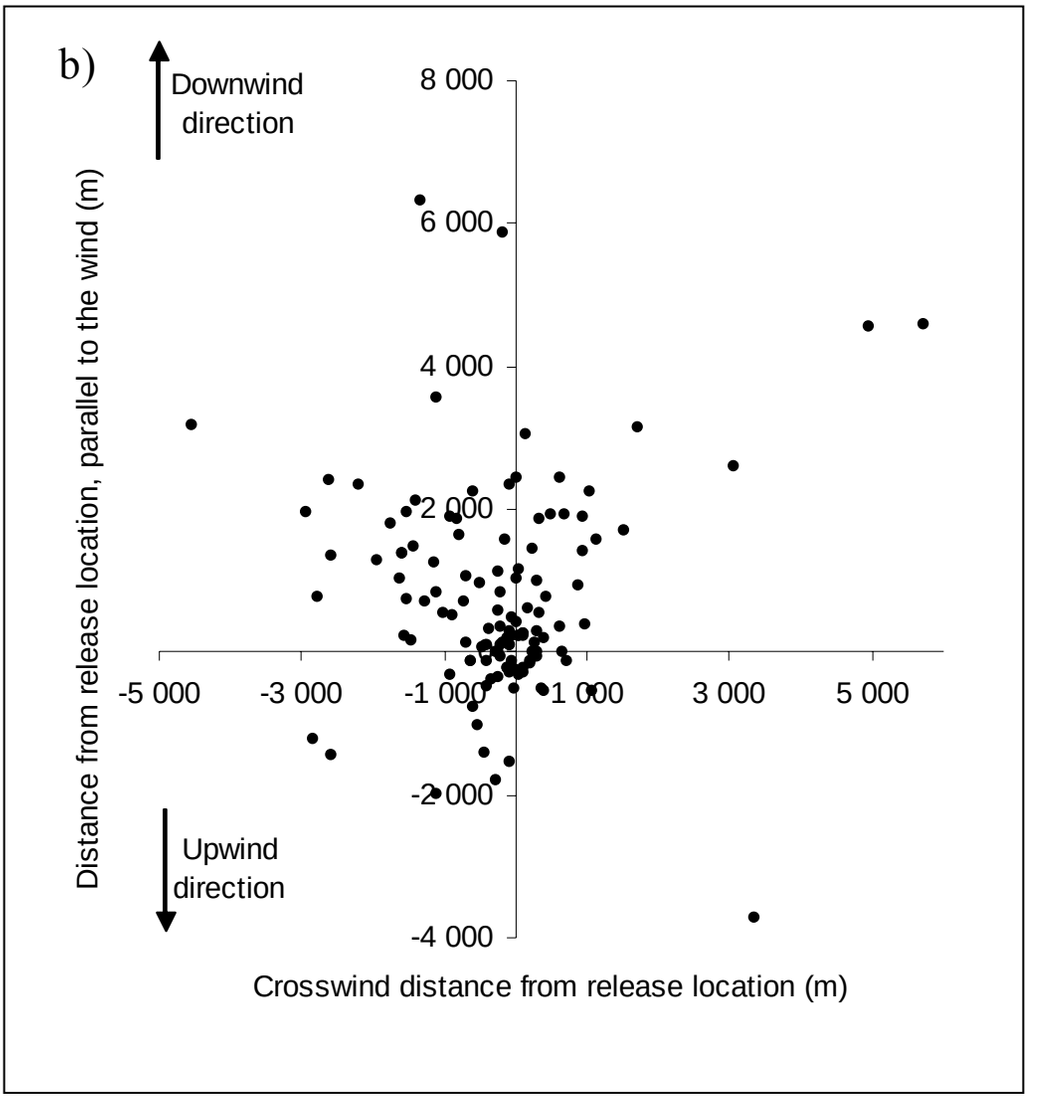

b) Waikumete Cemetery.

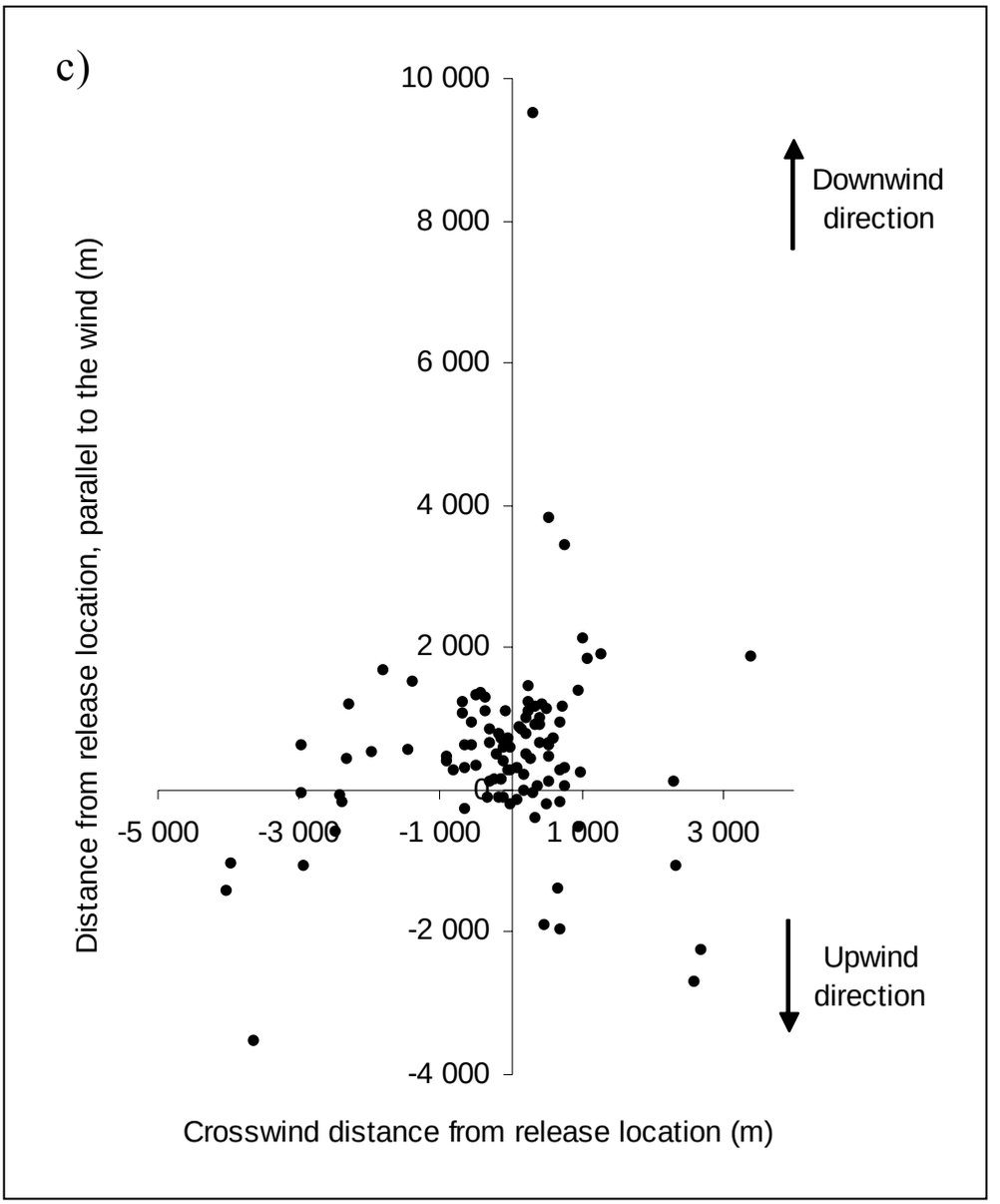
c)
10 000
8 000
6 000
4 000
2 000
0
-2 000
-4 000
-5 000
-3 000
-1 000
1 000
3 000
Downwind direction
Upwind direction
Distance from release location, parallel to the wind (m)
Crosswind distance from release location (m)

c) Ranui.

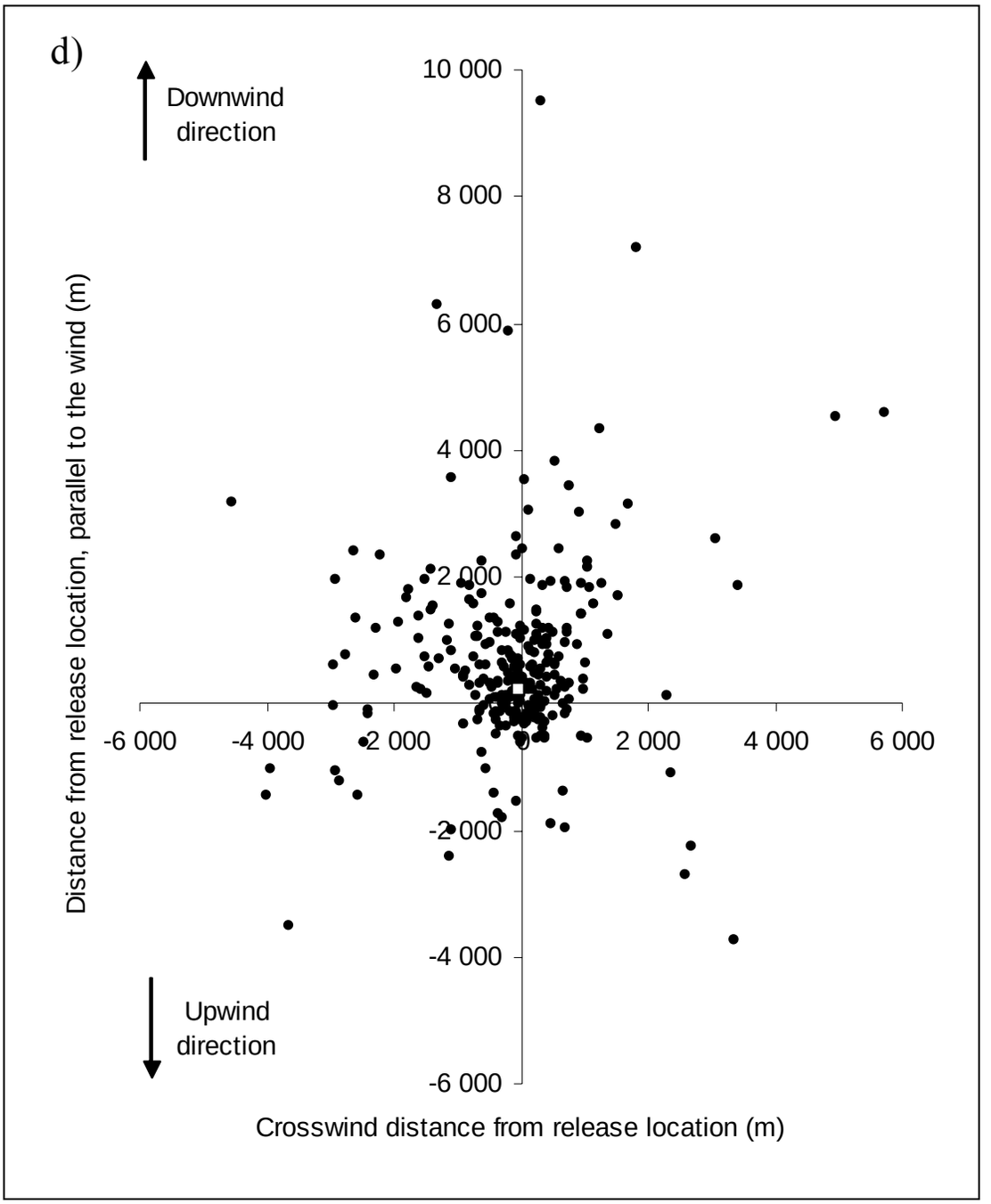

d) Whole dataset.

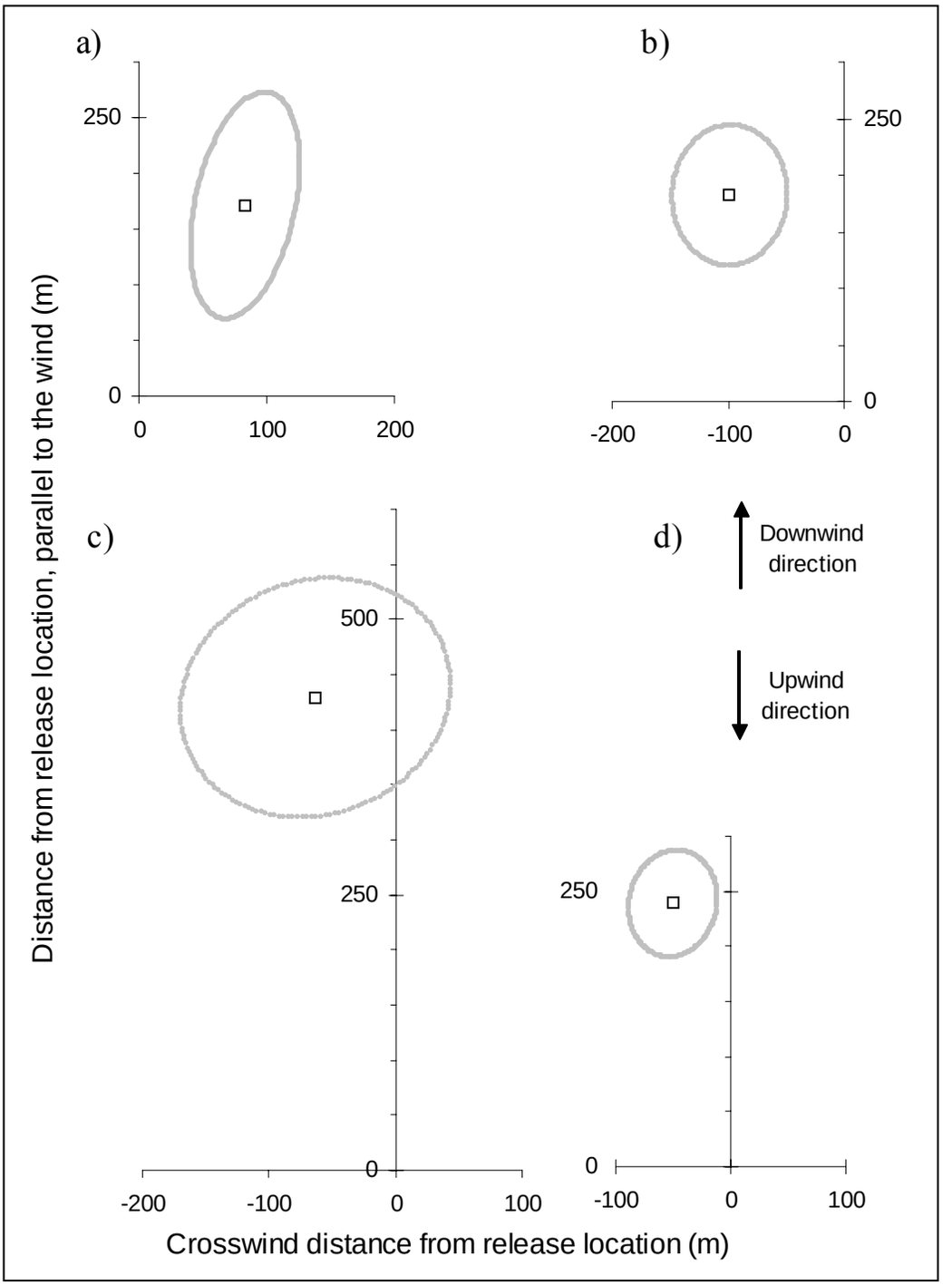

Figure III.4. *Centre of mass (▫) and confidence ellipse (——) of recapture patterns after normalization of the recapture direction by the mean wind for the three release locations: a) Hobsonville, b) Waikumete Cemetery, c) Ranui, and d) for the whole dataset. The downwind direction is represented by the positive ordinate axis.*

III.5 Discussion

Because the recapture dataset used in this study had insufficient temporal precision with respect to trap captures compared to the meteorological information, we were constrained to a comparison of the recapture pattern with declining survivorship over the next 4 days (Suckling *et al.*, 2005a) with the wind on the day of release. Despite that, the wind on subsequent days may have influenced the behaviour of moths; the wind on the day of release should have the greatest influence. Clearly, only a small proportion of insects would have survived over the week and we reasonably assumed that the wind direction during the day of release was the main driver for moth dispersal. The spatial recapture pattern over the week following the release had a significant downwind component in relation to first-day average wind direction. This suggests that either the moths have been passively blown downwind or an active behaviour has occurred on the day of release, such as an appetitive flight where insects needed to fly prior to encountering the pheromone. Appetitive downwind flight behaviour has been demonstrated in other species, such as bark beetles (Salom & McLean, 1989; Franklin & Grégoire, 1999).

The relationship between wind direction and recapture pattern has been investigated in light brown apple moth, *Epiphyas postvittana* (Walker) (Suckling *et al.*, 1994), but in the previous study, the authors did not account for the recapture distance which would bias the mean dispersal angle if recapture distances are not uniformly distributed in all directions. In the current study, we used Hotelling's test of significance to give an unbiased comparison. For the pooled data, the centre of mass of recapture locations is significantly distinct from the release location and deviated towards the downwind direction. The centre of mass of the pooled datasets (Figure III.4d) is located only 250 m downwind of the release location when data were normalized by the wind direction, whereas some recaptures occurred several kilometres away from the release location. This result is attributed to the fact that most of the recaptures were observed in traps close to the release location with several recaptures per trap, and less frequent recaptures over a long distance. Furthermore, the combination of downwind dispersal and anemotaxis behaviour to track a female by scent reduces the net downwind displacement contained in the recapture pattern

due to the mainly upwind and crosswind movements inherent to the anemotaxis behaviour. It would be interesting to record the behaviour of individual insects from the release site to the trap over a scale of hundreds of meters to some kilometres. In the present study we cannot explicitly segregate appetitive behaviour from passive downwind dispersal, but we demonstrate a downwind displacement in the recapture pattern. The active or passive downwind dispersal supports the findings of Reynolds *et al.* (2007) who used a harmonic radar study to record an initial downwind movement of *A. segetum* moths of a few hundreds of meters prior to anemotaxis behaviour.

The recapture distributions (Figure III.3) include a crosswind component that is important even for recaptures far from the release location. This could be attributed to moths heading at an angle different from the strict downwind direction, when dispersing downwind or the effect of anemotaxis behaviour following the downwind dispersal. However, the wind often shifts in strength and direction as it crosses this maritime-influenced landscape characterised by topography comprised of extinct volcanoes, and this is also likely to explain some of the crosswind component. For simplicity, and because of limited resources, we used only the wind characteristics at the release location rather than attempting to track the individual moths as they passed across the landscape.

Our study suggests the presence of an important downwind dispersal component in *T. anartoides* behaviour that would need to be incorporated into any model of its movement. Yamanaka *et al.* (2003) and Bisignanesi & Borgas (2007) developed agent-based models to simulate moth behaviour in an environment with pheromone traps but only included random or crosswind behaviour prior to pheromone detection. Given the potential for relatively high ground speed in comparison to other flight directions, even short-duration downwind flights may result in significant displacement and therefore have a significant impact on the final dispersal patterns of invasive organisms. This behaviour, either passive or active, is likely to be a critical component of any moth dispersal model aimed at identifying the proximal source of an incursion and subsequently to delimit the population. Previous work has suggested that the origin of an insect captured in a pheromone trap is likely to be located downwind, as would be suggested by standard anemotaxis theory alone (David *et al.*,

1983; Cardé, 1984; Ostrand *et al.*, 2000). Noting the downwind trapping results observed in this study, upon detecting an unwanted organism in a trap, delimitation surveys should include areas upwind of the capture site and around the capture site where the majority of recaptures were observed. In biosecurity incursion responses, minimizing ground search efforts to find the source of a pest incursion is critical both in terms of control efficiency and cost reduction (Myers *et al.*, 1998; 2000; Bogich *et al.*, 2008). Future work will focus on developing a modelling framework to improve incursion responses by better targeted searching for potential source populations.

III.6 Acknowledgments

We would like to thank A.M. Barrington and F. Bianchi for their helpful comments. We would like to acknowledge also the Ministry of Agriculture and Forestry Biosecurity New Zealand (MAFBNZ) and the New Zealand's National Climate Database for providing meteorological data and R.W. Turner from the National Institute of Water & Atmospheric Research (NIWA) for the interpretation and use of climatic data in CALMET. This work was funded by New Zealand's Foundation for Research, Science & Technology through contract C02X0501, the Better Border Biosecurity (B3) programme (www.b3nz.org).

Appendix III.A. Hotelling's test of significance

Hotelling's test of significance (Batschelet, 1981) was calculated with the following statistic (A1),

$$T^2 = \frac{n}{1-r^2}\left(\frac{\bar{x}^2}{s_x^2} - \frac{2r\bar{x}\bar{y}}{s_x s_y} + \frac{\bar{y}^2}{s_y^2}\right) \quad \text{(A1)}$$

where the variances s_x^2 and s_y^2 are given by equations (A2) and the correlation coefficient r by equation (A3).

$$s_x^2 = \frac{1}{n-1}\sum_i^n \left(x_i - \bar{x}\right)^2,\ s_y^2 = \frac{1}{n-1}\sum_i^n \left(y_i - \bar{y}\right)^2 \quad \text{(A2)}$$

$$r = \frac{\sum_i^n \left(x_i - \bar{x}\right)\left(y_i - \bar{y}\right)}{(n-1)s_x s_y} \quad \text{(A3)}$$

The critical value was calculated by equation (A4) where $4.787 < F_{2,n-2}(\alpha) < 4.605$ for respectively $120 < n-2 < \infty$ and $\alpha = 0.01$.

$$T^2(\alpha) = 2\frac{n-1}{n-2}F_{2,n-2}(\alpha) \quad \text{(A4)}$$

The equation of the confidence ellipse was of the form (A5):

$$s_y^2\left(x-\bar{x}\right)^2 - 2rs_x s_y\left(x-\bar{x}\right)\left(y-\bar{y}\right) + s_x^2\left(y-\bar{y}\right)^2 = \frac{\left(1-r^2\right)s_x^2 s_y^2 T^2(\alpha)}{n} \quad \text{(A5)}$$

CHAPTER IV

Objective fitness function

CHAPTER IV

Objective functions for comparing simulations with insect trap catch data

IV.1 Abstract

Targeted surveillance of high risk invasion sites using insect traps is becoming an important tool in border biosecurity, aiding in early detection and subsequent monitoring of eradication attempts. The mark-release-recapture technique is widely used to study the dispersal of insects, and to generate unbiased estimates of population density. It may also be used in the biosecurity context to quantify the efficacy of surveillance and eradication monitoring systems.

Marked painted apple moths were released at three different locations in Auckland, New Zealand over six weeks during a recent eradication campaign. The results of the mark-release-recapture experiment were used to parameterise a process-based mechanistic dispersal model in order to understand the moth dispersal pattern in relation to wind patterns, and to provide biosecurity agencies with an ability to predict moth dispersal patterns. A genetic algorithm was used to fit some model parameters. Different objective functions were tested: 1) Cohen's Kappa test, 2) the sum of squared difference on trap catches, 3) the sum of squared difference weighted by distance from the release site, 4) the sum of squared difference weighted on distance between best-fit paired data. The genetic algorithm proved to be a powerful fitting method, but the model results were highly dependant on the objective function used.

Objective functions for fitting spatial data need to characterise spatial patterns as well as density (*i.e*. recapture rate). For fitting stochastic models to datasets derived from stochastic spatial processes, objective functions need to accommodate the fact that a perfect fit is practically impossible, even if the models are the same.

Applied on mark-release-recapture data, the Cohen's Kappa test and the sum of squared difference on trap catches captured respectively the distance component of the spatial pattern and the density component adequately but failed to capture both requirements whereas the sum of squared difference weighted by distance from the release site did. However, in order to integrate the stochastic error generated by the model underlying stochastic process, only the sum of squared difference weighted on distance between best-fit paired data was adequate.
The relevance of each of the fitting methods is detailed, and their respective strengths and weaknesses are discussed in relation to their ability to capture the spatial patterns of insect recaptures.

Keywords: biosecurity, dispersal, individual based model, insect, goodness of fit

IV.2 Introduction

Biosecurity aims to protect economic and biodiversity values of a region from unwanted exotic organisms. One important tool for insect biosecurity is a targeted surveillance system comprising a network of attractive traps that are monitored regularly for early detection of the target species. This approach is a mainstay of gypsy moth and bark beetle biosecurity systems worldwide, and was particularly useful in the combating a recent major incursion of painted apple moth in New Zealand (Suckling *et al.*, 2007). In order to better respond to the detection of an unwanted species in a surveillance trap, a simulation model was developed to reproduce the likely flight path that led the insect into the trap, and in so doing, indicate where to search for the proximal source of the incursion. The simulation model uses an individual-based dispersal modelling approach, and is based on the well documented behaviour of insects in response to pheromone attractants. The model draws heavily on pheromone anemotaxis theory, which describes the optimal strategy used by male insects to track the pheromone plume emitted either by a female of the species or by a pheromone dispenser.

The dispersal model was partly parameterised using experimental data obtained from a mark-release-recapture experiment using the painted apple moth, *Teia anartoides*, in Auckland, New Zealand, in 2003 (Suckling *et al.*, 2005a). A genetic algorithm was used to fit inferentially some model parameters for which there was little knowledge available to inform their values. Genetic algorithms are methods inspired by natural selection processes in the evolution of biological organisms (Beasley *et al.*, 1993). A set of parameters represents a conceptual "genotype", within which, each parameter is a "gene". Using an appropriate fitness function, the algorithm scores the genotypes from a population, initially randomly generated, and selects the best genotype in order to "breed" a new population using cross-over and mutation processes. The selection of the best genotypes is crucial for the convergence of the population to a "perfect match" and is highly dependant on the fitness function. The rank of the scores for different genotypes reflects the goodness of fit of the simulation.

In this paper, we present a comparison of different objective functions for comparing simulated insect trap catches with observed recaptures in the mark-release-recapture experiment.

IV.3 Material and methods

IV.3.1 Observed recaptures

We chose a typical example of the recapture patterns observed from painted apple moth releases in Auckland, New Zealand in 2003. This example was from a release made on 6 March 2003 at Waikumete Cemetery (Figure IV.1).

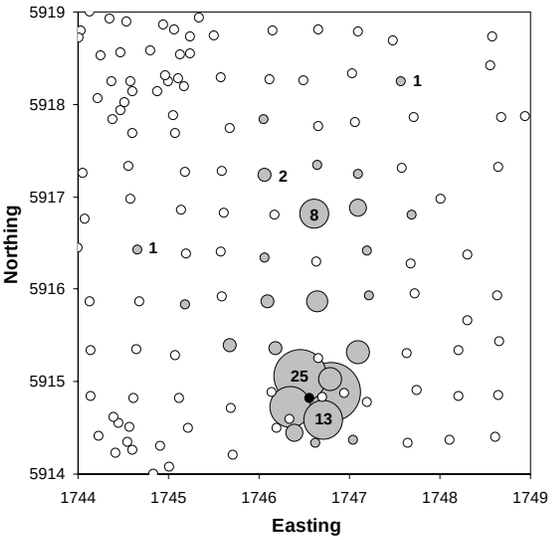

Figure IV.1. *Recapture pattern observed mark-release-recapture of painted apple moth at Waikumete Cemetery, Auckland, on 6 March 2003. Black dot represents the release site, grey dots indicate recaptures, with circle size proportional to the number captured and open dots indicate traps with no recaptures. The NZTM coordinate system has been used here with Easting and Northing expressed in kilometres.*

The spatial recapture pattern was characterised by three important features. Firstly, distance: most insects were recaptured close by, with recapture rates declining with distance from the release site. Secondly, direction: as a consequence of the particular meteorological patterns of the time, recaptures tended to occur to the north of the release site. Thirdly, stochastic error: since both insects and traps are discrete units in time and space, the observed outcomes from both simulation and experiment

represent single realisations of the underlying stochastic processes. Importantly, this means that the simulation results will practically never match exactly the observed field results, even when the same mechanisms and parameters are responsible for both.

The performance of any parameter fitting process for dispersal models such as this one depends on the ability of its objective function to assess adequately the distance, direction, and stochastic error of simulation results in relation to the observed recapture data.

IV.3.2 Objective functions

We evaluated the strengths and weaknesses of four different objective functions for adequately ranking the goodness of fit of different spatial patterns of insect recaptures:

- Cohen's Kappa statistic (Cohen, 1960). The score K evaluates the agreement between observed and simulated recaptures for each trap independently of the number of recaptures per trap (1). Trap catches are transformed to qualitative data and Pa is the proportion of agreement; Pc, the proportion of agreement expected by chance given the observed marginal totals. The higher the Kappa statistic, the better the agreement between observations and simulations is.

$$K = \frac{P_a - P_c}{1 - P_c} \quad (1)$$

- Sum of squared differences (SSD) between observed and simulated recaptures for each trap (2). This quantifies the errors generated by differences in trap catches between observations and simulations. In trap i the number of observed recaptures is O_i; the number of simulated recaptures is S_i for the trap i and n is the total number of traps. The lower the sum of square difference, the greater the similarity between observations and simulations.

$$SSD = \sum_{i=1}^{n} \left[(O_i - S_i)^2 \right] \quad (2)$$

- Distance-weighted sum of squared differences (DSSD). This is based on the sum of squared differences where each square difference is weighted against traps further from the release location (3). D_i is the distance in kilometres between each trap i and the release location.

$$DSSD = \sum_{i=1}^{n} \left[(O_i - S_i)^2 * D_i \right] \quad (3)$$

- Distance-weighted sum of squared differences on paired results (DSSDP). This calculates a sum of squared differences between observed and simulated recaptures where each simulated recapture is paired with the closest observed recapture and weighted according to equation (3) except that *Di* is now the distance between the paired traps. If the distance between paired traps is greater than the distance between the trap of the observed recapture and the release location, then the traps are not paired and the regular DSSD is applied. Furthermore, when the total numbers of simulated and observed recaptures are different, the DSSD is applied to the data remaining after pairing the best fits. Hence, each observed and simulated data point contributes only once to the sum of square differences. With a regular trapping grid, if the observed recaptures occur simultaneously in different traps separated by the same distance to one simulated recapture, the simulated recapture is randomly paired with one of the closest observed recaptures. Figure IV.2 and Table IV.1 illustrate the calculation method.

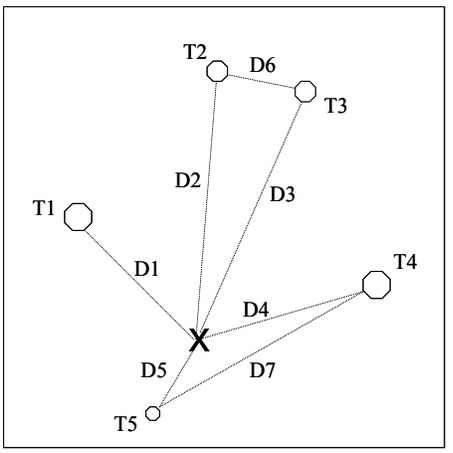

Figure IV.2. *Example map of trap locations to illustrate the DSSDP calculation. The cross denotes the release location. Traps Tn are separated by distances Dn.*

Compared to the SSD and DSSD, a recapture occurring in a trap close to an observation is penalized less: a near-miss in spatial terms is treated as almost a perfect match. This acknowledges that dispersal behaviour is a stochastic process, and that both simulated and observed recaptures are single realizations of similar stochastic processes. In this context, a recapture occurring in the closest trap could be considered as an approximation of a perfect match. This new objective function is inspired by the geostatistical principle of spatial inter-relationship between values of the same variable (for example, Rossi *et al.*, 1992) but applied to two variables with known underlying stochastic processes.

Table IV.1. *Details of the calculation of each components of the sum of square differences on paired trap catches weighted. In this example, trap T2 in which 3 recaptures were simulated and trap T3 in which 4 recaptures were observed, are paired. The calculation of the goodness of fit for T2 and T3 is: 3 simulated recaptures were paired with 3 observed recaptures and we applied Equation 3 with the distance D6; for the remaining recaptures in the trap T3 Equation 3 was used with the distance D3 as this observed recapture could not be paired with any simulated recapture. See Figure IV.2 for trap location and distance between traps.*

Trap	Observed recaptures	Simulated recaptures	Distances between traps	Results
T1	4	4	D1	$(4-4)^2$*D1
T2	0	3	D2 > D6	$(0-3)^2$*D6 + $(1-0)^2$*D3
T3	4	0	D3 > D6	
T4	4	0	D4 < D7	$(4-0)^2$ * D4
T5	0	1	D5 < D7	$(0-1)^2$ * D5

IV.3.3 Trap catch scenarios

The different fitness functions were evaluated against a set of trap catch scenarios (Figure IV.3) designed to represent different aspects of the distance, direction, and stochastic error of simulation results compared to the observed recapture data illustrated by Figure IV.1. These scenarios were, from least to most accurate:

- *Scenario 1 (null case)*: No moths were recaptured. This scenario represents one of the lower limits of each fitness function; although it doesn't represent the worst matching case which is when simulated recaptures occurred only in traps where no recapture was observed.
- *Scenario 2 (inverted dispersal pattern)*: The overall direction of recaptures is the same as observed, but the count of recaptures in individual traps is inverted, so that simulated recaptures tend to be distant from the release location. The primary source of error here is distance from the release point.
- *Scenarios 3 and 4 (truncated dispersal)*: Close to the release location, simulated results produce the observed pattern but no recaptures are observed far from the release location. In scenario 3 the errors begin closer to the release site than in scenario 4, so that the distance error is greater in the former scenario.
- *Scenario 5 (near-miss)*: This scenario is, for all practical purposes a desirable fit. The overall spatial pattern of abundance is similar between observation and simulation except for the traps far from the release location where simulated recaptures occurred in traps close to, but not coinciding with the observed recaptures. Although the errors appear greater here than in scenario 4, this is misleading since the individual recapture data are actually spatially closer to the observed recaptures. In scenario 5 there is very little direction or distance error but mostly just variation in the exact trap that catches an insect.
- *Scenario 6 (perfect match)*: All the simulated recaptures occurred where recaptures were observed. This scenario represents the upper limit of each fitness function.

IV.3.4 Rescaling of the objective functions

Scenarios 1 and 6, the null and perfect match cases respectively, were used to calibrate each of the fitness functions. We expressed the scores as a percentage between these two limits. Cohen's Kappa was multiplied by 100 as scenarios 1 and 6 gave rise to scores of 0 and 1 respectively. For the other fitness functions the raw scores (S_{raw}) were 0 for the perfect match scenario and they increased in value with decreasing similarity between the observed and simulated datasets. These scores were

transformed using equation (4) in order to adjust the score of null case scenario S_{null} to 0 and the score of the perfect match scenario to 100.

$$S = 100 - \left(\frac{S_{raw} * 100}{S_{null}} \right) \tag{4}$$

where S is the score after the rescaling, and $S < 0$ ranks the simulation worse than the null case. As the fitness function was designed to be used by a fitting algorithm, the critical aspect of each of the fitness scores was not its actual value but rather its rank in comparison to other simulations within the "population" of simulations.

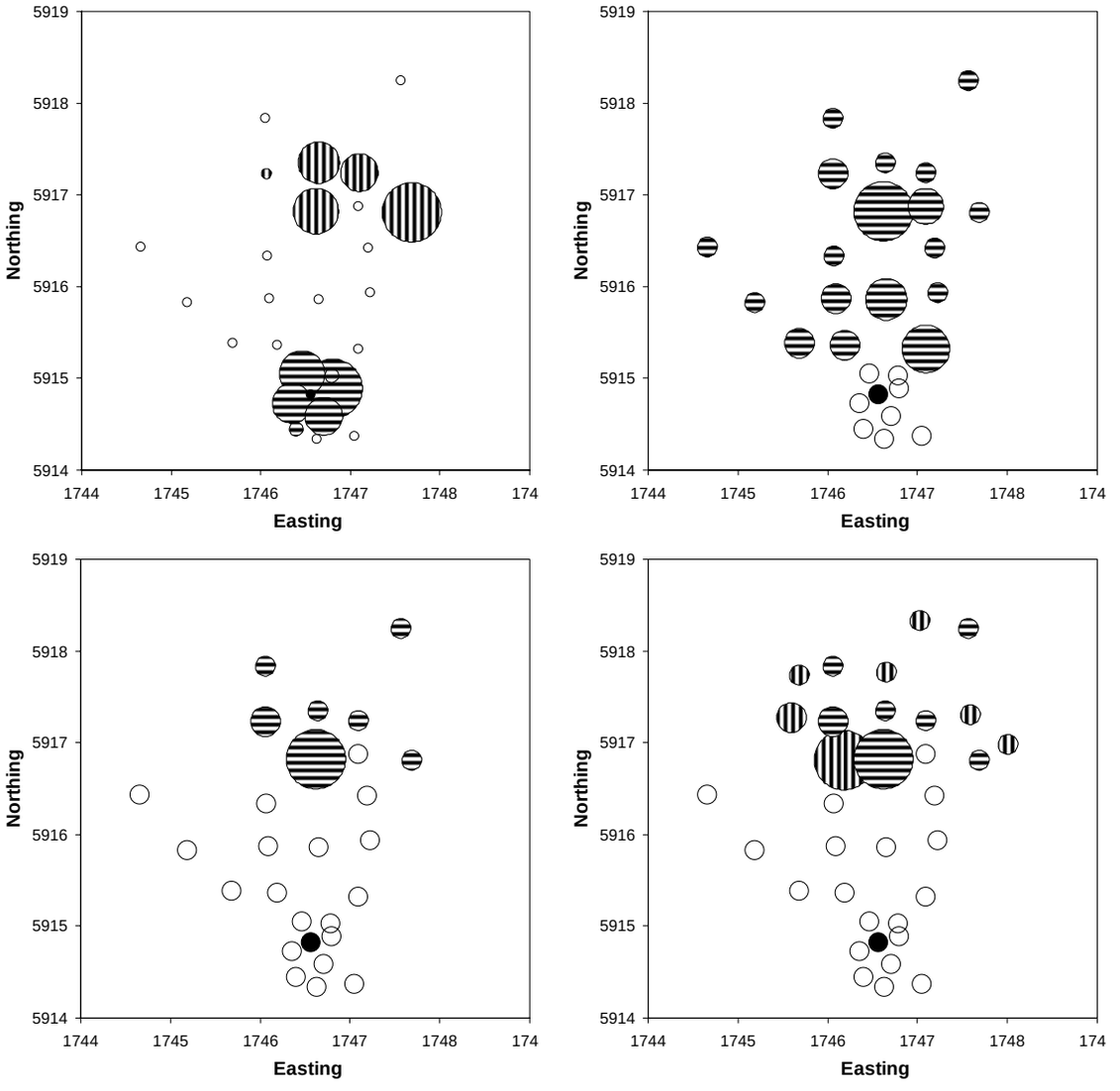

Figure IV.3. *Illustration of the magnitude of differences (size of hatched circle) between observed and simulated trap catches following scenarios 2 (top left), 3 (top right), 4 (bottom left) and 5 (bottom right). The horizontal cross-hatching indicates omission errors (simulated recaptures < observed) and vertical cross-hatching indicates commission errors*

(simulated recaptures > observed). Open circles indicate that simulated recaptures = observed.

IV.4 Results

The results (Table IV.2) showed that because of its qualitative nature, Cohen's Kappa was unable to discriminate against scenario 2, which is correct in terms of direction but maximises error in distance.

In contrast, the fitness functions based on sums of squared differences all ranked scenario 2 below the null case. The SSD detected the weakness of scenario 2 but scored all of the remaining scenarios very close to perfect, and provided little discrimination between scenarios 3 to 5. The SSD is highly influenced by the traps with the greatest recapture rates, and its performance was limited by the fact that recaptures were not uniformly distributed in space (Figure IV.1). Its inability to discriminate clearly between scenarios 3, 4, and 5 reflected the fact that the majority of the recaptures were found close to the release point. The DSSD correctly penalized scenario 2 and seemed to account adequately for the difference between scenarios 3 and 4. By weighting with distance from the release location, DSSD effectively accounted for the rapid decline in observed recaptures with distance from the release location. However, it also ranked scenario 5 lower than scenario 4, failing to capture the stochastic spatial error between simulation results and observed recapture data.

Table IV.2*. Scores of each fitness function evaluated on a set of scenarios after rescaling of their score in order to set one lower limit, the null case scenario, to 0 and the upper limit, the perfect match scenario, to 100; K: Cohen's Kappa; SSD: Sum of square difference on trap catches; DSSD: Distance-weighted sum of squared differences; DSSDP: Distance-weighted sum of squared differences on paired results.*

	K	**SSD**	**DSSD**	**DSSDP**
Null case	0	0	0	0
Scenario 2 (inverted distance)	100	-39	-419	-419
Scenario 3 (truncated dispersal)	46	93	68	68
Scenario 4 (mildly truncated dispersal)	83	96	78	78
Scenario 5 (near-miss pattern)	71	93	57	95
Perfect match	100	100	100	100

The DSSDP gave the same results as DSSD for scenarios 2 to 4, since the functions are by definition equal when simulated recaptures all occurred in the same traps as observed recaptures. However, DSSDP was also able to recognise stochastic error and accordingly ranked scenario 5 highly. DSSDP was clearly the best of the functions tested for fitting the model for insect dispersal against the observed mark-release-recapture data in terms of direction and distance, but also recognising that observation and simulation will necessarily differ even when the dispersal functions are the same or similar.

IV.5 Conclusions and Recommendations

The choice of a fitness function is critical in the process of fitting model parameters. For modelling biosecurity trap recaptures, the direction and distance of recaptures relative to the release location are both important, and the fitness function had to capture both aspects effectively. Cohen's Kappa captured the qualitative pattern but failed to discriminate based on distance. In contrast, SSD only considers the difference in distance from release to recapture sites, but takes no account of the direction of dispersal.

The DSSD performed well when simulated and observed recaptures all occurred within the same subset of available traps, as would be the case if presence-only data were available, if only a subset of traps were effective, or if limited traps were used so that all traps caught insects. However, the DSSDP method, based on sum of squared differences for paired data and weighted by the distance between traps or between traps and the release location, proved to be the best fitness function for our purpose. It correctly ranked the test scenarios, successfully accounting for distance and direction from the release site, as well as recognising the inherent stochastic nature of insect dispersal. More generally, simulation modelling of any stochastic spatial process could benefit from the use of objective functions that account for the inherent stochasticity in the process being modelled.

IV.6 Acknowledgments

This work was funded by New Zealand's Foundation for Research, Science & Technology through contract C02X0501, the Better Border Biosecurity (B3) programme (www.b3nz.org).

CHAPTER V

Application of the hindcast model

CHAPTER V

Individual based modelling of moth dispersal to improve biosecurity incursion response

V.1 Abstract

Some biosecurity systems, aimed at preventing the establishment and spread of invasive alien species, employ sentinel trapping systems to detect the presence of unwanted organisms. Having identified the presence of an invasive alien species through a trap catch, the next challenge is to locate the source of the incursion. Tools that can direct search effort towards the most likely sources of an incursion can improve the chances of identifying the introduction pathway, and consequently delimiting and eradicating the local population. The ground-based detection and delimitation surveys can be very expensive, and methods to focus search effort to those areas most likely to contain the target organisms can make these efforts more effective and efficient.

An individual-based semi-mechanistic model was developed to simulate the spatio-temporal dispersal patterns of an invasive moth. The model combines appetitive and pheromone anemotaxis behaviours in response to wind, temperature and pheromone conditions. The model was trained using data from a series of mark-release-recapture experiments on painted apple moth, *Teia anartoides*.

The model was used to create hindcast simulations by reversing the time course of environmental conditions. The ability of the model to encompass the release location was evaluated using individual trap locations as starting points for the hindcast simulations.

The hindcast modelling generated a pattern of moth flights that successfully encompassed the origin from 86% of trap locations, representing 95% of the 1 464 recaptures observed in the mark-release-recapture experiments.

Comparing the guided search area defined using the hindcast model with the area of a simple point-diffusion search strategy revealed an optimized search strategy that combined searching a circle of 1 km radius around the trap followed by the area indicated by hindcast model predictions.

Incorporating this novel moth dispersal model into biosecurity sentinel systems will allow incursion managers to direct search effort for the proximal source of the incursion toward those areas most likely to contain natal sites for the unwanted moth. This targeted effort should reduce costs and reduce the time taken to detect the proximal source of the incursion.

Keywords: anemotaxis, appetitive behaviour, CALMET, genetic algorithm, hindcast, Lymantriidae, *Lymantria dispar, Teia anartoides*

V.2 Introduction

To manage the increasing risk of biological invasions under globalization and climate change, management policies need to be backed up by effective biosecurity systems (Cannon, 1998; Mack *et al.*, 2000; Perrings *et al.*, 2005; Lodge *et al.*, 2006; Hulme *et al.*, 2008). An important characteristic of an effective biosecurity system is the ability to detect and respond rapidly and efficiently to an incursion when prevention fails, as this enhances the likelihood of eradication success (Myers *et al.*, 2000; Byers *et al.*, 2002). Modelling can assist to optimize the balance between surveillance and eradication in a biosecurity strategy (Bogich *et al.*, 2008). We suggest that modelling can also improve the incursion response capacity of a biosecurity system by optimising surveys to determine the geographic source of the founder population of an incursion: increasing the likelihood of detecting the proximal source of the incursion, and reducing the time and costs of the survey.

One way to detect some types of insect incursions is the use of sentinel traps baited with an odour attractant. This practice is used for targeted biosecurity threats such as gypsy moth (Maynard *et al.*, 2004; Biosecurity New Zealand, 2006) but also fruit flies (Maynard *et al.*, 2004; Suckling *et al.*, 2008). Surveillance programmes typically deploy traps around perceived high risk sites such as airports, seaports and shipping container transitional facilities and can cover hundreds of square kilometres (Bulman, 2008; Wylie *et al.*, 2008). Insects caught in these sentinel traps can inform biosecurity managers on the origin of the incursion, in other words on the location of the local founder population. If the proximal source of an incursion can be identified, then the pathway of introduction can be investigated and perhaps attenuated, reducing the risk of future introductions of invasive alien species. Knowledge of the spatial and temporal origin of an incursion can also anchor the modelling of spread of the organism to help guide efforts to delimit the extent of the incursion.

To enable more rapid and efficient detection of founder populations of moths, we developed an individual-based dispersal model to simulate the dispersal paths of moths in relation to dynamic wind fields, air temperature and time of day. The model can be run in a forward (forecast) or backward (hindcast) mode.

When run in the forecast mode, the model can simulate the paths by which a moth can disperse from a point such as a natal site or an intentional mark-recapture release point. When run in hindcast mode, it can simulate paths by which a moth could have arrived at a sentinel trap. The stochastic mechanistic model was based on insect flight behaviour, parameterized from published mark-release-recapture observations, and subsequently validated and applied in hindcast mode. It was trained on a subset of mark-release-recapture data from Suckling *et al.* (2005a) and validated on another subset. Although the mark-release-recapture experiment was undertaken with painted apple moth, *Teia anartoides* (Walker), characteristics of moth biology were taken from gypsy moth, *Lymantria dispar* (Linnaeus), another Lymantriid species that shares common traits (especially the diurnal flight of males and the flightless females), and for which there is sufficient detailed knowledge of its flight behaviour.

The benefits of the model run in the hindcast mode as an operational biosecurity tool were also tested in relation to its efficiency, delimitation strategy and potential to reduce costs of surveillance.

V.3 Materials and methods

V.3.1 Release recapture dataset

Weekly release recapture data (Suckling *et al.*, 2005a) over the period February to March 2003 where the highest recapture rates were observed (Table V.1) were used to develop and test the model. The study area, which covered 400 km^2, was separated into three zones depending on the release location and associated recaptures. The three zones were Hobsonville 36º47'35"S 174º39'12"E, Ranui 36º51'59"S 174º35'52"E and Waikumete Cemetery 36º54'04"S 174º38'42"E (Figure V.1). For the three regions, 116, 621 and 762 traps respectively, were baited with virgin females and deployed in each zone. The model was trained on four replicates (Table V.1, 659 recaptures) and validated on the remaining twelve replicates (805 recaptures).

Table V.1. *Number of moths released and recaptured at the different locations and release date considered in the present study. The dataset used to train the model is indicated by bold font and validation dataset by normal font.*

Location	**Hobsonville**		**Waikumete Cemetery**		**Ranui**	
Release date	***Release***	***Recapture***	***Release***	***Recapture***	***Release***	***Recapture***
19 February 2003	413	63	434	32	-	-
28 February 2003	**1128**	**103**	**1436**	**324**	330	39
6 March 2003	814	81	**795**	**131**	892	175
13 March 2003	1444	34	**1292**	**101**	1440	111
21 March 2003	1191	25	1129	59	1036	13
28 March 2003	866	19	850	154	-	-

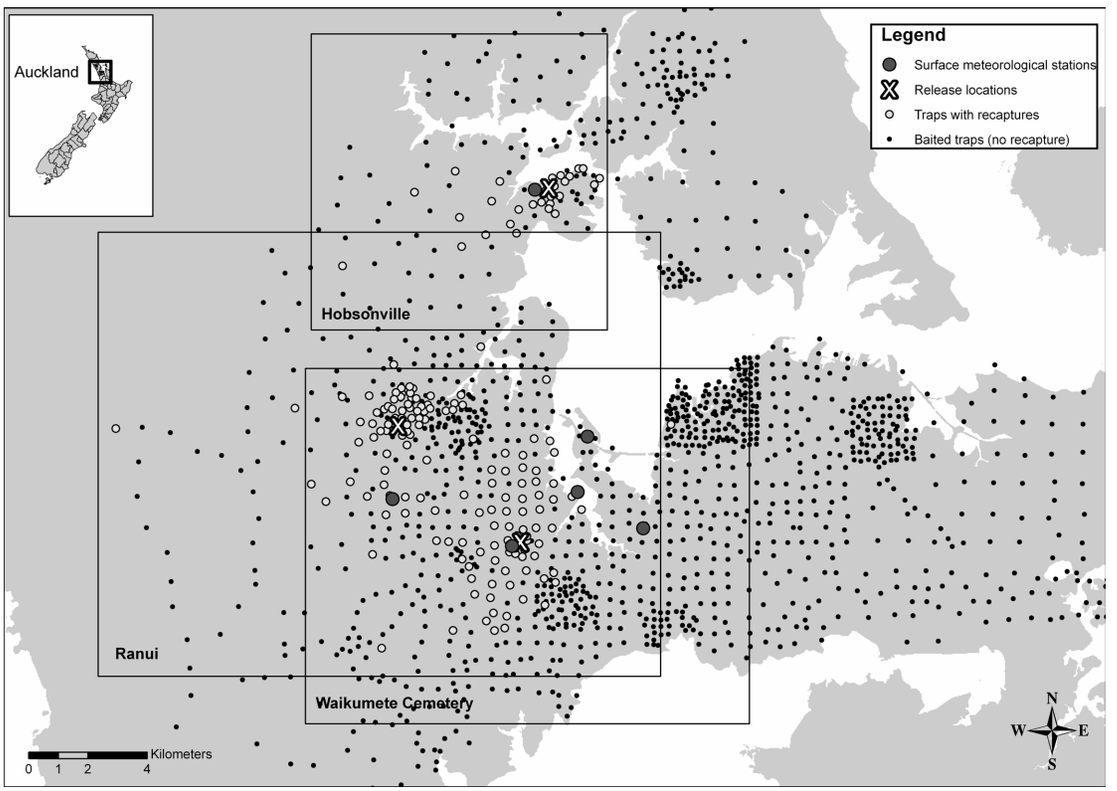

Figure V.1. *Situation map of the three different zones (Hobsonville, Ranui and Waikumete Cemetery, respectively from North to South) of the mark-release-recapture experiment (adapted from Suckling* et al.*, 2005a) highlighting the baited traps where recaptures were observed.*

V.3.2 Environmental data

CALMET and CALPUFF air quality modelling systems (Scire *et al.*, 1998; Wang *et al.*, 2008) were used to generate spatio-temporally gridded estimates of the environmental conditions of wind and pheromone concentration for the modelling period and across the study area at a temporal scale of 10 minutes and a spatial scale of 200 m. CALMET requires information on wind direction and strength, elevation and land cover. Weather data recorded at six meteorological stations at 1 minute and 10 minute intervals and at hourly intervals at other three meteorological stations of the New Zealand Climate Database (Figure V.1) were used. Information regarding land cover was extracted from the New Zealand land cover database (LCDB2, http://www.mfe.govt.nz/issues/land/land-cover-dbase/).

CALPUFF can use meteorological grids generated by CALMET to estimate the pheromone concentration through time across the landscape as it emanates from a network of lures. The pheromone emission rate of caged virgin PAM is unknown. Therefore, we assumed a rate measured for laboratory reared and wild gypsy moths, which averaged 15 ng for a two hour period (Charlton & Cardé, 1982). This rate was used in CALPUFF and assumed to apply at a constant rate over a daytime emission period from 8 am to 8 pm.

V.3.3 Modelling approach

The model described in this study is a semi mechanistic individual based model (IBM), written as a series of modules in the Python object oriented programming language. The IBM approach introduces stochasticity in the model as each insect responds slightly differently to environmental conditions and behavioural rules. The semi-mechanistic nature of the model supports hindcasting by applying the same behaviour rules but reversing the flight direction, the wind direction and the chronology. The object oriented language optimizes the algorithm by invoking the same modules in both forecast and hindcast modes.

We use the model in forecast mode to track an insect from a release location to a pheromone trap. We use it in hindcast mode to model the potential paths by which an insect could have dispersed to a pheromone trap. To distinguish between biological observations and the simulation modelling, we will reserve the term agent to describe an individual simulated flying moth.

V.3.4 Forecast modelling

From the commencement of dispersal flight, an insect potentially flies some distance before encountering a pheromone plume. This *appetitive* behaviour (Elkinton & Cardé, 1983) during this initial flying period has been described as random (Yamanaka *et al.*, 2003) or a downwind flight pattern (Chapter III; Reynolds *et al.*, 2007). Following this initial appetitive behaviour, moths then typically start orienting their flight patterns in relation to the wind in ways that depend upon the concentration of pheromones or other chemical elicitors: anemotaxis. It is unclear what triggers the changing of moth behaviour from appetitive to anemotaxic, and a variety of plausible functions can be suggested. In this study, we used the collective appetitive behaviour inferred in Chapter III on the same insect species and the same dataset. In forecast mode the male moths initially fly downwind during the appetitive phase of their dispersal, followed by the anemotaxic phase. Whilst in the appetitive phase insects do not respond to the concentration of pheromone.

The appetitive behaviour was simulated as passive downwind displacement at the current wind speed. This decision was based on the observation that recapture patterns between different replicates seemed to extend further downwind when the wind speed was greater (Chapter III). The downwind direction of the agent deviated for the whole downwind course by a randomly selected angle within a uniform distribution of a defined range (Table V.2), that we call the downwind deviation range. The sign of the deviation angle was also selected randomly. This modelling process was designed to account for insect downwind headings as well as to account for the averaging of wind direction over the scale of 10 minutes.

Table V.2. *List of parameters fitted by the genetic algorithm with their respective range and the value for the best fitted set of parameter. Ranges in which the genetic algorithm was allowed to select values were defined* ad hoc.

Parameter	**Range in the genetic algorithm**	**Best fitted value**
Downwind deviation range (º)	[25 , 45]	38
Downwind exit rate (probability per time step)	[0.0014 , 0.0035]	0.0026
Anemotaxis frequency of direction reversal (reversal by time step)	[1/10 , 1]	1/6
Minimum temperature (ºC)	[8.0 , 12.0]	8.2
Maximum wind speed (ms^{-1})	[6.0 , 10.0]	7.2
Mortality (day^{-1})*	[0.1 , 2.0]	1.0
Trap range (m)	[2.5 , 5.0]	4.4

**The mortality function is defined as the proportion of the population that dies during one day; a value of 2 should be interpreted as: the whole population dies in half a day.*

The function used to shift between the appetitive phase and the anemotaxic phase depends on whether the model is deployed in forecast or hindcast mode (Figure V.2). In forecast mode, all agents disperse downwind after they commence flying, with a constant probability of shifting to the anemotaxic phase at each time step, the downwind exit rate in Table V.2.

Thresholds for insect flight were also defined for the minimum temperature and the maximum wind speed. The flight was stopped if the temperature was below the flight temperature threshold or if the wind speed exceeded the wind speed threshold.

When an insect in an appropriate physiological state (anemotaxic phase) detects the presence of its pheromone, it attempts to track the plume upwind to the source. This pheromone anemotaxis behaviour has been well studied since an original study by Kennedy and Marsh (1974), and is a behaviour that has been widely described for a wide range of species (reviewed by Kennedy, 1983; Cardé & Willis, 2008).

Pheromone anemotaxis can be summarized as a series of upwind and sideways displacements elicited by the detection of a pheromone plume, interspersed with sideways casting behaviour during those periods when a pheromone has not been encountered for some time. Anemotaxis behaviour has been well documented at a fine scale (centimetres) but less so at a scale of metres. Here, we applied the behavioural rules quantified by David *et al.* (1983) and in Chapter II for insect flight orientation and speed, and scaled this behaviour up to a scale of two metre granularity for use in a broader setting (Figure V.3).

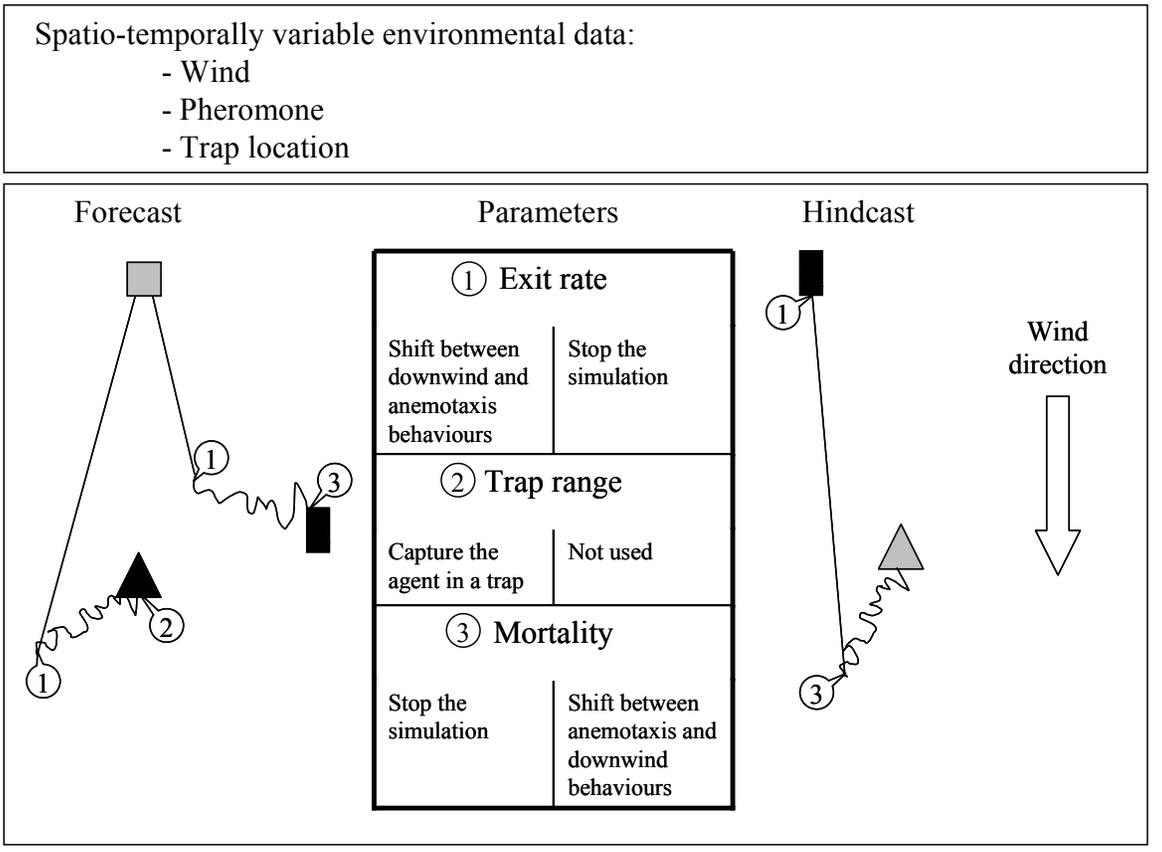

Figure V.2. *Design of the model showing the key parameters used in hindcast and forecast modes. Trap location is represented by a triangle, the simulation starting point in grey and ending point in black.*

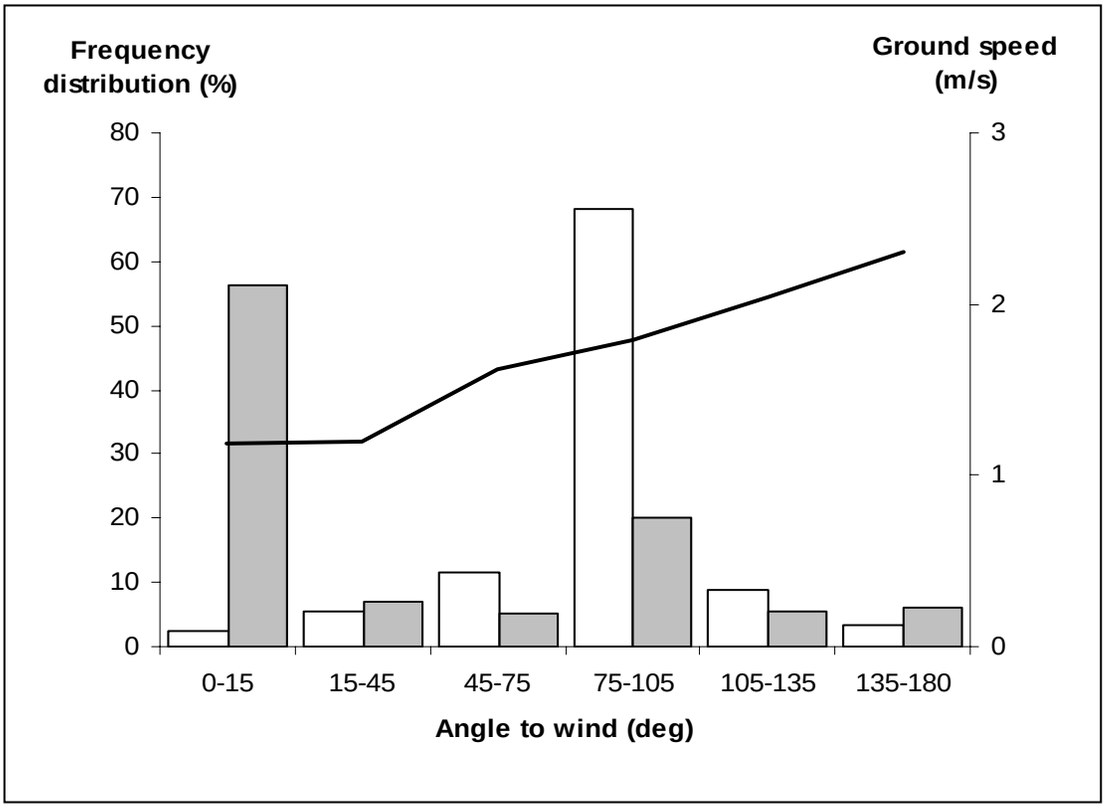

Figure V.3. *Behaviour rules applied for insects flying in the anemotaxis mode. Probability density functions of insect flying direction as a function of a flight inside (white bars) or outside (grey bars) of the pheromone plume (David* et al.*, 1983) and speed of the insect (black line) associated with its flying direction (Chapter II).*

We used the anemotaxis rules (Figure V.3) based on the frequency distribution of flight direction by David *et al.* (1983) for the deviation to the wind in the range 0-180º and associated ground speed derived in Chapter II in the range 0-135º. To be consistent with the agent movement in the range 0-135º, we linearly extrapolate the ground speed to 2.3 ms^{-1} for deviations between 135º and 180º to the wind. The time step for flight was set to 1.5s to reproduce track segments at least 2m long as defined in David *et al.* (1983) and in Chapter II. Insect anemotaxis is a combination of mainly upwind behaviour when insects are inside a pheromone plume, and mainly crosswind behaviours when they are outside of a pheromone plume (David *et al.*, 1983). In the model, at each time step, the agent selects a flight direction randomly from one of these two frequency distributions depending on the pheromone concentration and the probability of detecting the pheromone. These rules (Figure V.3) defined the movement of the agent in the range 0-180º and 180-360º to the wind; we defined a

parameter to shift from one side of the wind to the other allowing the agent to reverse direction (Table V.2).

Inside of the pheromone plume, the insect experiences an environment composed of a complex fine scale structure of successions of filaments of pheromone separated by gaps of clean air (Murlis & Jones, 1981; Baker & Haynes, 1989; Riffell *et al.*, 2008). To be useful in a biosecurity context the model was developed at a scale covering several square kilometres, and the ability of an insect to detect the pheromone was simplified to detection of the mean concentration of the pheromone. The pheromone detection function switched the agent behaviour between *inside* and *outside* of the pheromone plume. The pheromone detection function was derived from observations of wing fanning behaviour (Hagaman & Cardé, 1984), and the percentage of wing fanning was interpreted as a probability for the agent to detect the pheromone (Appendix V.A).

In the forecast mode, the agent flight is stopped by either mortality or trapping. The mortality represents all processes (such as predation, exhaustion, etc.) involved in the difference between the number of insects released and the number recaptured. The mortality is defined by the proportion of the population that dies during one day and is applied on randomly selected agents by reduction of the population every 10 minutes. The agent is assumed to be captured in a trap if it flies within a defined distance to a trap. The temperature and wind speed thresholds, mortality rate and trap range parameters (Table V.2) were all fitted during the model training.

V.3.5 Hindcast modelling

In hindcast mode, all the agents were flown in reverse (the chronology and wind directions were simply reversed). The appetitive and anemotaxic phases were also reversed so that agents commenced in the anemotaxic phase. The mortality function was used to identify when each agent should exit the anemotaxic phase and enter the appetitive phase, flying upwind until stopped by the reversed downwind exit rate function (Figure V.2).

In hindcast mode, during the anemotaxic phase, insects respond to the concentration of the pheromone but in the reverse direction. Clearly, the trap capture routine is not applied. The main difference between forecast and hindcast models was a slight overestimation of anemotaxic phase in the hindcast model as agents stopped their anemotaxic phase by only one process. As the objective of the hindcast modelling was to encompass the origin, we judged this simplification appropriate.

V.3.6 Parameter fitting

A Genetic Algorithm (GA) was used to explore the ranges of the different parameters and was used to fit the parameters on four replicates (bold entries in Table V.1). Genetic algorithms are optimization methods inspired by genetic processes of evolutionary biology (inheritance, mutation, selection and crossover) where candidate solutions, called "genomes", are grouped into a "population" evolving according to the principle of survival of the fittest (Beasley *et al.*, 1993).

Genetic algorithms utilise a "population" of vectors, each containing values for each of the parameters to be fitted. Each of the vectors was initialised with values that were randomly assigned to each parameter from within the ranges given in Table V.2. The "fitness" of each vector was determined by comparing the model projections with observations from the mark-release-recapture experiments where the model used the same meteorological conditions and the same initial number of agents as the field experiments (Table V.1). The fitness score was used to rank the vectors, and the best were hybridized and used in the next iteration of the algorithm. By repeating this procedure many times it is possible to select sets of parameter values that produce models with the highest possible fitness (in this study defined as the level of model agreement with the field data).

Different fitness functions were tested: 1) the sum of squared differences on trap catches was adapted to fit the density of recapture, 2) Cohen's kappa (Cohen, 1960) was adapted to fit the recapture pattern. An *ad hoc* fitness function, the distance weighted sum of squared differences on paired results (DSSDP), was developed to integrate in a single estimate, both density and pattern of recaptures derived from

stochastic processes: 1) the further from the release location a trap was, the higher the impact of each recapture on the fitness score; 2) an allowance was included for the stochasticity in the recapture pattern due to both the behaviour of the insects during the mark-release-recapture experiment and during the simulation in our model (Chapter IV). The developed fitness function rewarded agreement in the vicinity of traps where the highest number of recaptures was observed (usually close to the release location) and also for traps far away from the release location where the number of recaptures was often weak (Figure V.4).

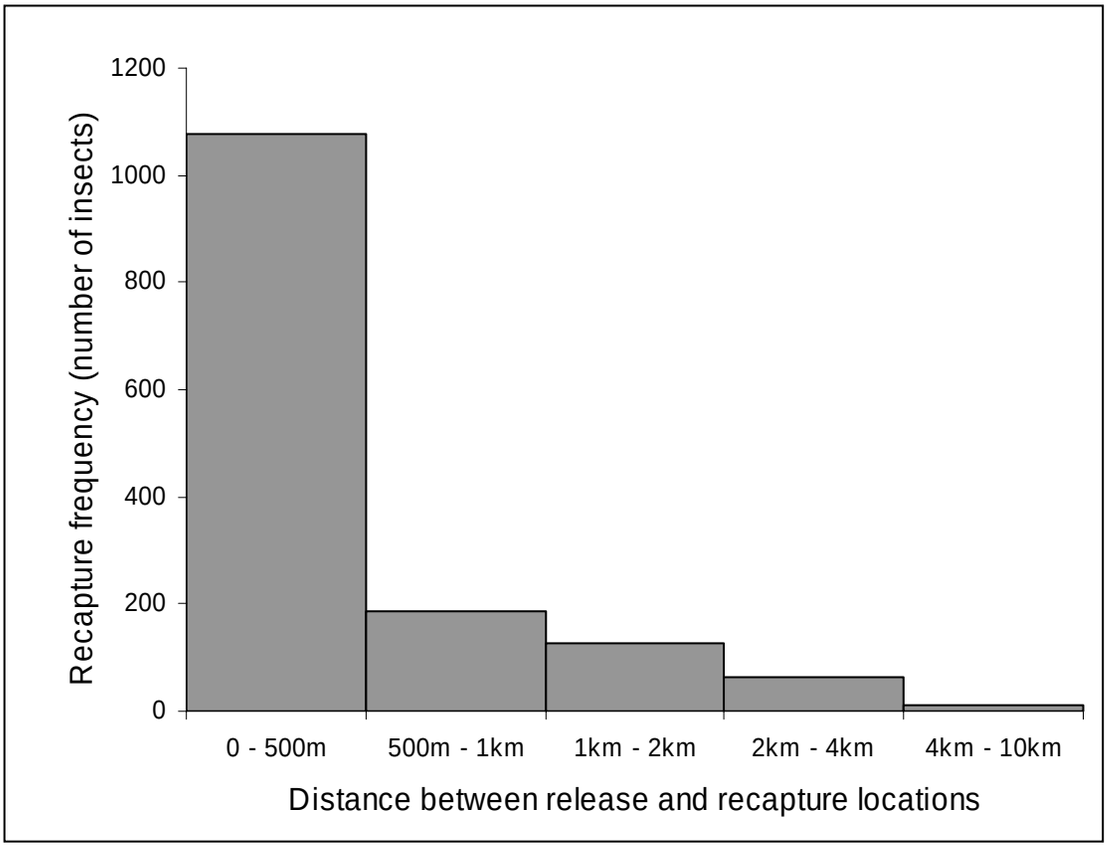

Figure V.4. *Recapture abundance in relation to the distance between trap and release locations. Note the variable size of the distance classes on the x-axis.*

V.3.7 Model Validation

With the best fitted set of parameters, hindcast simulations were run on the training dataset (bold entries in Table V.1) but also on all other scenarios (plain font entries in Table V.1).

Each recapture location from mark-release-recapture observations became a release location in hindcast simulations, and the release locations from mark-release-recapture experiment became the model target locations. For each recapture location we tested if the target location was included within the convex hull enclosing the cloud of agent locations at the end of the hindcast simulation for 1000 simulated insects.

The trap catch patterns from the mark-release-recapture experiment exhibited a distinct over-dispersion, and trap catch numbers were proportionately much higher nearer to the release point than further away (Figure V.4). This particular pattern was attributed to the high density of pheromone traps, where traps close to the release point acted as filter for the insects reducing recapture probabilities in those further away. In the biosecurity context, where small numbers of moths may be caught, it is much more likely that the traps are closer to the release point than further away if the density of surveillance traps is high.

The proportion of hindcast simulations originating from different traps for one scenario that included the target location inside the convex hull represented the sensitivity of our model for a particular scenario. The model accuracy was tested under two scenarios: Firstly considering only the spatial extent of the trap captures (naïve), and secondly including consideration of the abundance of trap captures (abundance informed). For the naïve analysis we identified the proportion of convex hulls that encompassed the origin. This frequency has a maximum of 1 if all hindcast simulations from different trap locations encompassed the origin. In the abundance informed analysis the number of convex hulls included in the proportion that encompassed the origin was weighted by the trap recapture abundance for the scenario. The abundance informed scenario provides a correction for the fact that in an incursion setting, the hindcast simulation is likely to only have a single trap for initialising the simulations, and that the spatial distribution of this trap in relation to the source site is likely to be described by the patterns of recaptures observed in the mark-release-recapture experiments. We would generally expect a better fit from the abundance informed assessment than the naïve assessment.

The hindcast model was designed to target the origin of a trap catch in a biosecurity context. To quantify the benefit of using the model, we compared the minimum survey areas indicated by the hindcast model and the use of a simple point diffusion searching strategy. The minimum survey area indicated by the hindcast model is defined by the minimum area to encompass the origin when we decreased the number of dots included in the construction of the convex hull, from a convex hull with all the 1 000 simulated agents to a smaller convex hull centred to the highest density of agent locations (Figure V.5). From a convex hull with an initial cloud of agent locations, the subset of agent locations with the highest aggregation was obtained by sequentially removing, dot by dot, the agent location furthest from the centre of mass of the cloud of agent locations (Appendix V.B). The minimum survey area based on a simple point diffusion searching strategy is the area of a circle with the radius equal to the distance between the trap location and the origin location (Figure V.5).

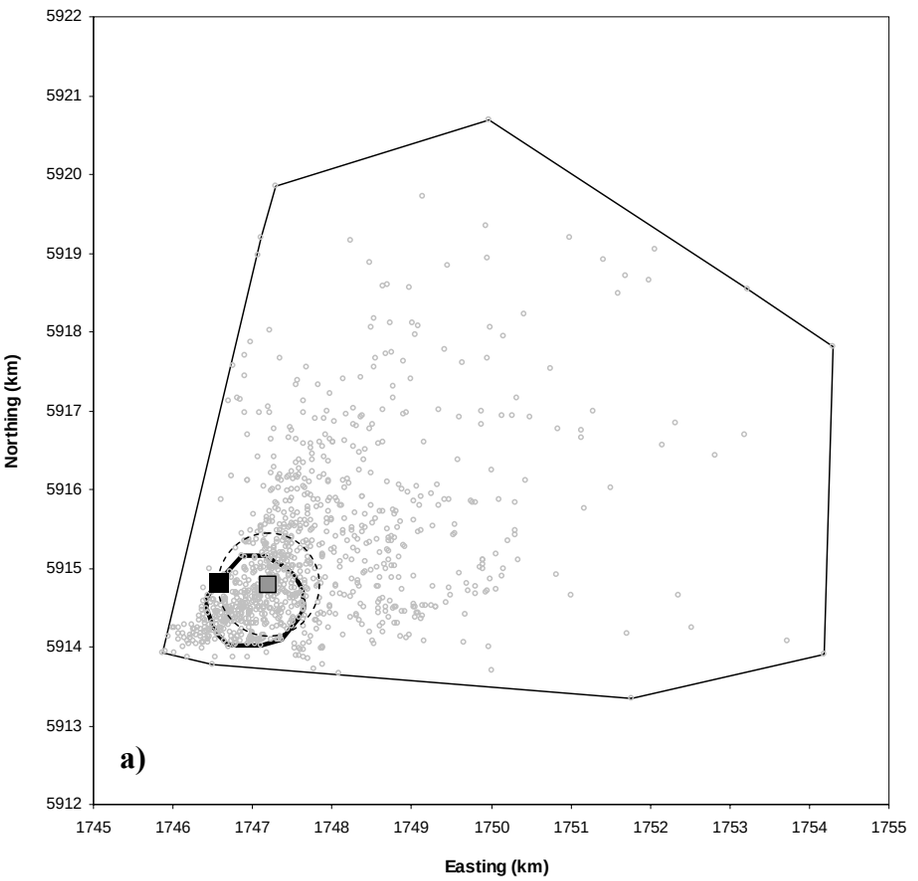

Figure V.5. *Hindcast simulations, based on a release from the Cemetery Waikumete location (black square) on the 28th of February 2003, from two different trap locations: a) the trap (grey square) is located 632m away from the release location, b) (next page) the trap (grey square) is located 5 892m away from the release location (note the differences in scale*

between graphs a) and b). Representation of the convex hull (thin line) for all the 1 000 simulated agents (open circles) at the end of the simulation. Minimum survey areas to detect the origin with hindcast model (thick line) and simple point-diffusion (dashed circle).

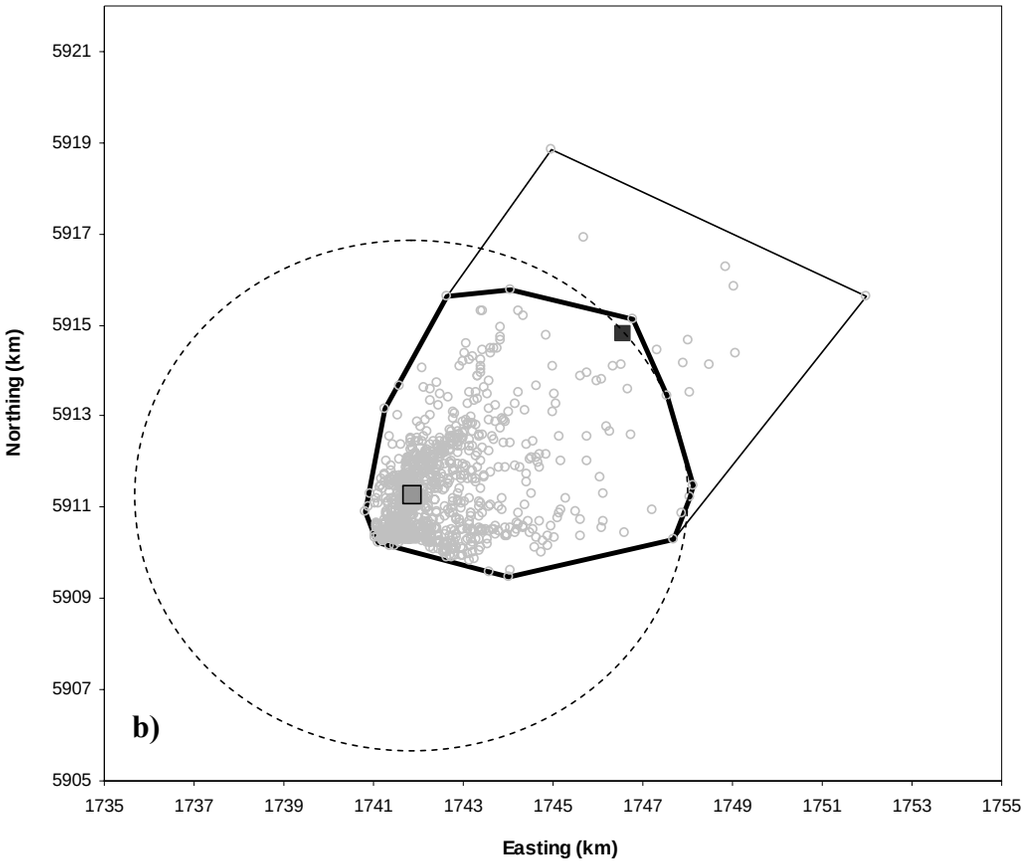

V.4 Results

The goodness of fit for the best fitted parameter set for the training dataset in forecast mode is summarised in Table V.3. These were not the best fitting parameters in each of the four scenarios individually, but gave the best fit across the training datasets and performed well for three out of four scenarios (Table V.3).

The best parameter set was used in hindcast mode from each of the traps where at least one recapture was observed using the meteorological conditions for the release day. Figure V.5 illustrates the location of the 1,000 agents for each of 2 traps at the end of the hindcast simulation and the minimum survey area. Searching the convex hull from the highest to lowest density of agent activity for all the 1,000 agents would have successfully enabled the detection of the release location of the mark-release-recapture experiment once the defined "minimum survey area" is surveying

Table V.3. *Average estimates of the goodness of fit for the training dataset (four replicates) simulated in forecast mode. DSSDP means Distance weighted sum of square differences on paired results (Chapter IV). The sum of squared difference is calculated on recaptures normalized by the number of released insects in so that scenarios are comparable.*

Scenario	**Hobsonville**	**Waikumete Cemetery**		
Estimate	***28 February***	***28 February***	***6 March***	***13 March***
DSSDP [-∞,100]	-167	63	65	60
Total number of recapture	192 (103)*	233 (324)*	97 (131)*	159 (101)*
Number of trap with recapture	24 (15)*	57 (28)*	38 (26)*	41 (22)*
Shared extent area (%)	39%	57%	70%	61%
Kappa [0,1]	0.28	0.35	0.47	0.45
Sum of square difference [0,+∞]	0.00175	0.01094	0.00058	0.00268

**Numbers in parenthesis are the values from mark-release-recapture experiment.*

In order to estimate the performance of the hindcast model, the naive and abundance corrected model sensitivity was calculated on respectively the 265 traps in which recaptures were observed and the 1 464 insect recaptures on the whole dataset or splitting the dataset by explanatory variables (the release time, classes of distance or release locations). Overall, the trap locations were encompassed by the largest convex hulls 86% of the time which represents 95% of all recaptures for the whole dataset (Table V.4). When the accuracy error or the precision error was equally distributed on the different subsets, the Pearson chi square test was not significant. Pearson chi-square tests didn't show any significant differences in raw frequency distributions when the dataset was split by release dates or by release locations (Table V.4). However, the distributions were significantly different for precision when the dataset was split by distance classes, but not for accuracy.

The failure of the model to encompass the source location is more accentuated in traps located further from release location in which only a few insects were recaptured (Table V.4, Figure V.6).

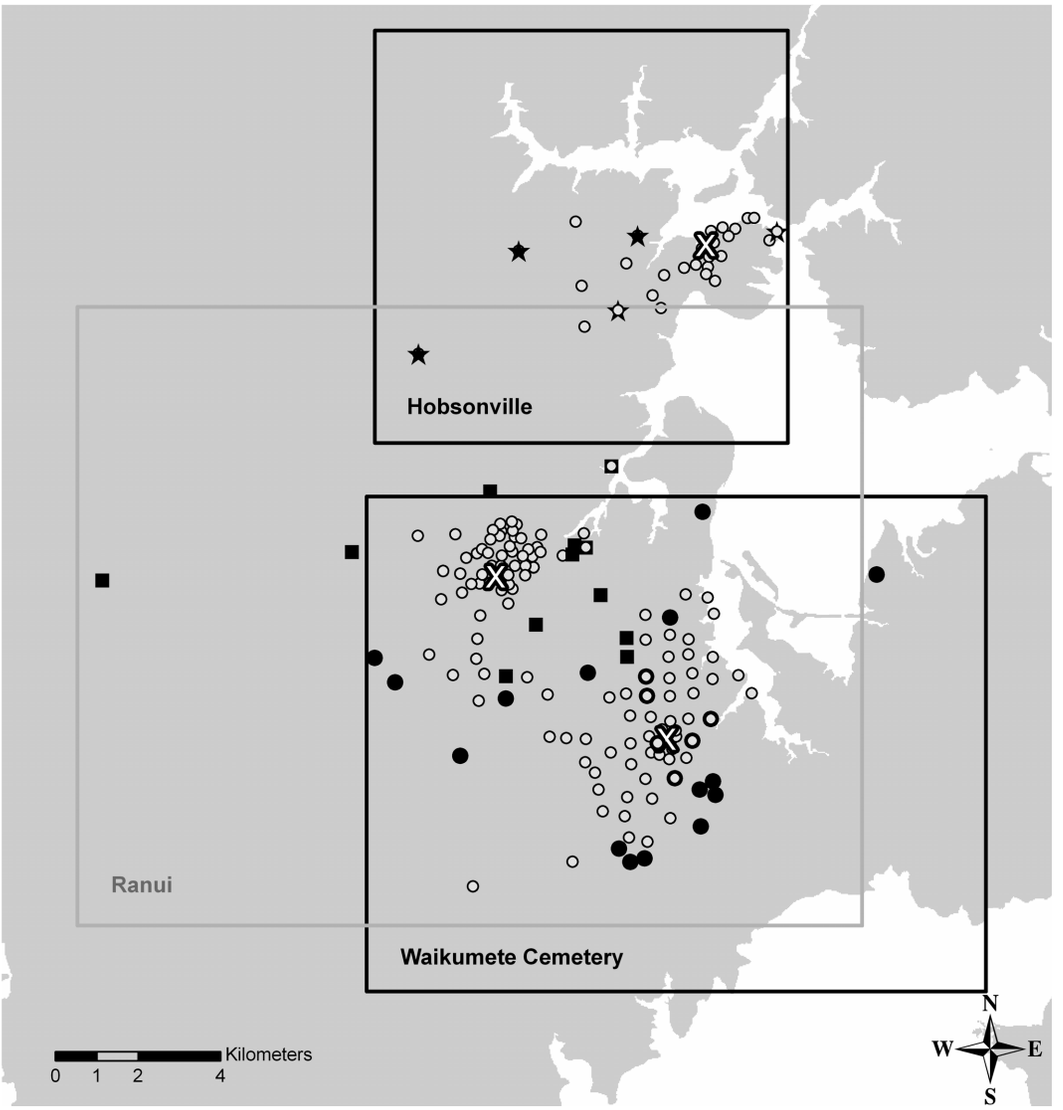

Figure V.6. *Location of the traps from which the hindcast model failed to encompass the release location into the convex hull with the maximum size. Black stars, black squares and black dots represent failures to detect release points for Hobsonville, Ranui and Wikumete cemetery release locations respectively. Open dots represent the trap from which the hindcast model successfully detects the release location. A combination of two symbols shows locations where detection of the release location occurred for some weeks but not others.*

The differences in the minimum area required to identify successfully the release location with our hindcasting model, in comparison with the minimum area of the simple point-diffusion search strategy that is generally employed in current

biosecurity operations to identify source populations and to subsequently delimit the population, are presented in Figure V.7. The differences in the area searched using the two approaches are similar for traps located close to the release location but increasingly favour the use of our model for traps located further from the release location. However, even if search areas are small for traps close to the release location, the search area using a point-diffusion strategy is smaller in 100 cases out of 137 cases for distance between release and recapture locations below 1 km (110 cases out of 227 for the whole dataset, Figure V.7). The critical distance between trap and release location, at which a point diffusion searching strategy becomes less efficient than using the hindcast model, is around 1km (Figure V.7). Below this value, the average difference in area to search to successfully encompass the origin is 0.5 ± 0.9 km^2 (1 240 recaptures in 59 traps) whereas it reaches 5.8 ± 11.3 km^2 (161 recaptures in 76 traps) for recaptures observed more than 1 km from the origin.

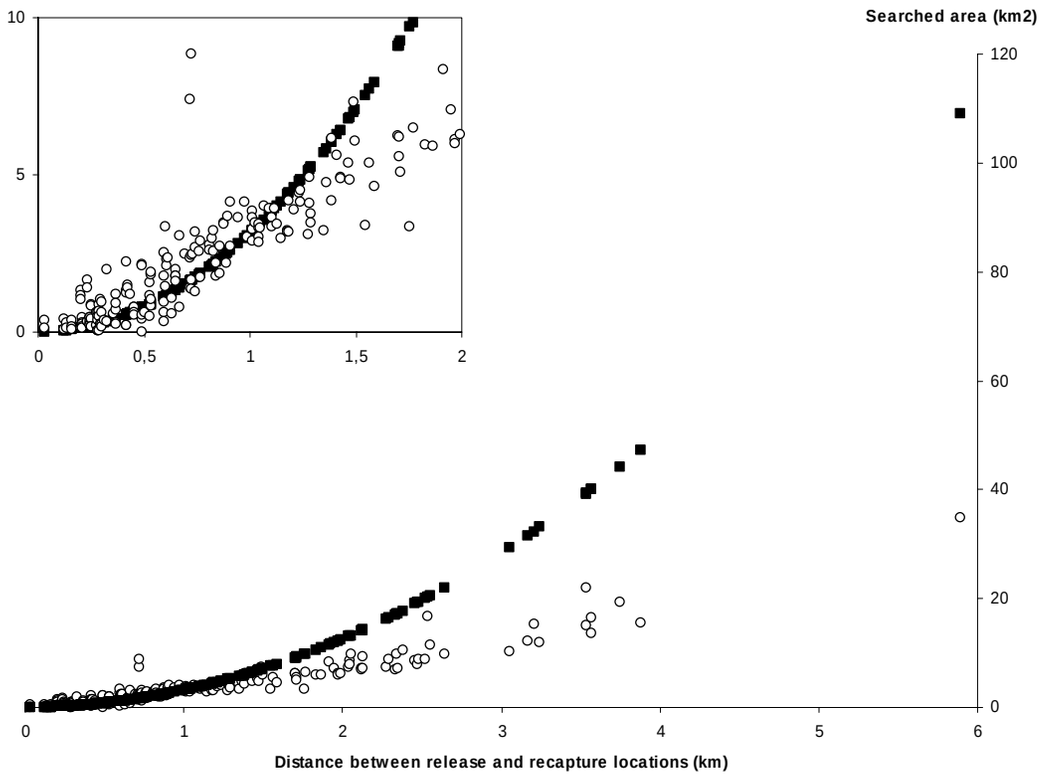

Figure V.7. *Difference in the minimum area with potential to detect the origin between the hindcast model (open circles) and a point-diffusion search strategy (black squares). Insert is focused on the differences for situations where trap and origin were close.*

Table V.4. *Performance of hindcast modelling segregated either by the release time, trap distance, release location or over the whole dataset. For each trap location, accuracy represented the correct hindcast model prediction of the origin in relation to the number of traps. For each recapture, precision represented the correct hindcast model prediction of the origin in relation to the number of recaptures. The Pearson chi square was calculated on the raw distributions of hindcast prediction and total number of trap or recaptures.*

Dataset	**Accuracy (total number of traps)**	**Chi square test on accuracy**	**Precision (total number of recaptures)**	**Chi square test on precision**
Release 19th of February	88% (16)		98% (95)	
Release 28th of February	93% (59)		99% (466)	
Release 6th of March	88% (67)	χ^2=1.25 df=5 p=0.939	98% (387)	χ^2=1.13 df=5 p=0.951
Release 13th of March	89% (61)		91% (246)	
Release 21st of March	79% (34)		93% (97)	
Release 28th of March	64% (28)		90% (173)	

Table V.4 (suite).

Dataset	**Accuracy (total number of traps)**	**Chi square test on accuracy**	**Precision (total number of recaptures)**	**Chi square test on precision**
Distance (0-500m)	99% (78)	χ^2=8.59 df=4 p=0.072	99% (1061)	χ^2=9.83 df=4 p=0.044
Distance (500m-1km)	97% (62)		95% (188)	
Distance (1km-2km)	85% (68)		91% (126)	
Distance (2km-4km)	66% (47)		71% (63)	
Distance (4km-10km)	10% (10)		10% (10)	
Hobsonville	91% (53)	χ^2=0.16 df=2 p=0.921	98% (325)	χ^2=0.21 df=2 p=0.901
Cemetery Waikumete	83% (120)		94% (801)	
Ranui	87% (92)		96% (338)	
All data	86% (265)	-	95% (1464)	-

V.5 Discussion

The parameterization of the model using the number of insects released as input and the density and pattern of insects recaptured as comparison data, is powerful but is highly dependant on the total number of insects released and recaptured. In accordance Chapter IV, we found the distance weighted sum of squared difference on paired results (DSSDP) handled the right skewed distribution of the frequency of trap recaptures with respect to the distance to the release location (Figure V.4), and the inherent stochasticity in the real and simulated processes of insect dispersal and recapture. However, this fitness function penalized both commission and omission errors. Except for extreme cases, the DSSDP would reward simulated and observed patterns that shared the exact total number of recaptures more than the comparisons where the total numbers were mismatched, but the spatial patterns were similar.

We found that the trap range parameter and the variations in initial population and total number of recaptures between different scenarios (Table V.2) greatly influenced the DSSDP scores (Table V.3). The goodness of fit of forecasts would be optimized for situations where the number of recaptures in the observation and the simulations are similar, and it explains both why the fitness function performed well on one scenario only and why we found that the trap range parameter has a great influence between scenarios. However, variations in the trap range between traps but also amongst different days would not be surprising as the trap range is dependant on surface roughness and also on meteorological conditions such as the wind strength and its variability (Olafsson & Bougeault, 1997; Britter & Hanna, 2003).

The hindcast model generally performed well but shows its limitations when modelling the origin from traps located furthest away from the release location. However, if the observed density of recaptures from the mark-release-recapture experiment reflects the probability of detecting an incursion in a sentinel trap; then, in a biosecurity context we have to concentrate search effort and resources to the most highly probable areas identified by the hindcast model. So, while the model has limitations, we recommend its use for improving the detection of proximal source populations. Indeed, the comparison between a point diffusion searching strategy and

the use of our model clearly indicates an advantage in targeting the source location using our modelling approach. However, for distances within 1 km of the trap location, even if our model can predict a search area in which the release location was located, a point-diffusion search was often more efficient. The best searching strategy would be a combination of a point-diffusion search up to a radius of 1 km, and then the use of our model to direct the search pattern (Figure V.8). Applying our model in hindcast mode can improve the search for the source population. Once the source has been identified, our model could be used in forecast mode to delimit the area occupied by the invading organism, and in which to concentrate eradication measures (Figure V.8). Before applying our model in this manner however, the parameters would need to be re-fitted using a slightly modified goodness of fit function that increased the sensitivity of the projections at the expense of model specificity. The rationale for this being that when delimiting the area occupied by an invasive organism during an incursion, the costs of underestimating the area occupied and perhaps missing some individuals may be far greater than overestimating it and searching an area that does not contain the target organism.

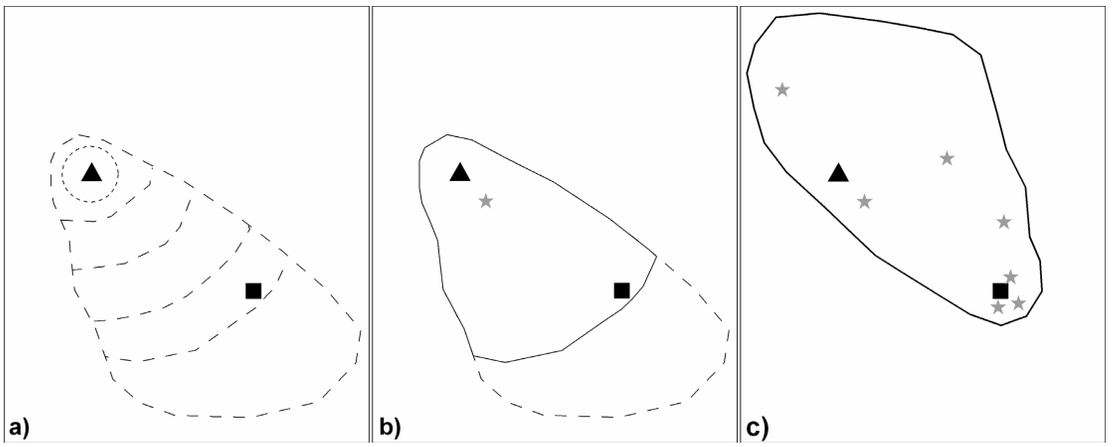

Figure V.8. *Sequence of the use of hindast and forecast modelling in different biosecurity applications. a) After the detection of an incursion in a sentinel trap (▲), a delimitation survey concentrates firstly inside of a 1 km circle (dotted line) and extends to survey areas of increasing size predicted by the hindcast model (dashed line). b) Delimitation survey (thin line) stops when the perceived source (■) is found (*eg. *presence of old egg mass, damages). Detection of a secondary population (★) (*eg. *fresh egg mass, adults) can also occur during this survey. c) Survey area (thin line) predicted by the forecast model from the identified source (■) and subsequent detection of other secondary populations (★) originating from the same source.*

Some aspects of operational searching have not been included in the two searching strategies, such as the presence of water bodies or any other landscape features that constitute unsuitable habitat. We recommend that the search area identified by the model is intersected with land use layers to restrict the search area to suitable habitat.

As far as we know our model is the first biosecurity tool based on insect behaviour to improve delimitation surveys. Developed on painted apple moth, it provides the framework for an application on other insect species but further research is required to investigate the transferability of the parameters to other case study species. Future research will also need to assess the sensitivity of the simulation results to the frequency with which meteorological data is collected, and the density of meteorological stations in relation to landscape roughness characteristics. This knowledge can guide the development of a meteorological monitoring system that can support desired levels of model precision.

In order to support a timely biosecurity response it is critical that the wind field data is processed into gridded form in near real-time. This modelling step is time-consuming, and to have it calculated automatically would cost little to maintain once processes of automatically capturing and cleaning field meteorological data was established. If the meteorological datasets are available, then simulations could be commenced as soon as an incursion detection is reported.

The sensitivity of our model parameters to the specific organism needs to be tested through multiple case studies. The obvious priority should be given to those species that hierarchically: are thought to pose the greatest threat, can benefit from early detection, and can be readily researched. In making this decision, thought should be given to applying effort across broad taxonomic groups, as well as radiating away from the Lymantriid used in this case study, and for which we have promising results.

Combining our model with an automated detection trapping system such as those currently being developed for monitoring purposes (Jiang *et al.*, 2008), would enable the detection of the organism to be precisely time-stamped. This would allow the hindcast simulations to be more precisely synchronised with the environmental datasets, allowing our model to be initialised at the correct time and place.

V.6 Acknowledgment

This work was funded by New Zealand's Foundation for Research, Science & Technology through contract C02X0501, the Better Border Biosecurity (B3) programme (www.b3nz.org).

AppendixV.A Pheromone detection function

The pheromone dosages in Hagaman and Cardé (1984) were converted into densities of pheromone around the male using the following procedure:

- Volume of pheromone plume between the source and the male (pheromone plume as a cone), $V = \frac{1}{3}\pi.r^2.d$ where r is the radius of the cone at the male location and d is the distance between the male and the pheromone source (d = 2.55). r is given by a constant expansion rate of the plume (0.02 .s^{-1}) during the time separating the source and the male (3.64).

- Density of pheromone = $\frac{D_0.t}{V}$ where D_0 is the release rate ($D_0 = 5x10^{-6}$ ng.s^{-1} for 1000 ng dose and $D_0 = 2.5x10^{-6}$ for 100 ng dose) and t is given by the distance d divided by the wind speed (0.7 m.s^{-1})

We fitted a logarithmic model for insect response to the density of pheromone (Figure V.A1) and used the percentage of wing fanning as a probability to detect the pheromone in our model.

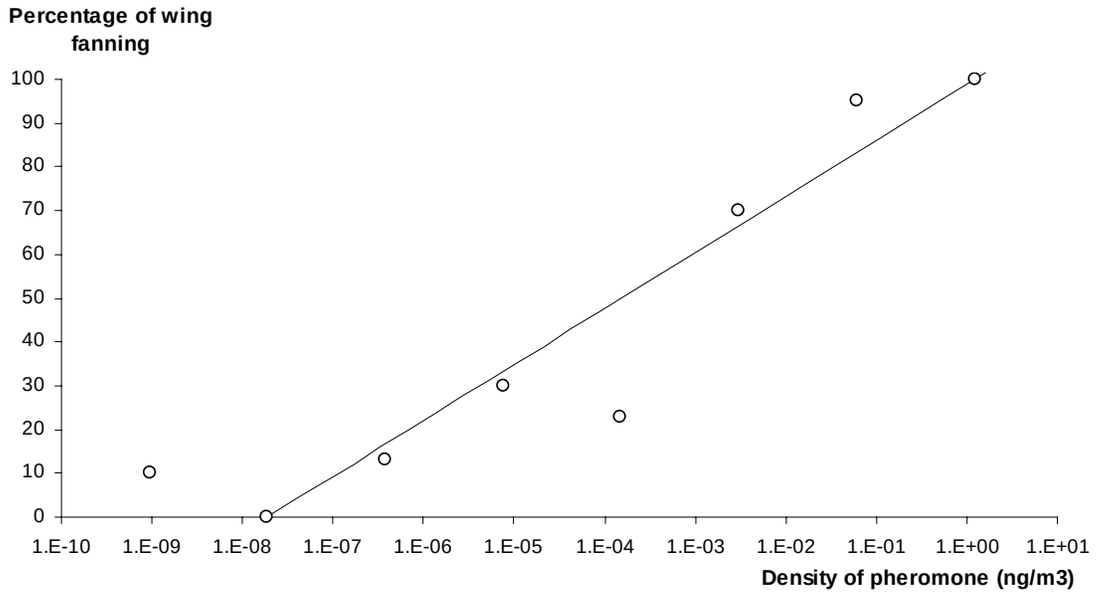

Figure V.A1. *Pheromone detection function:* $y = 0.05563 * \ln(x) + 0.98924$ *(R^2 = 0.85) where* y *is probability of detection and* x *the pheromone concentration in ng/m^3. Note the logarithmic scale of x-axis.*

Appendix V.B Methodology to concentrate a convex hull of a cloud of dots around the nugget of highest density

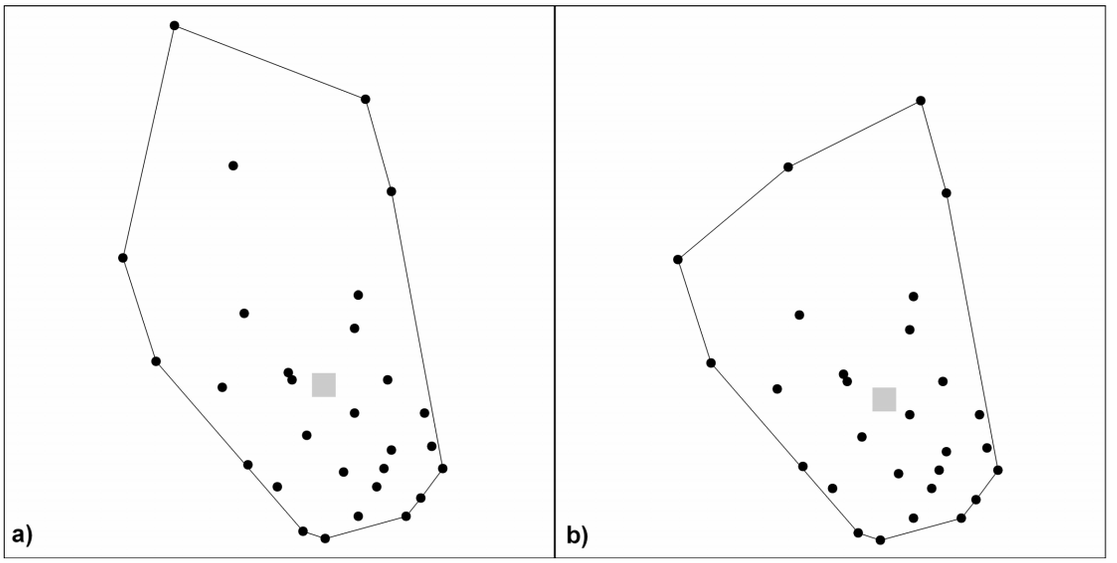

Figure V.B1. *Illustration of methodology to delineate a convex hull (black line) of a cloud of dots (black circles) around the nugget of highest density (grey square). Cloud of dots and associated convex hull and centre of mass: (a) before and (b) after the deletion of the furthest dot to the centre of mass.*

The convex hull was drawn around a cloud of dots (Figure V.B1a). Convex hull extremities were identified from the cloud of dots by recursively eliminating each dot inside of two neighbouring dots. The position of the centre of mass was calculated as the average x and y coordinates of all the dots (Figure V.B1a). For each dot, the distance to the centre of mass was calculated and the furthest dot to the centre of mass was deleted. The convex hull was drawn around the remaining cloud of dots (Figure V.B1b). The position of the new centre of mass was calculated. Note the difference in the location of the centre of mass between (Figure V.B1a) and (Figure V.B1b): the centre of mass "migrated" to the highest nugget of density of the cloud of dots. These iterations were repeated until the cloud of dots did not allow a convex hull to be drawn. This methodology was used to calculate the minimum area in which the origin was found following a hindcast strategy. The hindcast model generated a cloud of agent locations and the hindcast strategy comprised a progressively larger search area: in this example, the search area (Figure V.B1b) would be extended to the area (Figure V.B1a) if the source was not detected in the search area (Figure V.B1b).

CHAPTER VI

Discussion

CHAPTER VI

Discussion

VI.1 Overview of the study

The aim of this project was to develop a model to assist the biosecurity incursion response to invasive species. The model was designed to simulate insect dispersal patterns based on theoretical insect flight behaviour patterns, and on results of a mark-release-recapture experiment. In an operational biosecurity setting, the resulting model could then be used to "back-track" from a trapped specimen to produce a probability surface, predicting its potential origin, and thereby inform delimitation and pathway analysis.

Several technical challenges had to be overcome to achieve this aim:
Pheromone tracking insect flight behaviour has been well documented in the literature at a fine scale, but this study required broader-scale behaviour to be simulated. Thus, a method to **up-scale the pheromone anemotaxis** behavioural patterns was designed and is described in Chapter II in order to set the rules for simulating insect flight patterns in a pheromone trapping grid at a landscape scale.

The experimental dataset revealed an important **downwind shift in the pattern of recaptured moths** which was unexpected under pheromone anemotaxis theory. This downwind dispersal is illustrated, and its ecological implications are discussed in Chapter III.

The goodness of fit between simulated trap catches and observations, required the spatial pattern and abundance of recaptures, as well as the inherent stochasticity of the dispersal process, to be considered. A novel fitness function is developed in

Chapter IV that combines these three aspects of the trap catches, and allows the performance of the model to be objectively quantified.

The moth flight simulation model was designed to operate in **forecast mode,** from a release location to a trap, **and hindcast mode,** from a trap to the source location. A process based approach was selected (Chapter V) to reproduce insect dispersal in both directions satisfactorily. The model was trained on a subset of a mark-release-recapture experimental dataset in forecast mode, validated in hindcast mode with respect to its ability to identify the original location, in other words the release location, from a recapture location.

This study has resulted in the emergence of a number of perspectives and recommendations applicable to the general fields of modelling, biosecurity and ecology.

VI.2 Perspectives and recommendations in modelling

In biosecurity, the costs and probability of success of an incursion response depend critically on the ability to rapidly detect and accurately delimit the source population. Typically, sentinel traps are not distributed in a regular grid pattern, but are rather focused around perceived high risk sites. In addition, detection usually involves catches of only a few insects, which prevents robust evaluation of the population density from sentinel trap results. Interpretation of trap catches is therefore difficult, even if we can assume that nearby populations are more readily detected. In mark-release-recapture experiments or during monitoring of the spread at the edge of a species distribution, the pattern of trap catches is typically right skewed with respect to distance from the source population; in other words, the majority of recaptures occur in traps close to the population source, with progressively fewer recaptures occurring further from the source. Prior to analysing such data, trap catches are usually log-transformed to address the problem of heteroscedasticity in the data (Zar, 1984). However, analysis of trap catches in a biosecurity context aims to use high density catches to identify the most probable location of incursion foci, but also to

utilise low density catches occurring further away to delimit the range of the invasive population. I found that the **log transformation was not useful for modelling trap catches in a biosecurity context** because it weakens the importance of catches distal to the source and untransformed trap catches are recommended.

The model developed in this study was trained and validated on untransformed trap catches. However, modelled trap catches were dependant on a range of variables such as insect behaviour and its response to temperature, wind speed and wind direction, which are highly variable in space and time. Therefore, it was recognised that trap recapture events involve a high level of stochasticity, and that each experiment of mark-release-recapture was a single realization of a stochastic process from a pool of many other possible realizations. Thus, exact replicates of an experiment with exactly the same insect population in the same conditions would clearly have given different recapture results. The design of the model needed to take account of this variability, such that an **Individual Based Modelling** system was employed as a modelling framework so that each individual could follow different routes, **thereby introducing stochasticity into the model**.

The objective function for comparing simulated results with experimental results, needed to take account of **stochastic realisation** of both the dispersal process and the model realisations. This requirement was incorporated into the objective function developed in Chapter III. That function allowed for local stochasticity in trap catches whilst objectively comparing the larger scale patterns arising from simulations and in data from the field studies. Both the experimental and simulated recapture patterns shared high intrinsic stochasticity, but the new objective function took this into account by allowing for a **spatially explicit relationship between trap catch results in the fitness function**.

In this study, we also faced **scaling variability** in the different processes of the model. The recapture pattern was observed at a scale of several meters (around 2 to 100 m) and over a time period of at most 7 days. The meteorological data were recorded at time steps of 1 and 10 minutes and wind strength, wind direction and pheromone concentration were interpolated every 10 minutes for grids of 200 m cells due to computational limitations imposed by the large number of pheromone traps per zone

(116, 621 and 762 over respectively 100, 285 and 180 km^2). While pheromone tracking behaviour component is well described by pheromone anemotaxis theory from observations in wind tunnels at scales of 1 x 10^{-1} s, over a distance of a few centimetres (e.g. review by Cardé & Willis, 2008), it was necessary to up-scale the movement rules derived from pheromone anemotaxis theory to match the spatial and temporal scale of the available field data. The differences in scale between the meteorological dataset, flying behaviour and recapture pattern were handled more efficiently **using an object oriented programming language**. Time and location in space became attributes of flying individuals and the different processes were represented in the modelling algorithm as different objects. The interactions of processes evolving at different scales were facilitated by the object-oriented structure of the algorithm.

Effective use of the model relies on accurate knowledge of the date and time of capture so that the relevant meteorological values can be used. However, traps are often checked relatively infrequently (e.g. weekly). Given that weather is changeable, the model is probably of limited use without the use of "smart traps" that can detect and report captures rapidly (Jiang *et al.*, 2008). Even if the identity of the insect cannot be confirmed until some time later, having a temporally precise knowledge of the time of capture provides the critical biofix data with which to initialise the dispersal model.

The model developed in this study reproduced the recapture pattern from mark-release-recapture experiments and we argued its use in order to forecast the origin of the source population of an incursion detected in a sentinel trap. However, some **improvements** could be implemented in the model. The **integration of meteorological processes** directly into the model instead of the use of external modelling systems such as Calmet and Calpuff could simplify the use of the model, and potentially increase its efficiency. Models for insect pheromone dispersion (for example Bisignanesi & Borgas, 2007; Strand *et al.*, 2009) would be interesting to implement.

Rules to **constrain the maximum dispersal range** could be investigated and implemented. For example, lipid content and consumption may limit the potential dispersal range of insects such as gypsy moth and painted apple moth that cannot feed

during their adult dispersal. Identification of the maximum dispersal range of an insect would provide a stopping rule for the simulated insect flight, and further constrain the possible range of source locations that need to be explored for the delimitation survey.

The model presented in this study has been developed on Lymantriid moths, and parameterized on mark-release-recapture of painted apple moth (*T. anartoides*) in Auckland, New Zealand, between February and March 2003. The model should only be applied to other insect species, places or at different dates, with caution. Firstly, the generality of the observed combination of appetitive downwind dispersal followed by pheromone anemotaxis behaviour needs to be confirmed, especially for a different insect species. Secondly, the parameters presented may be specific to the conditions of the study. Even if, due to its mechanistic structure, the model processes could be transferred, it would be prudent to collect dispersal information similar to the mark-release-recapture experiment in order to transfer parameters of the model to different conditions.

VI.3 Recommendations for incursion management

The model presented in this study has not been tested during operational management of an incursion response. **Prerequisites to use the model** are to generate pheromone and wind conditions for the period and the area of interest, and initialise the model for the time and place of the capture.

To do this the following steps are required:

1) Acquire and format meteorological data for the Calmet modelling system.

2) Generate altitudinal and land use datasets for the area of interest in Calmet format.

3) Initialize and run the Calmet model to generate spatio-temporal wind datasets.

4) Initialize and run the Calpuff model to generate spatio-temporal pheromone concentration datasets.

Depending mainly on the time frame considered and the size and the number of traps in the area of interest, this process could take from one day to around a week. However, once the system has been established and calibrated for an area of interest such as a high-risk surveillance region, it is possible to run the system in near real-

time using automated weather station data. This approach would ensure that the model framework was ready to commence a hindcast simulation as soon as a trap catch for an unwanted organism has been reported.

With a constantly updated spatio-temporal dataset for wind strength, wind direction and pheromone concentration, the model that back-tracks an insect from a recapture location to its potential origin would be available in a maximum of a day for painted apple moth. This assumes the use of a single high-end computer workstation. Using a grid computing facility, the time to generate a hindcast map indicating the priority areas upon which to focus surveillance attention could be reduced to an hour.
In order to get the model integrated into a generic incursion management system, some investments would be required:
1) Recording of fine scale meteorological data (especially the wind) at 10 minutes intervals for several permanent stations covering the area of interest. In the present study, only six meteorological stations provided meteorological data for the area of Auckland.
2) Computational facilities to run the different models
3) Regular, high frequency sentinel trap inspection, either manual or smart trap technology
4) Further research on insect dispersal to transfer the model to different conditions, especially for its use with another insect species.

The results of this study are encouraging for targeting detection activities for delimiting incursion source populations more efficiently, and **general practical recommendations** have been confirmed and emerged regarding the future response to painted apple moth incursion in Auckland. Ground searches should concentrate in the immediate vicinity of the trap catch in all directions but with a downwind emphasis, taking into consideration the prevailing wind direction for the period since the trap was last cleared.

VI.4 Ecological perspectives

The model developed in this study integrated two different dispersal behaviours: 1) **downwind dispersal**, either active or passive, and assumed to be appetitive (Elkinton & Cardé, 1983), prior to encountering pheromone stimulus and 2) **anemotaxis behaviour** to track the source of a pheromone plume. These two behaviours have opposite consequences in terms of spatial displacement; they respectively resulted in downwind displacement and net upwind displacement, even if insects are alternating upwind, zigzagging and casting behaviours in the latter. Following Dobzhansky (1973) in his essay "Nothing in biology makes sense except in the light of Evolution", one can speculate on the evolutionary advantages of these behaviours. Painted apple moth is a day flying moth but **females are flightless** (Common, 1990). The evolution of wing reduction is strongly associated with spring feeding in Lymantriidae in forest habitat (Hunter, 1995).

For Lymantriids, **ballooning behaviour of larva** has been observed (Zlotina et al., 1999). Although Lepidopteran ballooning has not been intensively studied, it is thought to disperse mostly early instars' larvae up to a few hundred of meters (Bell et al., 2005). Consequently, from a single egg mass, the larval population may disperse across an area of 1-2 km diameter with a spatial pattern determined by the fluctuations of the wind direction. Furthermore, adult males disperse some months later than the larvae, and consequently the main wind direction will almost certainly be different.
During the adult phase, the flightless female will stay in the near vicinity to where she landed as a larva after ballooning. The **success of mating** will depend primarily on the ability of the males to detect and locate the females. It could be advantageous to detect a calling female in downwind dispersion followed by anemotaxis behaviour, since it may enable males to firstly get out of the area of larval dispersal, in the downwind direction, and therefore be more likely to encounter a pheromone cloud located in the downwind direction of a calling female. That is consistent with theoretical studies by Dusenbery (1990) and Reynolds et al. (2007) on **optimal searching strategies** in shifting winds.

Increased mate finding efficiency could provide an evolutionary advantage in the survival of the population by mitigating the Allee effect (Gascoigne *et al.*, 2009). In a biosecurity context, the transition between arrival of alien species propagules and an established or invasive population may depend on mate finding capacities at low population densities. Determination of mate finding efficiency under different scenarios would also be of particular importance for evaluating the invasiveness of a species in different environments. More evidence is required to support this suggestion, but clearly prioritizations of pest species in pest risk assessment studies should consider mate finding ability as one of the indices of invasiveness.

VI.6 General conclusion

The development of an applied modelling tool for insect behaviour provides the basis for future biosecurity tools, and raises fundamental questions about different modelling approaches, scaling and stochasticity but also on mechanisms employed by flying insects to locate a mate.

CHAPTER VII

References

Anderbrant O **(1988)**. Survival of parent and brood adult bark beetles, *Ips typographus*, in relation to size, lipid content and re-emergence or emergence day. *Physiological Entomology*, **13:** 121-129.

Armstrong KF, McHugh P, Chinn W, Frampton ER & Walsh PJ **(2003)**. Tussock moth species arriving on imported used vehicles determined by DNA analysis. *New Zealand Plant Protection, Volume 56*, (Zydenbos SM, Ed.), Christchurch, New Zealand, The New Zealand Plant Protection Society Inc., 16-20.

Augustin S, Guichard S, Svatos A & Gilbert M **(2004)**. Monitoring the regional spread of the invasive leafminer *Cameraria ohridella* (Lepidoptera: Gracillariidae) by damage assessment and pheromone trapping. *Environmental Entomology*, **33:** 1584-1592.

Baker R, Cannon R, Bartlett P & Barker I **(2005)**. Novel strategies for assessing and managing the risks posed by invasive alien species to global crop production and biodiversity. *Annals of Applied Biology*, **146:** 177-191.

Baker TC & Roelofs WL **(1981)**. Initiation and termination of oriental fruit moth male response to pheromone concentrations in the field. *Environmental Entomology*, **10:** 211-218.

Baker TC & Haynes KF **(1987)**. Manoeuvres used by flying male oriental fruit moths to relocate a sex pheromone plume in an experimentally shifted wind-field. *Physiological Entomology*, **12:** 263-279.

Baker TC & Haynes KF **(1989)**. Field and laboratory electroantennographic measurements of pheromone plume structure correlated with oriental fruit moth behaviour. *Physiological Entomology*, **14:** 1-12.

Baker TC & Haynes KF **(1996)**. Pheromone-mediated optomotor anemotaxis and altitude control exhibited by male oriental fruit moths in the field. *Physiological Entomology*, **21:** 20-32.

Balkovsky E & Shraiman BI **(2002)**. Olfactory search at high Reynolds number. *Proceedings of the National Academy of Sciences, USA*, **99:** 12589-12593.

Barker GM, Stephens A, Hunter C, Rutledge D, Harris RJ, Lariviere MC & Gough JD **(2003)**. Biosecure - a model for analysis of biosecurity risk profiles. *Defending the Green Oasis: New Zealand Biosecurity and Science. Proceedings of a New Zealand Plant Protection Symposium*, (Goldson SL & Suckling DM, Eds.), Rotorua, New Zealand, New Zealand Plant Protection Society, 73-91.

Barlow ND & Goldson SL **(2002)**. Alien invertebrates in New Zealand. *Biological invasions: economic and environmental costs of alien plant, animal, and microbe species.*, (Pimentel D, Ed.), CRC Press, 195-216.

Batschelet E **(1981)**. *Circular statistics in biology*. Academic Press.

Beasley D, Bull DR & Martin RR **(1993)**. An overview of genetic algorithms: part 1, fundamentals. *University Computing*, **15:** 58-69.

Beenakkers AMT, Horst DJ & Marrewijk WJA **(1984)**. Insect flight muscle metabolism. *Insect Biochemistry*, **14:** 243-260.

Beggs JR & Wilson PR **(1991)**. The kaka *Nestor meridionalis*, a New Zealand parrot endangered by introduced wasps and mammals. *Biological Conservation*, **56:** 23-38.

Bell JR, Bohan DA, Shaw EM & Weyman GS **(2005)**. Ballooning dispersal using silk: World fauna, phylogenies, genetics and models. *Bulletin of Entomological Research*, **95:** 69-114.

Biosecurity New Zealand **(2006)**. *Standard for gypsy moth (Lymantria dispar) surveillance*, pp. 27.

Bisignanesi V & Borgas MS **(2007)**. Models for integrated pest management with chemicals in atmospheric surface layers. *Ecological Modelling*, **201:** 2-10.

Blacklock BJ & Ryan RO **(1994)**. Hemolymph lipid transport. *Insect Biochemistry and Molecular Biology*, **24:** 855-873.

Bogich TL, Liebhold AM & Shea K **(2008)**. To sample or eradicate? A cost minimization model for monitoring and managing an invasive species. *Journal of Applied Ecology*, **45:** 1134-1142.

Britter RE & Hanna SR **(2003)**. Flow and dispersion in urban areas. *Annual Review of Fluid Mechanics*, **35:** 469-496.

Bulman LS **(2008)**. Pest detection surveys on high-risk sites in New Zealand. *Australian Forestry*, **71:** 242-244.

Byers JE, Reichard S, Randall JM, Parker IM, Smith CS, Lonsdale WM, Atkinson IAE, Seastedt TR, Williamson M, Chornesky E & Hayes D **(2002)**. Directing research to reduce the impacts of nonindigenous species. *Conservation Biology*, **16:** 630-640.

Canadian Food Inspection Agency **(2007)**. *Comparative report of engagement strategies for invasive alien species among "QUAD" countries: case studies of forest pest insects*, pp. 116.

Cannon RJC **(1998)**. The implications of predicted climate change for insect pests in the UK, with emphasis on non-indigenous species. *Global Change Biology*, **4:** 785-796.

Cannon RJC, Koerper D, Ashby S, Baker R, Bartlett PW, Brookes G, Burgess R, Cheek S, Evans HF, Hammon R, Head J, Nettleton G, Robinson J, Slawson D, Taylor MC, Tilbury CA & Ward M **(2004)**. Gypsy moth, *Lymantria dispar*, outbreak in northeast London, 1995-2003. *International Journal of Pest Management*, **50:** 259-273.

Cardé RT & Hagaman TE **(1979)**. Behavioral responses of the gypsy moth in a wind tunnel to air-borne enantiomers of disparlure. *Environmental Entomology*, **8:** 475-484.

Cardé RT **(1984)**. Chemo-orientation in flying insects. *Chemical ecology of insects*, (Bell WJ & Cardé RT, Eds.), Chapman and Hall, 111-124.

Cardé RT & Knols BGJ **(2000)**. Effects of light levels and plume structure on the orientation manoeuvres of male gypsy moths flying along pheromone plumes. *Physiological Entomology*, **25:** 141-150.

Cardé RT & Willis MA **(2008)**. Navigational strategies used by insects to find distant, wind-borne sources of odor. *Journal of Chemical Ecology*, **34:** 854-866.

Carter PCS **(1989)**. Risk assessment and pest detection surveys for exotic pests and diseases which threaten commercial forestry in New Zealand. *New Zealand Journal of Forestry Science*, **19:** 353-374.

Charlton RE & Cardé RT **(1982)**. Rate and diel periodicity of pheromone emission from female gypsy moths, (*Lymantria dispar*) determined with a glass-adsorption collection system. *Journal of Insect Physiology*, **28:** 423-430.

Charlton RE, Kanno H, Collins RD & Cardé RT **(1993)**. Influence of pheromone concentration and ambient temperature on flight of the gypsy moth, *Lymantria dispar* (L.), in a sustained-light wind tunnel. *Physiological Entomology*, **18:** 349-362.

Clark JM, Marion JR, Scarano LJ, Potter TL, Gosselin PF, Argentine JA & Elkinton JS **(1990)**. Neutral lipid content and fatty acid composition of 1,2-diacylglycerols in the hemolymph of the male gypsy moth, *Lymantria dispar* L. (Lepidoptera: Lymantriidae). *Canadian Entomologist*, **122:** 1101-1109.

Cohen J **(1960)**. A coefficient of agreement for nominal scales. *Educational and Psychological Measurement*, **20:** 37-46.

Colautti RI, Bailey SA, Van Overdijk CDA, Amundsen K & MacIsaac HJ **(2006)**. Characterised and projected costs of nonindigenous species in Canada. *Biological Invasions*, **8:** 45-59.

Colvin J, Brady J & Gibson G **(1989)**. Visually-guided, upwind turning behaviour of free-flying tsetse flies in odour-laden wind: a wind-tunnel study. *Physiological Entomology*, **14:** 31-39.

Common IFB **(1990)**. *Moths of Australia*. Melbourne University Press, pp. 535.

Conner WE, Webster RP & Itagaki H **(1985)**. Calling behaviour in arctiid moths: the effects of temperature and wind speed on the rhythmic exposure of the sex attractant gland. *Journal of Insect Physiology*, **31:** 815-820.

Convention on Biological Diversity **(2004, cited 2009)**. Decision VII/13. Alien species that threaten ecosystems, habitats or species (Article 8 (h)). Report of the Seventh Meeting of the Conference of the Parties to the Convention on Biological Diversity. [Available online from http://www.biodiv.org/doc/meetings/cop/cop-07/official/cop-07-21-part2-en.pdf.]

Cook A, Weinstein P & Woodward A **(2002)**. The impact of exotic insects in New Zealand. *Biological invasions: economic and environmental costs of alien plant, animal, and microbe species.*, (Pimentel D, Ed.), CRC Press, 217-239.

Craig J, Anderson S, Clout M, Creese B, Mitchell N, Ogden J, Roberts M & Ussher G **(2000)**. Conservation issues in New Zealand. *Annual Review of Ecology and Systematics*, **31:** 61-78.

Currano ED, Wilf P, Wing SL, Labandeira CC, Lovelock EC & Royer DL **(2008)**. Sharply increased insect herbivory during the Paleocene-Eocene thermal maximum. *Proceedings of the National Academy of Sciences, USA*, **105:** 1960-1964.

David CT, Kennedy JS, Ludlow AR, Perry JN & Wall C **(1982)**. A reappraisal of insect flight towards a distant point source of wind-borne odor. *Journal of Chemical Ecology*, **8:** 1207-1215.

David CT, Kennedy JS & Ludlow AR **(1983)**. Finding of a sex pheromone source by gypsy moths released in the field. *Nature*, **303:** 804-806.

Dobzhansky T **(1973)**. Nothing in biology makes sense except in light of evolution. *American Biology Teacher*, **35:** 125-129.

Downer RGH & Matthews JR **(1976)**. Patterns of lipid distribution and utilisation in insects. *American Zoologist*, **16:** 733-745.

Dudley R & DeVries PJ **(1990)**. Flight physiology of migrating *Urania fulgens* (Uraniidae) moths: Kinematics and aerodynamics of natural free flight. *Journal of Comparative Physiology - A Sensory, Neural, and Behavioral Physiology*, **167:** 145-154.

Dudley R & Ellington CP **(1990)**. Mechanics of forward flight in bumblebees 2. Quasi-steady lift and power requirements. *Journal of Experimental Biology*, **148:** 53-88.

Dusenbery DB **(1989a)**. Optimal search direction for an animal flying or swimming in a wind or current. *Journal of Chemical Ecology*, **15:** 2511-2519.

Dusenbery DB **(1989b)**. Calculated effect of pulsed pheromone release on range of attraction. *Journal of Chemical Ecology*, **15:** 971-977.

Dusenbery DB **(1990)**. Upwind searching for an odor plume is sometimes optimal. *Journal of Chemical Ecology*, **16:** 1971-1976.

El-Sayed AM & Trimble RM **(2002)**. Relative attractiveness, of natural and synthetic pheromone of three tortricid tree fruit pests. *Environmental Entomology*, **31:** 960-964.

El-Sayed AM, Gibb AR, Suckling DM, Bunn B, Fielder S, Comeskey D, Manning LA, Foster SP, Morris BD, Ando T & Mori K **(2005)**. Identification of sex pheromone components of the painted apple moth: A tussock moth with a thermally labile pheromone component. *Journal of Chemical Ecology*, **31:** 621-646.

Elkinton JS & Cardé RT **(1983)**. Appetitive flight behavior of male gypsy moths (Lepidoptera: Lymantridae). *Environmental Entomology*, **12:** 1702-1707.

Elkinton JS, Cardé RT & Mason CJ **(1984)**. Evaluation of time-average dispersion models for estimating pheromone concentration in a deciduous forest. *Journal of Chemical Ecology*, **10:** 1081-1108.

Elkinton JS, Schal C, Ono T & Cardé RT **(1987)**. Pheromone puff trajectory and upwind flight of male gypsy moths in a forest. *Physiological Entomology*, **12:** 399-406.

Fadamiro HY, Wyatt TD & Birch MC **(1998)**. Flying beetles respond as moths predict: Optomotor anemotaxis to pheromone plumes at different heights. *Journal of Insect Behavior*, **11:** 549-557.

Farkas SR & Shorey HH **(1972)**. Chemical trial following by flying insects: A mechanism for orientation to a distant odor source. *Science, USA*, **178:** 67-68.

Fox KJ **(1978)**. The transoceanic migration of Lepidoptera to New Zealand - a history and a hypothesis on colonisation. *New Zealand Entomologist*, **6:** 368-380.

Franklin AJ & Grégoire JC **(1999)**. Flight behaviour of *Ips typographus* L. (Col., Scolytidae) in an environment without pheromones. *Annals of Forest Science*, **56:** 591-598.

Gascoigne J, Berec L, Gregory S & Courchamp F **(2009)**. Dangerously few liaisons: a review of mate-finding Allee effects. *Population Ecology*, **51:** 355-372.

Gear I **(2004)**. Painted apple moth's days are numbered. *Biosecurity magazine*, **51:** 11.

Gordon MS **(1977)**. *Animal physiology: principles and adaptations*. Macmillan Publishing Company, pp. 699.

Green GW **(1962)**. Flight and dispersal of the European Pine Shoot Moth, *Rhyacionia buoliana* (Schiff.) I. Factors affecting flight, and flight potential of females. *Canadian Entomologist*, **94:** 282-299.

Green OR **(1984)**. New Zealand host and locality records for an introduced tortricid parasite, *Trigonospila brevifacies* (Diptera: Tachinidae). *New Zealand Entomologist*, **8:** 69-71.

Hagaman TE & Cardé RT **(1984)**. Effect of pheromone concentration on organization of preflight behaviors of the male gypsy moth, *Lymantria dispar* (L.). *Journal of Chemical Ecology*, **10:** 17-23.

Hardie J, Gibson G & Wyatt TD **(2001)**. Insect behaviours associated with resource finding. *Insect movement: mechanisms and consequences. Proceedings of the Royal Entomological Society's 20th Symposium.*, (Woiwod IP, Reynolds DR, & Thomas CD, Eds.), Oxon, CABI Publishing, 87-109.

Hardwick S, Baltus JG & Willoughby BE **(2000)**. Seasonal distribution of *Herpetogramma licarsisalis* (Walker) (Lepidoptera: Pyralidae) in northern Northland. *New Zealand Entomologist*, **23:** 77-83.

Heran H & Lindauer M **(1963)**. Windkompensation und Seitenwindkorrektur der Bienen beim Flug uber Wasser. *Journal of Comparative Physiology A: Sensory, Neural, and Behavioral Physiology*, **47:** 39-55.

Hoare RJB **(2001)**. Adventive species of Lepidoptera recorded for the first time in New Zealand since 1988. *New Zealand Entomologist*, **24:** 23-47.

Hosking G, Clearwater J, Handiside J, Kay M, Ray J & Simmons N **(2003)**. Tussock moth eradication - a success story from New Zealand. *International Journal of Pest Management*, **49:** 17-24.

Hulme PE, Bacher S, Kenis M, Klotz S, Kuhn I, Minchin D, Nentwig W, Olenin S, Panov V, Pergl J, Pysek P, Roques A, Sol D, Solarz W & Vila M **(2008)**. Grasping at the routes of biological invasions: a framework for integrating pathways into policy. *Journal of Applied Ecology*, **45:** 403-414.

Hunter AF **(1995)**. The ecology and evolution of reduced wings in forest Macrolepidoptera. *Evolutionary Ecology*, **9:** 275-287.

IPPC **(2008)**. *International standards for phytosanitary measures ISPM No. 5. Glossary of phytosanitary terms*. International Plant Protection Convention, pp. 22.

IUCN **(2000)**. *2000 IUCN Red list of threatened species*. International Union for Conservation of Nature, pp. 64.

Jactel H & Gaillard J **(1991)**. A preliminary study of the dispersal potential of *Ips sexdentatus* (Boern) (Col., Scolytidae) with an automatically recording flight mill. *Journal of Applied Entomology*, **112:** 138-145.

Jeschke JM & Strayer DL **(2008)**. Are threat status and invasion success two sides of the same coin? *Ecography*, **31:** 124-130.

Jiang JA, Tseng CL, Lu FM, Yang EC, Wu ZS, Chen CP, Lin SH, Lin KC & Liao CS **(2008)**. A GSM-based remote wireless automatic monitoring system for field information: A case study for ecological monitoring of the oriental fruit fly, *Bactrocera dorsalis* (Hendel). *Computers and Electronics in Agriculture*, **62:** 243-259.

Johnson CG **(1963)**. Physiological factors in insect migration by flight. *Nature*, **198:** 423-427.

Johnson CG **(1969)**. *Migration and dispersal of insects by flight*. Methuen, pp. 763.

Kean JM & Suckling DM **(2005)**. Estimating the probability of eradication of painted apple moth from Auckland. *New Zealand Plant Protection, Volume 58*, (Zydenbos SM, Ed.), Wellington, New Zealand, The New Zealand Plant Protection Society Inc., 7-11.

Kennedy JS **(1939)**. The visual responses of flying mosquitoes. *Proceedings of the Zoological Society of London (A)*, **109:** 221-242.

Kennedy JS **(1951)**. The migration of the Desert Locust (*Schistocerca gregaria* Forsk.). I. The behaviour of swarms. II. A theory of long-range migration. *Philosophical Transactions of the Royal Society of London, B*, **235:** 163-290.

Kennedy JS & Marsh D **(1974)**. Pheromone-regulated anemotaxis in flying moths. *Science*, **184:** 999-1001.

Kennedy JS, Ludlow AR & Sanders CJ **(1980)**. Guidance system used in moth sex attraction. *Nature*, **288:** 475-477.

Kennedy JS **(1983)**. Zigzagging and casting as a programmed response to wind-borne odour: a review. *Physiological Entomology*, **8:** 109-120.

Kishaba AN, Toba HH, Wolf WW & Vail PV **(1970)**. Response of laboratory-reared male cabbage looper to synthetic sex pheromone in the field. *Journal of Economic Entomology*, **63:** 178-181.

Kriticos DJ, Phillips CB & Suckling DM **(2005)**. Improving border biosecurity: potential economic benefits to New Zealand. *New Zealand Plant Protection, Volume 58*, (Zydenbos SM, Ed.), Wellington, New Zealand, The New Zealand Plant Protection Society Inc., 1-6.

Kriticos DJ, Potter KJB, Alexander NS, Gibb AR & Suckling DM **(2007)**. Using a pheromone lure survey to establish the native and potential distribution of an invasive Lepidopteran, *Uraba lugens*. *Journal of Applied Ecology*, **44:** 853-863.

Kuenen LPS & Baker TC **(1982)**. Optomotor regulation of ground velocity in moths during flight to sex pheromone at different heights. *Physiological Entomology*, **7:** 193-202.

Kuenen LPS & Cardé RT **(1994)**. Strategies for recontacting a lost pheromone plume: casting and upwind flight in the male gypsy moth. *Physiological Entomology*, **19:** 15-29.

Kuenen LPS & Rowe HC **(2006)**. Cowpea weevil flights to a point source of female sex pheromone: Analyses of flight tracks at three wind speeds. *Physiological Entomology*, **31:** 103-109.

Liebhold AM & Tobin PC **(2008)**. Population ecology of insect invasions and their management. *Annual Review of Entomology*, **53:** 387-408.

Lodge DM, Williams S, MacIsaac HJ, Hayes KR, Leung B, Reichard S, Mack RN, Moyle PB, Smith M, Andow DA, Carlton JT & McMichael A **(2006)**. Biological invasions: Recommendations for US policy and management. *Ecological Applications*, **16:** 2035-2054.

Logan JA, Regniere J, Gray DR & Munson AS **(2007)**. Risk assessment in the face of a changing environment: Gypsy moth and climate change in Utah. *Ecological Applications*, **17:** 101-117.

Macaulay EDM **(1974)**. Lipid storage in the pre-imago and young adult *Plusia gamma*. *Entomologia Experimentalis et Applicata*, **17:** 53-60.

Mack RN, Simberloff D, Lonsdale WM, Evans H, Clout M & Bazzaz FA **(2000)**. Biotic invasions: Causes, epidemiology, global consequences, and control. *Ecological Applications*, **10:** 689-710.

Mafra-Neto A & Cardé RT **(1994)**. Fine-scale structure of pheromone plumes modulates upwind orientation of flying moths. *Nature*, **369:** 142-144.

Mafra-Neto A & Cardé RT **(1998)**. Rate of realized interception of pheromone pulses in different wind speeds modulates almond moth orientation. *Journal of Comparative Physiology A-Sensory, Neural, and Behavioral Physiology*, **182:** 563-572.

Marsh D, Kennedy JS & Ludlow AR **(1978)**. An analysis of anemotactic zigzagging flight in male moths stimulated by pheromone. *Physiological Entomology*, **3:** 221-240.

Marsh D, Kennedy JS & Ludlow AR **(1981)**. Analysis of zigzagging flight in moths: a correction. *Physiological Entomology*, **6:** 225.

Maynard GV, Hamilton JG & Grimshaw JF **(2004)**. Quarantine - Phytosanitary, sanitary and incursion management: an Australian entomological perspective. *Australian Journal of Entomology*, **43:** 318-328.

McCullough DG, Work TT, Cavey JF, Liebhold AM & Marshall D **(2006)**. Interceptions of nonindigenous plant pests at US ports of entry and border crossings over a 17-year period. *Biological Invasions*, **8:** 611-630.

Memmott J, Craze PG, Harman HM, Syrett P & Fowler SV **(2005)**. The effect of propagule size on the invasion of an alien insect. *Journal of Animal Ecology*, **74:** 50-62.

Mills NJ **(1981)**. The mortality and fat content of *Adalia bipunctata* during hibernation. *Entomologia Experimentalis et Applicata*, **30:** 265-268.

Ministry for the Environment **(1996, cited 2009)**. Hazardous Substances and New Organisms Act 1996. [Available online from http://www.mfe.govt.nz/laws/hsno.html.]

Ministry of Agriculture and Forestry **(2006a, cited 2009)**. Unwanted Organisms Database. [Available online from http://mafuwsp6.maf.govt.nz/uor/searchframe.htm.]

Ministry of Agriculture and Forestry **(2006b, cited 2009)**. Two Auckland pest moth populations declared eradicated. [Available online from http://www.maf.govt.nz/mafnet/press/200306pam.htm.]

Murlis J & Jones CD **(1981)**. Fine-scale structure of odour plumes in relation to insect orientation to distant pheromone and other attractant sources. *Physiological Entomology*, **6:** 71-86.

Murlis J, Elkinton JS & Cardé RT **(1992)**. Odor plumes and how insects use them. *Annual Review of Entomology*, **37:** 505-532.

Murlis J, Willis MA & Cardé RT **(2000)**. Spatial and temporal structures of pheromone plumes in fields and forests. *Physiological Entomology*, **25:** 211-222.

Murphy B **(2005)**. New era for high-risk site surveillance. *Biosecurity magazine*, **64:** 20.

Myers JH, Savoie A & van Randen E **(1998)**. Eradication and pest management. *Annual Review of Entomology*, **43:** 471-491.

Myers JH, Simberloff D, Kuris AM & Carey JR **(2000)**. Eradication revisited: Dealing with exotic species. *Trends in Ecology and Evolution*, **15:** 316-320.

O'Neil B **(2001)**. *Policy statement on responding to an exotic organism incursion*. MAF Biosecurity Authority Report, pp. 15.

Olafsson H & Bougeault P **(1997)**. The effect of rotation and surface friction on orographic drag. *Journal of the Atmospheric Sciences*, **54:** 193-210.

Ostrand F, Anderbrant O & Jonsson P **(2000)**. Behaviour of male pine sawflies, *Neodiprion sertifer*, released downwind from pheromone sources. *Entomologia Experimentalis et Applicata*, **95:** 119-128.

Ostrand F, Anderbrant O, Jonsson P & Lyytikainen-Saarenmaa P **(2001)**. Capture rates of the European pine sawfly, *Neodiprion sertifer*, in pheromone traps, with special regard to effects of wind speed. *Journal of Chemical Ecology*, **27:** 1561-1574.

Parliament of New Zealand **(1993, cited 2009)**. Biosecurity Act 1993. [Available online from http://rangi.knowledge-basket.co.nz/gpacts/public/text/1993/an/095.html.]

Perrings C, Dehnen-Schmutz K, Touza J & Williamson M **(2005)**. How to manage biological invasions under globalization. *Trends in Ecology & Evolution*, **20:** 212-215.

Pimentel D **(2002a)**. Introduction: non-native species in the world. *Biological invasions: economic and environmental costs of alien plant, animal, and microbe species.*, (Pimentel D, Ed.), CRC Press, 3-8.

Pimentel D **(2002b)**. *Biological invasions: economic and environmental costs of alien plant, animal, and microbe species*. CRC Press, pp. 376.

Preiss R & Kramer E **(1986)**. Mechanism of pheromone orientation in flying moths. *Naturwissenschaften*, **73:** 555-557.

Reynolds AM, Reynolds DR, Smith AD, Svensson GP & Lofstedt C **(2007)**. Appetitive flight patterns of male *Agrotis segetum* moths over landscape scales. *Journal of Theoretical Biology*, **245:** 141-149.

Richardson B, Kay MK, Kimberley MO, Charles JG & Gresham BA **(2005)**. Evaluating the benefits of dose-response bioassays during aerial pest eradication operations. *New Zealand Plant Protection*, **58:** 17-23.

Riffell JA, Abrell L & Hildebrand JG **(2008)**. Physical processes and real-time chemical measurement of the insect olfactory environment. *Journal of Chemical Ecology*, **34:** 837-853.

Riley JR, Valeur P, Smith AD, Reynolds DR, Poppy GM & Lofstedt C **(1998)**. Harmonic radar as a means of tracking the pheromone-finding and pheromone-following flight of male moths. *Journal of Insect Behavior*, **11:** 287-296.

Riley JR & Osborne JL **(2001)**. Flight trajectories of foraging insects: observations using harmonic radar. *Insect movement: mechanisms and consequences. Proceedings of the Royal Entomological Society's 20th Symposium.*, (Woiwod IP, Reynolds DR, & Thomas CD, Eds.), CABI Publishing, Oxon, 129-157.

Rossi RE, Mulla DJ, Journel AG & Franz EH **(1992)**. Geostatistical tools for modeling and interpreting ecological spatial dependence. *Ecological Monographs*, **62:** 277-314.

Sabelis MW & Schippers P **(1984)**. Variable wind directions and anemotactic strategies of searching for an odour plume. *Oecologia*, **63:** 225-228.

Sakamoto R, Murata M & Tojo S **(2004)**. Effects of larval diets on flight capacity and flight fuel in adults of the common cutworm, *Spodoptera litura* (Lepidoptera: Noctuidae). *Applied Entomology and Zoology*, **39:** 133-138.

Salom SM & McLean JA **(1989)**. Influence of wind on the spring flight of *Trypodendron lineatum* (Olivier) (Coleoptera, Scolytidae) in a second-growth coniferous forest. *Canadian Entomologist*, **121:** 109-119.

Scire JS, Robe FR, Fernau ME & Yamartino RJ **(1998)**. *A user's guide for the CALMET meteorogical model (version 5)*. Earth Tech. Inc., pp. 332.

Self M **(2003)**. Biosecurity: the implications for international forestry trade. *The Australian and New Zealand Institutes of Forestry Conference*, (Mason EG & Perley CJ, Eds.), Queenstown, New Zealand, 59-63.

Sharov AA, Liebhold AM & Ravlin FW **(1995)**. Prediction of gypsy moth (Lepidoptera: Lymantriidae) mating success from pheromone trap counts. *Environmental Entomology*, **24:** 1239-1244.

Sharov AA, Liebhold AM & Roberts EA **(1997)**. Methods for monitoring the spread of gypsy moth (Lepidoptera: Lymantriidae) populations in the Appalachian mountains. *Journal of Economic Entomology*, **90:** 1259-1266.

Sharov AA, Liebhold AM & Roberts EA **(1998)**. Optimizing the use of barrier zones to slow the spread of gypsy moth (Lepidoptera: Lymantriidae) in North America. *Journal of Economic Entomology*, **91:** 165-174.

Shigesada N & Kawasaki K **(1997)**. *Biological invasions: theory and practice*. Oxford University Press, pp. 205.

Stanaway MA, Zalucki MP, Gillespie PS, Rodriguez CM & Maynard V **(2001)**. Pest risk assessment of insects in sea cargo containers. *Australian Journal of Entomology*, **40:** 180-192.

Stephenson BP, Gill GSC, Randall JL & Wilson JA **(2003)**. Biosecurity approaches to surveillance and response for new plant pest species. *New Zealand Plant Protection, Volume 56*, (Zydenbos SM, Ed.), Christchurch, New Zealand, The New Zealand Plant Protection Society Inc., 5-9.

Strand T, Lamb B, Thistle H, Allwine E & Peterson H **(2009)**. A simple model for simulation of insect pheromone dispersion within forest canopies. *Ecological Modelling*, **220:** 640-656.

Suckling DM, Brunner JF, Burnip GM & Walker JTS **(1994)**. Dispersal of *Epiphyas postvittana* (Walker) and *Planotortrix octo* Dugdale (Lepidoptera, Tortricidae) at a Canterbury, New Zealand orchard. *New Zealand Journal of Crop and Horticultural Science*, **22:** 225-234.

Suckling DM, Charles J, Allan D, Chaggan A, Barrington A, Burnip GM & El-Sayed AM **(2005a)**. Performance of irradiated *Teia anartoides* (Lepidoptera: Lymantriidae) in urban Auckland, New Zealand. *Journal of Economic Entomology*, **98:** 1531-1538.

Suckling DM, Gibb AR, Dentener PR, Seldon DS, Clare GK, Jamieson L, Baird D, Kriticos DJ & El-Sayed AM **(2005b)**. *Uraba lugens* (Lepidoptera : Nolidae) in New Zealand: Pheromone trapping for delimitation and phenology. *Journal of Economic Entomology*, **98:** 1187-1192.

Suckling DM, Hackett JK, Chhagan A, Barrington A & El-Sayed AM **(2006)**. Effect of irradiation on female painted apple moth *Teia anartoides* (Lep., Lymantriidae) sterility and attractiveness to males. *Journal of Applied Entomology*, **130:** 167-170.

Suckling DM, Barrington AM, Chhagan A, Stephens AEA, Burnip GM, Charles JG & Wee SL **(2007)**. Eradication of the Australian painted apple moth *Teia anartoides* in New Zealand: Trapping, inherited sterility, and male competitiveness. *Area-wide control of insect pests: from research to field implementation*, (Vreysen MJB, Robinson AS, & Hendrichs J, Eds.), Springer, 603-615.

Suckling DM, Jang EB, Holder P, Carvalho L & Stephens AEA **(2008)**. Evaluation of lure dispensers for fruit fly surveillance in New Zealand. *Pest Management Science*, **64:** 848-856.

Tobin PC, Liebhold AM & Roberts EA **(2007)**. Comparison of methods for estimating the spread of a non-indigenous species. *Journal of Biogeography*, **34:** 305-312.

Turner JA, Bulman LS, Richardson B & Moore JR **(2004)**. Cost-benefit analysis of biosecurity and forest health research. *New Zealand Journal of Forestry Science*, **34:** 324-343.

Vickers NJ & Baker TC **(1994)**. Reiterative responses to single strands of odor promote sustained upwind flight and odor source location by moths. *Proceedings of the National Academy of Sciences of the United States of America*, **91:** 5756-5760.

Vickers NJ & Baker TC **(1996)**. Latencies of behavioral response to interception of filaments of sex pheromone and clean air influence flight track shape in *Heliothis virescens* (F.) males. *Journal of Comparative Physiology A: Neuroethology, Sensory, Neural, and Behavioral Physiology*, **178:** 831-847.

Vickers NJ & Baker TC **(1997)**. Flight of *Heliothis virescens* males in the field in response to sex pheromone. *Physiological Entomology*, **22:** 277-285.

Vickers NJ **(2000)**. Mechanisms of animal navigation in odor plumes. *Biological Bulletin*, **198:** 203-212.

Wall C & Perry JN **(1987)**. Range of action of moth sex-attractant sources. *Entomologia Experimentalis et Applicata*, **44:** 5-14.

Wang W, Shaw WJ, Seiple TE, Rishel JP & Xie Y **(2008)**. An evaluation of a diagnostic wind model (CALMET). *Journal of Applied Meteorology and Climatology*, **47:** 1739-1756.

Ward NL & Masters GJ **(2007)**. Linking climate change and species invasion: an illustration using insect herbivores. *Global Change Biology*, **13:** 1605-1615.

Whyte C **(2005)**. Science and biosecurity - monitoring the effectiveness of biosecurity interventions at New Zealand's borders. *Proceedings of the Royal Society of New Zealand*, (The Royal Society of New Zealand, Ed.), Wellington, New Zealand, The New Zealand Plant Protection Society Inc., 27-35.

Williams IH, Frearson D, Barari H & McCartney A **(2007)**. Migration to and dispersal from oilseed rape by the pollen beetle, *Meligethes aeneus*, in relation to wind direction. *Agricultural and Forest Entomology*, **9:** 279-286.

Williams JD & Meffe GK **(1998)**. Nonindigenous Species. *Status and Trends of the Nation's Biological Resources. Volume 1&2*, (Mac MJ, Opler PA, Puckett Haecker CE, & Doran PD, Eds.), U.S. Department of the Interior, U.S. Geological Survey, 117-129.

Williamson M & Fitter A **(1996)**. The varying success of invaders. *Ecology*, **77:** 1661-1666.

Willis MA & Cardé RT **(1990)**. Pheromone-modulated optomotor response in male gypsy moths, *Lymantria dispar* L.: upwind flight in a pheromone plume in different wind velocities. *Journal of Comparative Physiology A-Sensory, Neural, and Behavioral Physiology*, **167:** 699-706.

Willis MA & Arbas EA **(1991)**. Odor-modulated upwind flight of the sphinx moth, *Manduca-Sexta* L. *Journal of Comparative Physiology A-Sensory, Neural, and Behavioral Physiology*, **169:** 427-440.

Willis MA, Murlis WJ & Cardé RT **(1991)**. Pheromone-mediated upwind flight of male gypsy moths, *Lymantria dispar*, in a forest. *Physiological Entomology*, **16:** 507-521.

Willis MA, David CT, Murlis J & Cardé RT **(1994)**. Effects of pheromone plume structure and visual stimuli on the pheromone-modulated upwind flight of male

gypsy moths *Lymantria dispar* in a forest (Lepidoptera: Lymantriidae). *Journal of Insect Behavior*, **7:** 385-409.

Wilson JA, Stephenson BP, Gill GSC, Randall JL & Vieglais CMC **(2004)**. Principles of response to detections of new plant pest species and the effectiveness of surveillance. *New Zealand Plant Protection, Volume 57*, (Zydenbos SM, Ed.), Hamilton, New Zealand, The New Zealand Plant Protection Society Inc., 156-160.

Worner SP **(1991)**. Use of models in applied entomology - the need for perspective. *Environmental Entomology*, **20:** 768-773.

Wylie FR, Griffiths M & King J **(2008)**. Development of hazard site surveillance programs for forest invasive species: a case study from Brisbane, Australia. *Australian Forestry*, **71:** 229-235.

Yamanaka T, Tatsuki S & Shimada M **(2003)**. An individual-based model for sex-pheromone-oriented flight patterns of male moths in a local area. *Ecological Modelling*, **161:** 35-51.

Zanen PO & Cardé RT **(1999)**. Directional control by male gypsy moths of upwind flight along a pheromone plume in three wind speeds. *Journal of Comparative Physiology A-Sensory, Neural, and Behavioral Physiology*, **184:** 21-35.

Zar JH **(1984)**. *Biostatistical analysis*. Prentice-Hall, pp. 718.

Zera AJ, Mole S & Rokke K **(1994)**. Lipid, carbohydrate and nitrogen content of long- and short-winged *Gryllus firmus*: Implications for the physiological cost of flight capability. *Journal of Insect Physiology*, **40:** 1037-1044.

Zlotina MA, Elkinton JS, Mastro VC & Leonard DE **(1999)**. Dispersal tendencies of neonate larvae of *Lymantria mathura* and the Asian form of *Lymantria dispar* (Lepidoptera: Lymantriidae). *Environmental Entomology*, **28:** 240-245.